HAER
IOWA
85-AMES,
6-

# HISTORIC AMERICAN ENGINEERING RECORD

## STRUCTURAL STUDY OF IRON BOWSTRING BRIDGES

HAER No. IA-90

| | |
|---|---|
| Location: | Iowa Department of Transportation<br>Ames, Story County, Iowa |
| Dates of Construction: | 1873, 1875, 1878 |
| Designer/Builder: | Various — See HAER documentation for individual structures |
| Present Use/Owner: | Various — See HAER documentation for individual structures |
| Engineer: | Eugene M. Farrelly, August 1996 |
| Project Information: | Three iron bowstring bridges, built by three Ohio bridge fabricating companies in the 1870s, were selected for engineering analysis and evaluation based on modern structural theory and structural theory as it was known at the time the bridges were constructed.<br><br>This report is part of the Iowa Historic Bridges Recording Project II, conducted during the summer of 1996 by the Historic American Engineering Record (HAER). Dr. Dario Gasparini, Professor of Civil Engineering, Case Western Reserve University, Cleveland, Ohio, with assistance of civil engineering students Eugene M. Farrelly and Dawn M. Harrison, completed this report under contract with HAER.<br><br>(continued) |

Project Information (continued):

See HAER No. IA-19 for documentation of the Freeport Bridge (1878) and its fabricator, the Wrought Iron Bridge Company of Canton, Ohio.

See HAER No. IA-58 for documentation of the Fremont Mill Bridge (1873) and its fabricator, the Massillon Bridge Company of Massillon, Ohio.

See HAER No. WY-1 for documentation of the North Platte River Bowstring Truss Bridge (1875) and its fabricator, the King Bridge and Manufacturing Company of Cleveland, Ohio.

## INTRODUCTION

Llewellyn N. Edwards spent most of his life studying and designing bridges. In 1952, his wife posthumously published a manuscript which had been his life's work: a catalogue of his knowledge, understanding, and experience in the art of bridge building. In that book, Edwards wrote that "the engineer historian gathers a meed of satisfaction and pleasure in tracing the progress made by predecessors in his art; reviewing their accomplishments; analyzing their solutions of problems; and examining the monuments of their industry and skill."[1] His words more than adequately describe the reasons for engineers to study engineering history.

The general objective of this report is to provide an engineering perspective to HAER's effort to document America's bridges. In particular, this report complements HAER's Iowa Historic Bridge Recording Project II with an engineering analysis of three iron bowstring bridges: the Fremont Mill Bridge in Anamosa, Iowa, built by the Massillon Bridge Company of Massillon, Ohio, in 1873 (Figure 1); The Fort Laramie Bridge near Laramie, Wyoming, built by the King Iron Bridge and Manufacturing Company of Cleveland, Ohio, in 1875 (Figure 2); and the Freeport Bridge in Decorah, Iowa, built by the Wrought Iron Bridge Company of Canton, Ohio, in 1878 (Figure 3).

This engineering study applies modern structural theory to the three bridges to assess the lateral stability of their respective top chords and to determine their overall behavior under various static loading conditions.

This report then summarizes and interprets the structural analysis results and makes some observations on the bowstring bridge as a structural form.

The engineering evaluation of bridges requires an understanding of the technology that existed at the time they were built. Structural theory has changed dramatically in the 120 years since bowstring bridges were constructed, and so another focus of the report is reviewing the bowstring design in light of late nineteenth-century structural engineering knowledge.

A complete contextual evaluation of the bowstring design is not attempted. Rather, suggestions are made for additional historical and engineering studies of bowstring bridges.

To meet these objectives, the report is organized into ten sections:

- The conceptual design section introduces some engineering principles that are central to the study of bowstring bridges.
- The next section provides a detailed description of current models used for the lateral stability study of the bridges' top chords.

- The third section is a review of the bowstring patented by Squire Whipple in 1841. Since Whipple's bowstring bridge was the first to be built in America, it is appropriate to begin the study of bowstring bridges with the original design.
- The fourth section briefly summarizes previous studies on the marketing, design, fabrication, and construction of bowstring bridges. The three iron bowstring bridges are then discussed in light of the conceptual design issues.
- Each of the three bowstring bridges is described in its own section.
- Results of the lateral stability and static behavior studies are summarized, and the quantitative results are discussed.
- The report concludes with suggestions for further studies and appendices.

## CONCEPTUAL DESIGN

One of the most important conceptual design issues for bridges is the height-to-span ratio. The height-to-span ratio of a truss bridge determines the maximum force that exists in the top and bottom chords of the structure and determines its overall stiffness, namely the force required at mid-span to cause a unit vertical displacement.

Typical height-to-span ratios for bridges range from 1/10 to 1/20. A good design uses a height-to-span ratio that minimizes the material used to carry the design load, within aesthetic and construction constraints.

Another conceptual design issue for bowstring bridges is the top chord's profile. This profile determines how the force in the top chord varies with position along the span. For example, every member in a parabolic top chord will experience almost the same force under a uniform loading. In contrast, the end members of a horizontal top chord, such as that in a Pratt truss, carry much less force than the center members under a uniform loading.

There are advantages to having one particular profile over another. For example, since every member of a parabolic top chord experiences approximately the same force, the cross-sectional area required to carry this force will be constant along the chord's length. A member of constant cross-sectional area is called prismatic.

In the case of a horizontal top chord, the forces vary. Therefore the minimum cross-sectional area required to carry these forces will also vary. The engineer's dilemma is whether to design an efficient top chord of varying cross section, which increases manufacturing costs, or an easily-produced prismatic top chord, which is an inefficient use of material.

Clearly, the parabolic top chord has the advantage of both efficient use of material and ease of production.

Bowstring bridges may be modeled and designed as tied arches (Figure 4) or as trusses (Figure 5). However, most bridge company designs were hybrids (Figure 6). All three models are statically indeterminate, meaning that more unknown forces exist than equilibrium equations to solve them.

Continuity of the top chord implies that some bending moments will exist in the chords. For a particular loading, bending moments may be small or large depending on:

- the relative magnitudes of the flexural and axial stiffness of the members;
- whether equilibrium can be satisfied for the particular loading solely by axial forces (which in turn depends on the dead-load pretension in the vertical and diagonal members);
- the connection details of the diagonals.

It is difficult to estimate such moments, and it is therefore unlikely that bridge company designers used bending moments to size the top chord.

Floor systems and panel lengths are additional conceptual design issues. The design of a bridge deck involves two competing requirements: minimization of the number of connections of the deck to the superstructure and the minimization of the weight of the floor system. Connections are costly to construct. Consequently, a cost-effective bridge design has a minimum number of connections. However, to minimize connections, the bridge must also have widely-spaced panel points. The greater the spacing, the deeper stringers and floor beams must be to safely carry bending moments. Deeper stringers add weight, thus increasing the bridge's cost (Figure 7). A good floor system design is a compromise between number of connections and panel lengths.

Another major conceptual design issue is the definition of design loads. A uniformly distributed live load and a moving concentrated load were typically considered in nineteenth-century bridge design. The magnitude of these loads depended on the type of traffic the bridge was expected to experience over its lifetime. Wind pressures and dynamic loads from moving vehicles were generally not considered significant.

The various loading conditions considered in this study are uniform dead load on the structure, uniform dead load plus a full-span live load of 3.83 kN/m$^2$ (80 psf), uniform dead load and half-span live load of 3.83 kN/m$^2$ (80 psf), and uniform dead load with a concentrated load of 25 kN (5.6 kips) at each of the interior panel points. Two turn-of-the-century publications, Milo Ketchum's *The Design of Highway Bridges* and Joseph Balet's *Analysis of Elastic Arches*, corroborate the use of 3.83 kN/m$^2$ (80 psf) as a standard design load for bridges at the time.[2] The concentrated dead load of 25 kN (5.6 kips) represents the effects of a carriage with a team of

horses on the bridge. Dead load computations are based on information collected from HAER drawings and field data.[3]

The final conceptual design issue is lateral stability of the top chords in bowstring bridges. For each bridge, the top chord experiences compressive forces under various loading conditions. There are limits, however, to the amount of compressive force that a structural member can take before it buckles.

Early nineteenth-century bridge designers were aware of the problem of lateral stability. Colonel Stephen Harriman Long addresses the issue of lateral stability as early as 1836, when he received a patent for lateral bracing of wooden frame bridges.[4] Squire Whipple's original 1841 patent realizes the need "to produce stiffness and sustain it [the top chord] against lateral flexure."[5] His solution was a chord composed of two arches joined at the crown and spread out at the abutments (Figure 18). Patents held by Joseph Davenport, Zena King, and David Hammond, the designers of the Fremont Mill Bridge, the Fort Laramie Bridge, and the Freeport Bridge, respectively, also address the issue of lateral stability.[6] Hammond's patent is almost obsessed with the issue of lateral stability, addressing it numerous times in his patent.[7]

To understand the concerns of the nineteenth-century bowstring bridge designers, it is first necessary to understand their notion of structural stability. As noted before, there are limits to the amount of compressive force that a structural member can resist before it begins to buckle. For example, consider a pin-ended column member subjected to a gradually increasing compressive force. The member will remain straight until a certain load is reached, called the critical buckling load, and then it will begin to bow. This "bowing" is the characteristic deformed shape taken by a pin-ended compression member when it becomes unstable. It can be described as a half-wave (Figure 8a).[8]

The amount of load the member can resist before buckling can be increased by bracing the member. The new buckling load will produce two half-waves with an inflection point at the brace. This process continues as more braces are added. Each additional brace allows the member to resist more load before it buckles. When the new buckling load is reached, the member deforms with a node at each brace (Figures 8b-8d).

The buckled mode shape depends on the rigidity of the braces. Generally, the characteristic half-wave deformed shape is observed only when the braces are perfectly rigid. In reality, most braces are elastic to a certain degree. A better model for the lateral stability of a compression member, taking into account brace elasticity, is shown in Figure 8e.

In bowstring truss bridges, the top chord is in compression. Consequently, it will behave in a similar manner to the above example of the column member. A certain level of compressive force can be carried by the chord before any instability occurs. However, once the critical

buckling load is reached, the chord will deform in the shape of a half-wave. If the chord is braced, the critical buckling load increases, and the deformed shape changes to two half-waves. In the case of a fully-braced top chord, the fundamental buckling mode will take the shape of a series of half-waves (Figure 9).

The question is now one of sufficient bracing. For a sound structure, it is necessary to brace it so that the critical buckling load is much greater than any load the structure will experience.

In bridge design, three classic approaches are typically used to provide lateral bracing to chord members subject to compressive forces: outriggers, portal frames along the length of the span, and horizontal trusses with end portal frames (Figure 10).

Late nineteenth-century iron bowstring bridges had to rely mainly on outrigger bracing systems because of clearance issues. Because of a bowstring bridge's arched top chord, neither portal frames nor an overhead horizontal truss could be used near the ends of the span. However, in some longer spans, the height is great enough near the parabolic chord's vertex to allow overhead bracing. Both the Fremont Mill Bridge and the Fort Laramie Bridge employ outrigger braces in addition to some overhead bracing near mid-span. The Freeport Bridge is large enough to accommodate portal frames.

Even though these bracing systems can be found on some bridges constructed in America in the early nineteenth century, it was not until the 1880s that the problem of lateral stability was mathematically modeled and truly understood by bridge engineers. How much bracing is needed in a structure? How can the lateral stiffness be quantified? What are the buckling loads and the buckled mode shapes for a structure? These are the concerns of lateral stability analyses. Bleich points out, "The problem of the elastically supported bar was investigated first by Engesser, who derived an approximate formula for the required stiffness of the elastic supports."[9] The work to which Bleich refers was conducted by Friedrich Engesser, a German engineer, who published his findings in 1884.[10]

## MODELS FOR STABILITY ANALYSES

Before the buckling load and the buckled mode shape for the bowstring bridge's top chord can be computed, it is first necessary to quantify the amount of bracing provided by outriggers or portal frames. Analytical models are developed for the outriggers used on the Fremont Mill Bridge and the Fort Laramie Bridge and for the Freeport Bridge's portal frames.

The analytical model used for computing the bracing provided by the outriggers in the Fremont Mill and Fort Laramie bridges is shown in Figure 11.

Two of the most important parameters governing the outrigger's effectiveness are its length, *b,* and height, *h.* (The tangent of the angle $\alpha$ is a measure of the relationship between the parameters *b* and *h.*)

If the outrigger height is increased and its length remains constant, the lateral stiffness of the outrigger is decreased. This is important because the height of a bowstring truss varies along its span. If the outriggers were designed to provide an equal amount of bracing at every point along the span, there should be some evidence of the outrigger length, *b,* varying in accordance with the height to maintain a constant angle $\alpha$.

However, uniform bracing cannot be achieved just by varying *b* and *h* together to maintain a constant angle $\alpha$. The effectiveness of the outriggers will still be diminished if member properties are not increased along with geometric parameters. In other words, as the lengths *b* and *h* increase, the outrigger member's cross-sectional area and the floor beam's sectional moment of inertia must also increase.

In order to model the outrigger brace's effect on the top chord's stability, it is only necessary to know the effective lateral stiffness of the joint where the brace and the top chord meet. In the model, this is represented by the top roller.

To compute this effective stiffness, an arbitrary force *F* is applied to the top joint. Structural analysis is then used to compute the horizontal deflection $\Delta$ at the joint resulting from the load *F.*[11] The effective joint stiffness is then computed by dividing the load *F* by the horizontal displacement $\Delta$.

This model overestimates the effectiveness of the outriggers because it assumes perfect connections that do not add flexibility, which is not true for actual structures. Another limitation of the model is that it ignores potential instability within the outriggers. Because of the slenderness of the outriggers, buckling of the outriggers themselves is an issue. However, for the purpose of completing the lateral stability study of the Fremont Mill and Fort Laramie bridge top chords, it is assumed that the outriggers are stable in compression and have perfect connections that do not add flexibility.

Since the Freeport Bridge uses portal frames for braces, another model is needed for lateral stability study of that bridge. The analytical model used for computing the bracing provided by the portal frames is shown in Figure 12.

As with the outriggers, the portal frame parameters must be varied in accordance with the height along the bowstring truss' top chord if uniform bracing is to be provided. In particular, this means changing the section properties of the column members along with the height along the span.

Again, the model assumes perfect connections and ignores potential member instability. Consequently, it is also an overestimate of the Freeport Bridge's actual bracing.

The effective joint stiffness provided by the portal frame is computed in a similar manner as it was for the outriggers. An arbitrary horizontal force $F$ is applied to the top (Figure 12), and the corresponding deflection $\Delta$ is computed from structural analysis. The effective joint stiffness is the force $F$ divided by the displacement $\Delta$.

Once the effective joint stiffnesses of the outrigger braces and portal frames are computed, it is possible to perform a lateral stability analysis of the bowstring bridges' top chords. The computed effective joint stiffnesses allow each top chord to be modeled as a single member with a series of orthogonal elastic braces in the horizontal plane (Figure 13).

The buckling load and the buckled mode shape are computed using several subroutines programmed into a mathematical software program.[12]

The model uses pinned-end boundary conditions at the ends of the top chords, i.e., the ends of the top chord have no freedom of horizontal and vertical movement, but do have freedom of rotation (Figure 14). Fixed-end boundary conditions, on the other hand, allow no horizontal, vertical, or rotational movement. The connection details in the HAER drawings of the bowstring bridges substantiate the use of pinned-end boundary conditions.[13]

The last remark to be made about lateral stability is more quantitative. Exactly how much lateral stiffness must be provided to the top chords of these bowstring bridges for them to be fully braced? Surprisingly, not much stiffness is needed. This fact is best illustrated by an example. Consider a fixed-end beam with a single brace (Figure 15).

The deformed mode shape for a fully-braced member is a series of half-waves. For this particular example, the fully-braced buckled mode shape would resemble Figure 16a. Without any bracing at all, the beam would deform as shown in Figure 16b, and Figure 16c shows the buckled mode shape for the partially-braced beam. The property of the beam that governs its stability is its slenderness ratio, defined as the beam's length, $l$, divided by the smallest radius of gyration of its cross section, $r$.

The radius of gyration of a cross section is defined as the square root of the quotient of its sectional moment of inertia, $I$, divided by its cross-sectional area, $A$:

$$r = \sqrt{\frac{I}{A}} \qquad (1)$$

The slenderness ratio quantifies what is intuitively known about buckling behavior of

members. If a members is relatively slender, it will buckle at a much smaller load than a member which is stocky. That is, members with a large *l/r* will buckle at smaller loads than those with a small *l/r*. Typical slenderness ratios for modern structural members range from 10 to 200.

Figure 17 shows the buckling load for a beam with a slenderness ratio of 100 as a function of the ratio of the axial stiffness of the beam to that of the brace. The results show that the brace's axial stiffness need only be 0.0026 times the beam's axial stiffness to brace the beam completely. In other words, less than one percent of the axial stiffness of the beam is needed to fully brace it against buckling.

It is therefore evident that braces need not be very stiff in order to be effective.

## WHIPPLE BOWSTRING

The first bowstring bridge in America was built over the Erie Canal by Squire Whipple in 1840.[14] The design, which Whipple patented in 1841, is basically a tied arch. The patent's major claim is for the unique construction of a segmental cast-iron arch and "wrought iron . . . thrust ties to sustain the thrust and prevent the spreading of the arch in case the abutments and piers be not relied on for the purpose."[15] The patent's second claim is for the top chord's unique construction. Whipple's design provides lateral stiffness to the top chord by making it wider at the ends than at the center (See Figure 18).

This original bowstring bridge design is significant for two reasons. First, as the prototypical bowstring bridge, it undoubtedly influenced subsequent designs. Second, Whipple was the first to "develop a scientific approach to bridge construction" by publishing two books on bridge engineering in the nineteenth century: *A Work on Bridge Building* (1847) and *An Elementary and Practical Treatise on Bridge Building* (1872).[16] Hence, an evaluation of the bowstring design in light of structural theory known at the time can be readily made. Whipple's books are concerned mainly with conveying a knowledge of forces in structures, sizing members to carry those forces, and comparing general aspects of different bridge designs that existed at the time.

In both books, Whipple analyzes a seven-panel arch truss similar to the bowstring he patented in 1841. The results of a modern structural analysis of the same seven-panel arch truss are compared with those published by Whipple in 1872 to assess his understanding of the structural behavior of bowstring trusses.

Member dimensions and geometry for the modern analysis are estimated from Whipple's 1872 book and a photograph (Figure 18) from an article by David Simmons.[17] The comparison is made with Whipple's 1872 book because his 1847 discussion of a seven-panel arch truss uses the geometry of a circular arc and not a parabolic arc. In both books, Whipple assumes the

diagonals of his truss will take no axial force under a uniform load. This is largely true, but only for a parabolic arc with single diagonals, and not for a circular arc. Whipple, in his 1872 book, revises the geometry to a parabola and thus validates his assumption for the uniform load condition.

Results of the modern structural analysis of the seven-panel arch truss agrees with results published in Whipple's 1872 book (Figure 19). There are some slight differences. Under a uniform loading condition, the diagonals of the truss actually do carry some forces, but those forces are small enough in comparison to the loading to consider them negligible.

Whipple then notes that the diagonals only take a substantial force under non-uniform loading conditions. However, Whipple's truss is statically indeterminate, meaning that all the member forces cannot be determined using only the nodal equilibrium equations. In order to reduce the truss to a statically determinate problem, Whipple assumes that some of the truss's diagonals take no force under the various non-uniform loading conditions.

Whipple offers the results from this portion of his analysis as a means for sizing the members of the truss conservatively, i.e., choosing members which can safely carry the forces. If the members that Whipple eliminated from his analysis are similarly removed in a modern structural analysis, the member forces agree again (Figure 20).

If the diagonals are present and the statically indeterminate truss is analyzed for the non-uniform load cases prescribed by Whipple, it is found that the diagonals that Whipple eliminated from his study would take compressive forces. But the diagonals of his truss were usually about 2.54 cm (1") in diameter and very long. Such slender members could not withstand much compressive force without buckling. Therefore, Whipple's assumption to delete these diagonals from his calculations is therefore appropriate.

Since the three bowstring bridges in this study have diagonals of similar dimensions, the forces derived on the basis of deleting compression diagonals from the calculations are more representative of the bridges' behavior under different loadings.

In addition to the slender diagonals buckling at small compressive forces, the elimination of compression diagonals is further substantiated by the diagonal connection details in the bowstring bridges. The diagonals were not designed to take compressive force. In Whipple's bowstring bridge, the Fremont Mill Bridge, and the Fort Laramie Bridge, the diagonals have no resistance to compressive forces. Because the diagonal members are secured with a nut on only the outside of each connection, they can only resist extension from tensile forces (Figures 21 and 22). The member is free to slip in the other direction, and therefore will not resist compressive forces. The Freeport Bridge diagonals are eye-bars connected in such a way that they could carry compressive forces, but not of any significant magnitude.

The only remaining issue before accepting the deletion of some diagonals from the static analysis of bowstring bridges is that of prestressing. Two questions arise:

- Does the structure's dead load provide enough tensile prestressing for the diagonals to remain in tension despite whatever compressive forces are induced by non-uniform loading conditions?
- Can the diagonals be prestressed so as to preclude compressive forces in the diagonals?

The answer to both questions is no. Results from modern structural analysis reveal that pretensioning from dead loads is in fact too small to keep the diagonals in tension. As for pretensioning the diagonals by tightening the nuts of the connection, this might cause buckling in the slender vertical members of the structure. In light of this, elimination of compression diagonals is essential to a proper analysis of static behavior.

Whipple's 1847 method for sizing compression members does account for slenderness much in the same way that members are sized today. Whipple gives allowable stresses for a compression member whose length is expressed as an integral multiple of its diameter, i.e., member length divided by member diameter. His 1872 book gives an allowable stress of 233 MPa (33 ksi) for a wrought iron rod whose length is only twice its diameter and an allowable stress of 0.4 MPa (5 ksi) for a wrought iron rod whose length is forty times its diameter.

In contrast, modern theory determines the allowable stress for compression members based on the square of the ratio of the member length to the smallest radius of gyration of the member. Dimensionally, the radius of gyration has units of length. Modern theory determines allowable stresses by a ratio of lengths, similar to Whipple's 1847 book. For steel with a yield point of 252 MPa (36 ksi), modern standards set by the American Institute for Steel Construction (AISC) place allowable stresses at 151 MPa (21.56 ksi) for a slenderness ratio of 1, or 26 MPa (3.73 ksi) for a slenderness ratio of 200.[18]

As for the dimensioning of tensile members, Whipple's book mentions that "a bar of good wrought iron an inch square will sustain a positive strain of about 60,000 lbs. on the average," and the allowable stress was typically one-fourth of the tensile strength.[19] The AISC prescribes that tensile members carry no more stress than half of the ultimate strength of the material, nor 0.6 times its yield strength, which is typically 252 MPa (36 ksi).[20]

Whipple's 1872 book is an indication of the structural knowledge that existed at the time the Fremont Mill Bridge, the Fort Laramie Bridge, and the Freeport Bridge were constructed. However, there is no direct link except for the parabolic top chords between Whipple's 1872 publication and the designs of these bridges.

## BOWSTRING TRUSSES OF BRIDGE COMPANIES

The history of the bowstring truss is inextricably linked to the nineteenth century bridge companies. Bridge companies, though now a thing of the past, loomed as giants in the late nineteenth century. Improvements in the iron industry and westward expansion are two major events responsible for their rise.[21]

Once the West was settled, a network of farm-to-market roads created the need for thousands of bridges. As iron became more cost-effective, it began to challenge wood as a fundamental bridge-building material.[22] However, knowledge of material behavior was relatively esoteric.[23] Though bridge-building was in demand, there were no design specifications at the time. Bridge companies took advantage of this window of opportunity by creating their own proprietary, prefabricated bridges.

It was well known that the bowstring design offered great strength for a minimum amount of material.[24] But the peculiarities of the design were not easily mastered. Exactly how much strength for how little material was the question for every bridge company, and the late-nineteenth century saw a flurry of activity to find the answer.

Success depended not only on fabrication, but also on shipping and erection.[25] The successful bridge company found a shrewd way to master all three.

Several chord designs emerged over the years. Companies struggled with different designs trying to find a balance between structural integrity, manufacturing ease, and material economy.

Thomas Moseley of the Moseley Bridge Company of Cincinnati, Ohio, made a tubular bowstring girder, triangular in section, from two pieces of boiler plate. One pate was bent for the legs of the isosceles triangle.[26] The manufacturing time spent in bending the plate led him to change to a three-plate triangular section.

Zenas King, founder of the King Iron Bridge and Manufacturing Company and former employee of Moseley, was partial to a tubular girder composed of channel sections and boiler plate in a box formation.[27] His 1861 patent proposed non-prismatic chords (chords whose cross-sectional properties vary along the length of the member) in the interest of structural safety. It was six years before he was convinced of the manufacturing ease of a prismatic chord.[28]

Once a fundamental balance between design and manufacturing was well-established, the bridge companies sold their product through agents and with catalogs. These catalogs contained pictures and statistics of their products to entice communities to buy.[29]

Much of the success of the King Iron Bridge Manufacturing Company was due to King's business savvy.[30] He established a network of representatives in key cities in the west, that was unparalleled by any other company.[31] Representatives kept abreast of bridge needs in communities large and small, and maintained a steady stream of business.

## COMPARISON OF CONCEPTUAL DESIGNS

Despite the uniqueness of each of the bowstring bridges in this study, there are some similarities in their conceptual designs. Two distinct similarities are the height-to-span ratios of the bridges and the profile of their top chords. The height-to-span ratio of the Fremont Mill, Fort Laramie, and Freeport bridges are 1/8.7, 1/9.3, and 1/7.4 respectively. One indication of a structure's stiffness is the ratio of the mid-span live load deflection to the span length. Typically, if this ratio is lower than 1/400, the structure is quite rigid. Vertical mid-span deflections under a full-span live loading of 3.83 kN/m$^2$ (80 psf) are computed by modern structural analysis. The resulting deflection/span ratios for the Fremont Mill Bridge, the Fort Laramie Bridge, and the Freeport Bridge are 1/421, 1/673, and 1/615 respectively. All of these ratios are smaller than 1/400, so the bowstring bridges actually are quite stiff.

The other significant conceptual design similarity is the top chord profile of the bowstring bridges. All three bridges employ a parabolic top chord of similar parabolic geometry. Equations are fit to the coordinates of each bridge's top chord. In the following equations:

$x$ = distance along span from left-hand support
$y$ = height above bridge deck

Fremont Mill Bridge:

$y = -0.011769x^2 + 0.457091x + 0.005265$ m
($y = -0.003588x^2 + 0.457091x + 0.017271$ ft)

Fort Laramie Bridge:

$y = -0.011252x^2 + 0.428558x - 0.0052$ m
($y = -0.00343x^2 + 0.428558x - 0.017057$ ft)

Freeport Bridge:

$y = -0.011096x^2 + 0.539978x + 0.006433$ m
($y = -0.003383x^2 + 0.539978x + 0.021102$ ft)

The parabolic geometry specified by Whipple in his 1872 book is different from that of all three bridges in this report.[32] However, the similarities of the $x^2$ and $x$ term coefficients in the above equations suggest possible design imitations among the bridge companies that manufactured bowstring bridges.

Other conceptual design similarities include the floor systems and panel lengths. All the bridges, as originally built, had decks of wooden planks fastened to wooden stringers which rested on iron girders supported by the lower chords. The three bridges, however, employ different girder sections. The Fort Laramie Bridge contains wide-flange girders, the Fremont Mill Bridge employs girders of the same gas-pipe and boiler-plate Howe truss used in the top chord, and the Freeport Bridge has tapered girders composed of angles, tee sections, and iron plate.

The number of panels used for a given span are similar as well. The Fremont Mill Bridge and the Fort Laramie Bridge both have spans of about 38 m (125'). The Fremont Mill Bridge has 16 panels with irregular lengths that vary from 1.12 m (3.67') to 2.74 m (9'). The Fort Laramie bridge uses 14 panels for the same span, having panel lengths ranging from 2.16 m (7') to 3.023 m (10').

Recalling the trade-off between dead load and panel length, it is not surprising that the two bridges using the same number of panels for the same span have approximately the same ratio of dead weight to deck area. The dead load of the Fremont Mill Bridge is 225 kN (51 kips), and the Fort Laramie weight is 163 kN (37 kips). However, Fremont Mill Bridge has a wider deck than the Fort Laramie Bridge, 4.93 m (16') to 3.66 m (12') respectively. The ratio of dead weight to deck area is 1.17 kN/m$^2$ (0.025 kips/ft$^2$) for both the Fremont Mill and Fort Laramie bridges.

In comparison, the Freeport Bridge has a 48.66 m (160') span, and only 12 panels, with lengths around 4 m (13'). It is 4.88 m (16') wide, with a dead load of 241 kN (54 kips). Generally, the compromise for fewer panels and fewer connections is a greater dead load. However, when divided by the deck area, the normalized dead load is 1.01 kN/m$^2$ (0.021 kips/ft$^2$), which is less than the other two bridges.

The reason for the apparent inconsistency may be the design of the four center panels of the bridge (Figure 23).

Hammond decreased the dead load of the Freeport Bridge by adopting a method of construction developed by Job Abbott, a patent attorney from Canton who became the chief engineer of the Wrought Iron Bridge Company in 1872.[33] Abbot's patent reduces the amount of material used in the bridge by letting the diagonals span two panels and replacing vertical posts with "suspension rods . . . [that] serve as supports for the chords midway between the posts."[34]

His slender suspension rods weigh less than the other vertical posts, but they experience stresses as high as 150 MPa (21.5 ksi) under a full live load condition (Appendix D).

The most noticeable difference between the three bridges is the cross-sectional design of their top chords (Figure 24).

**Table 1.** Cross-sectional properties of the Fremont Mill, Freeport, and Fort Laramie bridges' top chords.

| | **Fremont Mill** | **Freeport** | **Fort Laramie** | |
|---|---|---|---|---|
| $A$ | 0.00774<br>12.0 | 0.01135<br>17.60 | 0.01089<br>16.88 | $m^2$<br>$in^2$ |
| $I_X$ | $2.81 \times 10^{-4}$<br>676.0 | $6.52 \times 10^{-5}$<br>156.60 | $8.17 \times 10^{-5}$<br>196.24 | $m^4$<br>$in^4$ |
| $r_X$ | 0.191<br>7.51 | 0.076<br>2.98 | 0.087<br>3.41 | m<br>in |
| $I_Y$ | $2.66 \times 10^{-5}$<br>64.0 | $1.11 \times 10^{-4}$<br>266.1 | $9.78 \times 10^{-5}$<br>234.92 | $m^4$<br>$in^4$ |
| $r_Y$ | 0.059<br>2.31 | 0.099<br>3.89 | 0.095<br>3.73 | m<br>in |

There are two issues to be discussed concerning the cross sections: stress and lateral stability. The stress on a member is a combination of the axial forces applied to the member and the bending moments experienced by the member. The total stress is determined by the algebraic sum of two terms. The first term is the axial force, $N$, divided by the area, $A$; the second is the product of the bending moment, $M_X$, with half of the section depth, $y$, divided by the moment of inertia about the x-axis (the strong axis), $I_X$:

$$Stress = \sigma = \frac{N}{A} + \frac{M_X\, y}{I_X} \qquad (2)$$

While the combined stress equation (Equation 2) was undoubtedly a tenet of structural knowledge of the time, it is not likely that the designers of these bowstring bridges ever computed the stresses due to bending moments in their structures. The reason for this is that exact analysis of plane frames with rigid joints is more difficult than for trusses.

Allowable stresses for compression members at the time were a function of the ratio of a member's length to its "diameter". They were typically on the order of 70 to 105 MPa (10 to 15

ksi). The axial stresses for each design are computed and discussed in the following sections on the three bowstrings.

The other issue regarding the cross sections is lateral stability. The lateral stability of the top chord is a function of the moment of inertia about the y-axis, or the weak axis. If this moment of inertia is large, the lateral stiffness of the cross section is better and its buckling load is higher. Consequently the amount of bracing needed to prevent buckling is much larger. From the standpoint of lateral stability, the Hammond top chord design is the most rigid. Of the three top chord designs (Figure 24), it has the largest moment of inertia about the y-axis. A visual inspection of the three cross sections confirms the rigidity of the Hammond chord, which is the widest of the three sections.

The stiffness of the Hammond design is not surprising; patents reveal that Hammond was keenly aware of the issues of lateral stability in bowstring bridges. In fact, in an effort to achieve even greater lateral rigidity in the top chord, his 1873 patent even proposes a top chord formed by placing two chords with the cross section shown in Figure 24 side by side.[35] However, as Clayton B. Fraser points out in the 1986 HAER study of the Freeport Bridge, no bowstring bridges using that design were ever fabricated.[36]

The last conceptual design similarities between the bridges are the connection details. In all three bridges, the connection details do not allow for force transfer from the diagonals to the bottom chord. In the Fort Laramie Bridge and the Fremont Bridge, the diagonals' lines of action meet outside of the bottom chord (Figure 22). In the Freeport Bridge, the diagonals connect to straps that are fastened on top of the tapered floor beams (Figure 25). Again, in that design, the lines of action meet outside the bottom chord, providing no means for stress transfer. These connection details decrease the effectiveness of the diagonals and the strength of the bridges.

**FREMONT MILL BRIDGE**

In the HAER study of the Fremont Mill Bridge, Geoff H. Goldberg points out that one of the major disadvantages of the late nineteenth-century bowstring bridge designs was that the top chord for each bridge required a unique curve for each span.[37] This variety of curves created manufacturing and mass production problems. In contrast, the Pratt trusses also being built at the same time did not have this problem. With the design patented by Thomas and Caleb Pratt in 1844, "Bridges of various spans could be accommodated by adding additional panels."[38] In designing the top chord of the Fremont Mill Bridge, Joseph Davenport created a combination of the two popular structural forms.

Davenport's top chord design does not draw on ideas of the Pratt truss but instead employs the principles of the Howe truss, patented by William Howe in 1840. The top chord of the Fremont Mill Bridge consists of a series of Howe truss panels with gas pipe for braces and

boiler plate for top and bottom chords. The gas-pipe braces are not fastened to the boiler plate, but are held in place on cast iron shoes by compressive forces induced by pretensioning the threaded rods (Figure 26).

In his 1867 patent, Davenport sought no recognition for the innovations patented by Howe in 1840: "I do not claim as my invention the shoes, arch shoes, angle irons, suspension rods, chords, nor any of the bolts taken separately, as all these have been before used."[39] Rather, his claim was based on his application of the well-known Howe design to the top chord of a bowstring bridge.

Despite its manufacturing advantages, the top chord design is responsible for some unusual static behavior in Fremont Mill Bridge. First, it should be pointed out that the Fremont Mill Bridge is asymmetric (Figure 27). The center vertical does not coincide with the structure's geometric center.

In fact, the bridge's geometric center coincides with a tension rod of a Howe panel in the top chord. Consequently, the center vertical of the bridge must be moved to the middle of one of the adjacent Howe panels to eliminate connection difficulties. The consequence is an asymmetric structure and local bending of the boiler plates. The difference in the width of the two center panels of the structure is about 0.4 m (15.75"), which is the length of one of the Howe panels in the top chord.

The next question is how the structure's asymmetry affects its behavior. Under a uniform full-span live load condition of 3.83 kN/m$^2$ (80 psf), the diagonals of the Fremont Mill Bridge experience substantial forces (Appendix B). For example, one diagonal carries a force of 64.25 kN (14.44 kips).

The Fremont Mill Bridge definitely behaves more like a tied arch than a truss. That is, the top chord carries significant bending moments because its moment of inertia about the strong axis, $I_X$, is comparatively large (Figure 24). Static analyses confirm that those bending moments are indeed significant, sometimes contributing up to 40 percent of the stress experienced by the top chord (Appendix B). Moments are largest at the ends of the top chord, where the combined stresses from both axial forces and bending moments are as high as 216 MPa (31 ksi).

Aside from the top chord, connections of the Fremont Mill Bridge's diagonals also indicate that tied-arch behavior is dominant. The diagonals are poorly connected for transferring forces to the top and bottom chords. In the top chord detail, the diagonals cause local bending in the boiler plates because their connection is eccentric from the panel points (Figure 28).

In the bottom chord detail (Figure 24), there is no positive means for force transfer to the bottom chord. Because the diagonals are not very effectively connected, the Fremont Mill Bridge is essentially a tied arch.

Static analyses of the Fremont Mill Bridge for a live load of 3.83 kN/m$^2$ (80 psf) show that the lower chord experiences intolerably high stresses, on the order of 270 MPa (39 ksi). Stress values of this magnitude are not allowed in iron. Therefore it is likely that the design load used by Joseph Davenport for the Fremont Mill Bridge was much smaller than 3.83 kN/m$^2$ (80 psf).

Indeed, the lower chord of the Fremont Mill Bridge has less area than the lower chords of both the Fort Laramie Bridge and the Freeport Bridge. The cross-sectional area of the lower chords of both of those structures are 5.16 x $10^{-3}$ m$^2$ (8 in$^2$), whereas the lower chord of the Fremont Mill Bridge has a cross-sectional area of only 3.87 x $10^{-3}$ m$^2$ (6 in$^2$).

The high stresses in the lower chord are not the only evidence that a smaller design load may have been used for the Fremont Mill Bridge. The stresses in the top chord due to axial forces are very high in comparison with allowable stresses of the time. The stresses of 136 MPa (19.4 ksi) fall outside of the range, 70 MPa (10 ksi) to 105 MPa (15 ksi), typically used in late nineteenth-century design of compression members.

Lastly, the lateral stability study of Davenport's bridge suggests that a smaller design load was used. The critical buckling load for the top chord is 873 kN (196 kips). The small buckling load is related to the fact that the top chord has a very small moment of inertia around the weak axis, $I_y$. Under a full-span live load of 3.83 kN/m$^2$ (80 psf), the maximum force in the top chord is 1053 kN (237 kips). In other words, under a full-span live load of 3.83 kN/m$^2$ (80 psf), the Fremont Mill Bridge would buckle. If a full-span live load of 2.87 kN/m2 (60 psf) were used, the maximum force in the top chord would only be 856 kN (192 kips), a value which essentially equals the critical buckling load.

Even assuming a design live load of 1.92 kN/m$^2$ (40 psf), the ratio of the buckling load to the axial compressive force in the top chord is only about 1.3, which is a relatively small factor of safety against lateral instability.

The buckling loads and corresponding buckled mode shapes for the Fremont Mill Bridge (Figure 29) are compared to buckled mode shapes obtained from a parametric study of the bracing stiffnesses. Buckling loads and buckled mode shapes for the Fremont Mill Bridge are found for outriggers 25, 75, 125, and 175 percent as stiff as those which actually exist in the structure.

The object of a parametric study of the lateral bracing system is to determine the sensitivity of the buckling loads to the bracing systems — to resolve the issue of how much lateral bracing is necessary to produce a different buckled mode shape. By quantifying the amount of bracing needed to produce a more laterally stable structure, it is possible to evaluate the efficiency and economy of the lateral bracing system used.

For the Fremont Mill Bridge, the lateral bracing is sufficient to induce a buckled mode shape of four half-waves (Figure 29). Three half-waves characterize the buckled mode shape at 75 percent of the actual outrigger stiffness, and a four-half-wave buckled mode shape is still present at 175 percent of the actual bracing provided by the outriggers.

It should be pointed out that the Fremont Mill Bridge outriggers are not designed to provide a uniform stiffness along the length of the top chord. The member properties of the outriggers do not vary at all, and the outrigger length (Figure 11) does not vary with the height. The result is that the stiffness of the bracing is significantly smaller at the structure's center. However, results from static analysis show that the largest axial forces and moments occur at the ends of the top chord. Consequently, the most bracing is needed at the ends, and the outriggers of the Fremont Mill Bridge actually provide the greatest bracing at the ends.

## FORT LARAMIE BRIDGE

The Fort Laramie Bridge, built in 1875, is representative of the tubular bowstring type built by Zenas King late in his career. King had no formal training in engineering, and his early patents reflect this.[40] His original tubular bowstring bridge patent in 1861 has a greater cross-sectional area at the crown of the arch than at the ends, a design which "renders the structure less liable to fracture."[41] The apparent concern of King was the fracturing of the center of the bowstring under maximum bending stresses at mid-span.[42] In fact, the maximum bending stresses occur in a bowstring at the ends of the top chord (Appendix C). After being enlightened to this knowledge by some worker, King redesigned his chord to place more cross-sectional area at the ends and received a patent for such in 1866.[43] The following year, King patented a prismatic chord under the suggestion of employee Cyrus G. Force, a trained civil engineer. It was with this design that King created a company able to fabricate a bridge in Cleveland, Ohio, and send it all the way out to Laramie, Wyoming, at the mere cost of $25.00 per foot.[44]

Like the Fremont Mill Bridge, the Fort Laramie Bridge is a tied arch; the top chord is continuous and carries significant bending moments (Appendix C). Unlike the Fremont Mill Bridge, the stresses in the lower chord are not unreasonable. The maximum stress under a full-span live load of 3.83 kN/m$^2$ (80 psf) is 156 MPa (22 ksi), below the allowable limit for iron.

The critical buckling load in the top chord is calculated to be 1383 kN (311 kips), and the largest force under the 3.83 kN/m$^2$ (80 psf) live load is 853 kN (192 kips), as shown in Appendix

C. Therefore, the factor of safety against lateral instability is approximately 1.6, which is similar to the factor of safety against yielding in the bottom chord.

Unlike Davenport's design for the outriggers of the Fremont Mill Bridge, King increases the outrigger length (Figure 11) with the increase in height along the length of the top chord. In fact, he maintains a constant outrigger angle $\alpha$ of 70 degrees. But he does not vary the depth of the floor girder or increase the area of the outrigger member to provide uniform bracing to the entire structure.

Much like the Fremont Mill Bridge, the outriggers of the Fort Laramie Bridge provide diminishing lateral stiffness to the top chord towards the crown. The fundamental buckled mode shape of the Fort Laramie Bridge (Figure 30) has only two half-waves, whereas the chord of the Fremont Mill Bridge has three (Figure 29). The weak-axis moment of inertia of the King chord is much greater than the weak-axis moment of inertia of the Davenport chord; therefore the lateral bracing stiffness required to achieve a three-half-wave buckled mode shape is greater for the King bowstring.

A parametric study varying the outrigger stiffness shows that with a 25 percent increase in the original stiffness provided by the braces, a buckled mode shape having three half-waves occurs (Figure 30).

Nonetheless, King's bracing provides a factor of safety against lateral instability commensurate with the factor of safety against yielding of the bottom chord, for a live load of 3.83 kN/m$^2$ (80 psf).

**FREEPORT BRIDGE**

It has been said that "Whipple may have invented the bowstring, but no other inventor in nineteenth century America did as much as David Hammond to perfect the form."[45] This distinction is substantiated by the sixteen bridge patents that were produced by the Wrought Iron Bridge Company in the 1860s and 1870s under Hammond's guidance.[46]

Hammond's 1873 patent was the basis for the thousands of bowstring bridges built by the Wrought Iron Bridge Company in North America.[47] It contained six pages of drawings alone and twenty individual claims, which gives a sense of his bowstring bridge design's complexity.

The most noticeable feature of the Freeport Bridge is its detailing. There are a number of different members used in the structure: asymmetric tees, angles, square rods, circular rods, tapered floor beams, and, of course, a tubular arch. The bridge's floor beams even have cast-iron end plates embossed with eight-pointed stars to enhance the bridge's overall aesthetics.

The question of overall design efficiency naturally arises from such an array of members. Is there some rational basis for the design of each member? Or is there waste? Based on the consistency of factors of safety for member stresses, the design is not wasteful. However, it should be pointed out that the factors of safety are consistently low, a fact which suggests that a design load different from 3.83 kN/m$^2$ (80 psf) was used for the Freeport Bridge.

Just as with the Fremont Mill Bridge and the Fort Laramie Bridge, the static behavior of the Freeport Bridge is that of a tied arch. The diagonals are not connected for proper transfer of forces to the chords. While the bending moment stresses in the Freeport Bridge are almost 10 percent less than those in the other two bridges for the same full-span live load (Appendix D), they are still significant: 30 percent of the total stress in the top chord.

The lower percentage of stresses due to bending moments suggests higher axial stresses. Static analyses reveal that the stresses in the lower chord are high (Appendix D). For the full-span live load condition, the maximum stress in the lower chord is 204 MPa (29 ksi), which is close to the bottom chord's probable yield stress.

The critical buckling load also has a comparable factor of safety. The critical buckling load for the Freeport Bridge's top chord is 1418 kN (319 kips). The maximum force in the top chord is 1177 kN (265 kips) for a design load of 3.83 kN/m$^2$ (80 psf), making for a factor of safety of only 1.2 against buckling. With all of the concern that Hammond focused on stability, it is surprising that his factors of safety are not higher.

The dominant feature of the top chord's buckled-mode shape (Figure 31) is the long unbraced length that exists at each end of the top chord. This is not surprising, because the Freeport Bridge does not employ outriggers for bracing, but uses portal frames instead. Because of clearance issues, the portal frames could not be placed near the ends of the structure, but only toward the center. The consequence is a long unbraced length at each end of the top chord. This unbraced length has the most impact on the buckling load and the buckled mode shape. In fact, a parametric study varying the stiffness of the portal frame bracing system reveals virtually no change in the buckled mode shape. Clearly, the unbraced lengths at the ends is central to the instability behavior.

Ironically, of the bracing systems on the three structures, the Hammond portal frames have the greatest stiffness. Unfortunately, the nature of the portal frame design precludes their use at the ends of the top chord, where both the bending moments and axial forces are largest — an ideal location for buckling failures.

Despite the issue of the proper design load and the unbraced lengths at the ends of the top chord, the Freeport Bridge is a remarkably consistent design. The consistent factors of safety throughout the bridge indicate its overall design efficiency.

## EVALUATION OF DESIGNS

Despite the limitations in modeling and the uncertainty regarding design loads, it is possible to compare the designs of the three bowstring bridges and evaluate which is the most effective.

Given the findings of this report, it is most reasonable to conclude that King's Fort Laramie Bridge is the best design. The Fort Laramie Bridge had the smallest dead load 163 kN (37 kips) of the three bridges and a comparable span 38 m (125'). This suggests design efficiency.

The outrigger bracing system on the Fort Laramie bridge suggests a better understanding of the parameters governing lateral stability. King's bridge maintains a constant outrigger angle along the span, clearly indicating an attempt to provide uniform bracing along the span.

The outrigger angles on the Fremont Mill Bridge do not remain constant, suggesting that no attempt is made at uniform bracing. The long unbraced lengths at the ends of the Freeport Bridge's top chords (where bending moments are largest) cannot be considered a good design.

Lastly, the Fort Laramie Bridge has the largest factor of safety, 1.6, against bottom chord yielding and against top chord buckling. The Freeport Bridge, in comparison, has a factor of safety of only 1.2 against yielding and buckling, and the Fremont Mill Bridge has a factor of safety less than one for the assumed loading, indicating that the bridge was designed for smaller loads.

## SUGGESTIONS FOR FURTHER STUDY

Ambiguity about design loads used by the bowstring bridge companies must be resolved. A more complete description of the designer's rationale has yet to be formulated. Such a reconstruction might be possible from a study of historical documents.

There is still much to be done in the area of the contextual structural evaluation of the bowstring design. The quantity of structural knowledge the bowstring bridge designers actually possessed and used in their designs remains elusive. Again, historical documents may offer some assistance, but in the absence of such, the only recourse may be to conduct a survey of structures of different spans built by the same bridge company. Modifications in the design from one span to the next can reveal much about the structural knowledge of the designer.

Bowstring bridges fell into disuse by the 1880s. Diffusion of engineering and fabrication technologies, user demands for standardization, and the emergence of reinforced concrete changed perceptions regarding the strength, stability, durability, and relative economy of the

bridge company bowstring. Charting this change will not be easy, but as Llewellyn Edwards pointed out, "a meed of satisfaction" awaits the engineer historian at the end of such work.[48]

**ENDNOTES**

1. L. N. Edwards, *A Record of History and Evolution of Early American Bridges* (Orono: University of Maine Press, 1952). Although a bowstring bridge was built under Edwards' guidance as late as 1921, the book does not say much about the structural form.

2. Joseph W. Balet, *Analysis of Elastic Arches*, (New York: Engineering News Publishing, 1908), p. 214. Balet's section on design loads is reprinted from J. A. L. Waddell's *The Design of Ordinary Iron Highway Bridges.* Milo S. Ketchum, *The Design of Highway Bridges*, (New York: Engineering News Publishing, 1909), p. 514.

3. For computations of properties of some rolled shapes used in bowstring bridges, see Herbert W. Ferris, *Dimensions and Properties of Rolled Shapes, Steel and Wrought Iron Beams & Columns, as Rolled in the U.S.A., Period 1873 to 1952* (Chicago: American Institute of Steel Construction, 1953).

4. S. H. Long, U.S. Patent, January 23, 1836.

5. Squire Whipple, U.S. Patent No. 2,064 (April 24, 1841).

6. Joseph Davenport, U.S. Patent No. 72,611 (December 24, 1867). Phrases about the "great strength and rigidity" of the girder design are generally references to lateral stability. Zenas King, U.S. Patent No. 33,384 (October 1, 1861). David Hammond, U.S. Patent No. 135,802 (February 11, 1873).

7. Hammond, U.S. Patent No. 135,802.

8. Friedrich Bleich, *Buckling Strength of Metal Structures,* (New York: McGraw-Hill, 1952), p. 268.

9. Ibid., p. 269.

10. The article by Bleich references the following works by Engesser: "Die Sicherung offener Brücken gegen Ausknicken," *Zentralblatt der Bauverwaltung,* 1884, p. 415; 1885, p. 93; *Die Zusatzkräfte und Nebenspannungen eiserner Fachwerkbrücken,* vol. 2 (Berlin: 1893).

11. STAN2D is a structural analysis program for the linear elastic analysis of plane frames. It assembles the linear elastic element stiffness matrix, modifies it for known forces and displacements, and solves for force unknowns.

12. The subroutines of the Mathematica code used for the lateral stability analysis use the geometric stiffness matrix approximation to the non-linear secant stiffness matrix. The geometric stiffness matrix approximation gives good results and is easier to compute than

the secant stiffness matrix. The complete code is included in Appendix A along with an example of how the program is used to determine the buckling load and buckled mode shape of the Freeport Bridge's top chord.

13. As the length of a member increases, the effects of the boundary conditions on its critical buckling load diminish, as is the case with bowstring bridges' long chords. However, the Mathematica code was modified for fixed-end boundary conditions and tested on the Fremont Mill Bridge. The buckling load is 885 kN (199 kips) for the fixed-end condition and 873 kN (196 kips) for the pinned-end condition, less than 2 percent difference.

14. David A. Simmons, "Engineering and Enterprise: Early Metal-Truss Bridges in Ohio," *Timeline,* vol. 2, no. 1 (February-March 1985): 21.

15. Whipple, U.S. Patent No. 2,064.

16. Simmons, "Engineering and Enterprise," p. 20. Squire Whipple, *A Work on Bridge Building*, (Utica: H. H. Curtiss, 1847), *An Elementary and Practical Treatise on Bridge Building*, (New York: D. Van Nostrand, 1872).

17. Whipple, *An Elementary and Practical Treatise on Bridge Building*, p. 67. Simmons, "Engineering and Enterprise," p. 21.

18. American Institute of Steel Construction, *Manual of Steel Construction, Allowable Stress Design*, 9th ed. (Chicago: AISC, 1989), p. 3-16.

19. Whipple, *A Work on Bridge Building,* p. 52.

20. American Institute of Steel Construction, *Manual of Steel Construction,* p. 5-133.

21. Eric DeLony, "Surviving Cast- and Wrought-Iron Bridges in America," *Industrial Archeology,* vol. 19, no. 2 (1993): 17.

22. David A. Simmons, "Bridge Building on a National Scale: The King Iron Bridge and Manufacturing Company," *Industrial Archeology,* vol. 15, no. 2 (1989): 23.

23. DeLony, "Surviving Cast- and Wrought-Iron Bridges in America," p. 20.

24. David A. Simmons, "Bridges and Boilers: Americans Discover the Wrought-Iron Tubular Bowstring Bridge," *Industrial Archeology,* vol. 19, no. 2 (1993): 63.

25. Ibid.

26. Ibid., p. 67.

27. Simmons, "Bridge Building on a National Scale," p. 25.

28. Ibid., p. 26.

29. Clayton B. Fraser in U.S. Department of the Interior, Historic American Engineering Record (HAER), No. IA-19, "Freeport Bridge," 1985, p. 11, Prints and Photographs Division, Library of Congress, Washington, D.C.

30. Simmons, "Bridge Building on a National Scale," p. 23.

31. Ibid., p. 31.

32. Whipple, *An Elementary and Practical Treatise on Bridge Building,* p. 31. The top chord of Whipple's seven-panel arch truss has the following equation: $y/v = 1/12*(x/h)^2 - 1/48$. At a height-to-span ratio of 1:10, this becomes $y = -0.0408x^2 + 0.0208$, quite different from the other bowstring bridges in the study.

33. David A. Simmons, "Uncommon Wrought-Iron Bridge in Morrow County," *Ohio County Engineer,* Spring 1992, pp. 12-13.

34. Job Abbott, U.S. Patent No. 184,490 (November 21, 1876).

35. Hammond, U.S. Patent No. 135,802.

36. Fraser, "Freeport Bridge," p. 9.

37. Geoffrey H. Goldberg in U.S. Department of the Interior, Historic American Engineering Record (HAER), No. IA-58, "Fremont Mill Bridge," 1995, p. 8, Prints and Photographs Division, Library of Congress, Washington, D.C.

38. Ibid., p. 9.

39. Davenport, U.S. Patent No. 72,611.

40. Simmons, "Bridge Building on a National Scale," p. 23.

41. King, U.S. Patent No. 33,384.

42. Simmons, "Bridge Building on a National Scale," p. 24.

43. Ibid., p. 26. Zenas King, U.S. Patent No. 58,266, (September 25, 1866).

44. Dan Clement in U.S. Department of the Interior, Historic American Engineering Record (HAER), No. WY-1, "North Platte River Bowstring Truss Bridge," 1995, p. 3, Prints and

Photographs Division, Library of Congress, Washington, D.C.

45. Fraser, "Freeport Bridge," p. 18.

46. Simmons, "Uncommon Wrought-Iron Bridge in Morrow County," p. 12.

47. Hammond, U.S. Patent No. 135,802.

48. Edwards, *A Record of History and Evolution of Early American Bridges.*

**SOURCES CONSULTED**

Abbott, Job. U.S. Patent No. 184,490 (November 21, 1876).

American Institute of Steel Construction. *Manual of Steel Construction, Allowable Stress Design.* 9th ed. Chicago: AISC, 1989.

Balet, Joseph W. *Analysis of Elastic Arches.* New York: Engineering News Publishing, 1908.

Bleich, Friedrich. *Buckling Strength of Metal Structures.* New York: McGraw-Hill, 1952.

Davenport, Joseph. U.S. Patent No. 72,611 (December 24, 1867).

DeLony, Eric. "Surviving Cast- and Wrought-Iron Bridges in America." *Industrial Archaeology,* vol. 19, no. 2 (1993).

Edwards, L. N. *A Record of History and Evolution of Early American Bridges.* Orono: University of Maine Press, 1952.

Engesser, Friedrich. "Die Sicherung offener Brücken gegen Ausknicken." *Zentralblatt der Bauverweltung,* 1884, 1885.

_____. *Die Zusatzkräfte und Nebenspannungen eisener Fachwerkbrücken.* Vol. 2. Berlin: 1893.

Ferris, Herbert W. *Dimensions and Properties of Rolled Shapes, Steel and Wrought Iron Beams & Columns, as Rolled in the U.S.A., Period 1873 to 1952.* Chicago: American Institute of Steel Construction, 1953.

Hammond, David. U.S. Patent No. 135,802 (February 11, 1873).

Ketchum, Milo S. *The Design of Highway Bridges.* New York: Engineering News Publishing, 1909.

King, Zenas. U.S. Patent No. 33,384 (October 1, 1861).

_____. U.S. Patent No. 58,266 (September 25, 1866).

Long, S. H. U.S. Patent, January 23, 1836.

Simmons, David A. "Bridge Building on a National Scale: The King Iron Bridge and Manufacturing Company." *Industrial Archaeology,* vol. 15, no. 2 (1989).

_____. "Bridges and Boilers: Americans Discover the Wrought-Iron Tubular Bowstring Bridge." *Industrial Archaeology,* vol. 19, no. 2 (1993).

_____. "Engineering and Enterprise: Early Metal-Truss Bridges in Ohio." *Timeline,* vol. 2, no. 1 (February-March 1985).

_____. "Uncommon Wrought-Iron Bridge in Morrow County." *Ohio County Engineer,* Spring 1992.

U.S. Department of the Interior, Historic American Engineering Record (HAER), No. IA-19, "Freeport Bridge," 1985. Prints and Photographs Division, Library of Congress, Washington, D.C.

_____, No. WY-1, "North Platte River Bowstring Truss Bridge," 1995. Prints and Photographs Division, Library of Congress, Washington, D.C.

Waddell, J. A. L. *The Design of Ordinary Iron Highway Bridges.*

Whipple, Squire. *A Work on Bridge Building.* Utica: H. H. Curtiss, 1847.

_____. *An Elementary and Practical Treatise on Bridge Building.* New York: D. Van Nostrand, 1872.

_____. U.S. Patent No. 2,064 (April 24, 1841).

## FIGURES

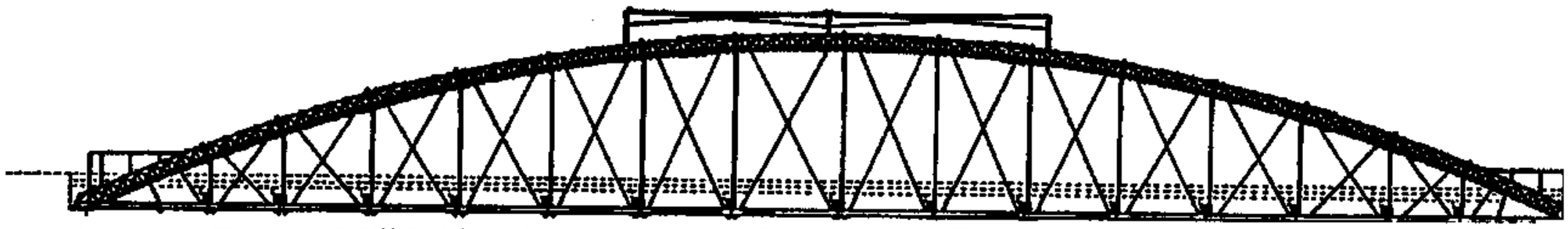

**Figure 1.** Fremont Mill Bridge, Anamosa, Iowa. Delineated by Erick McEvoy in U.S. Department of the Interior, Historic American Engineering Record (HAER), No. IA-58, "Fremont Mill Bridge," 1995. Prints and Photographs Division, Library of Congress, Washington, D.C.

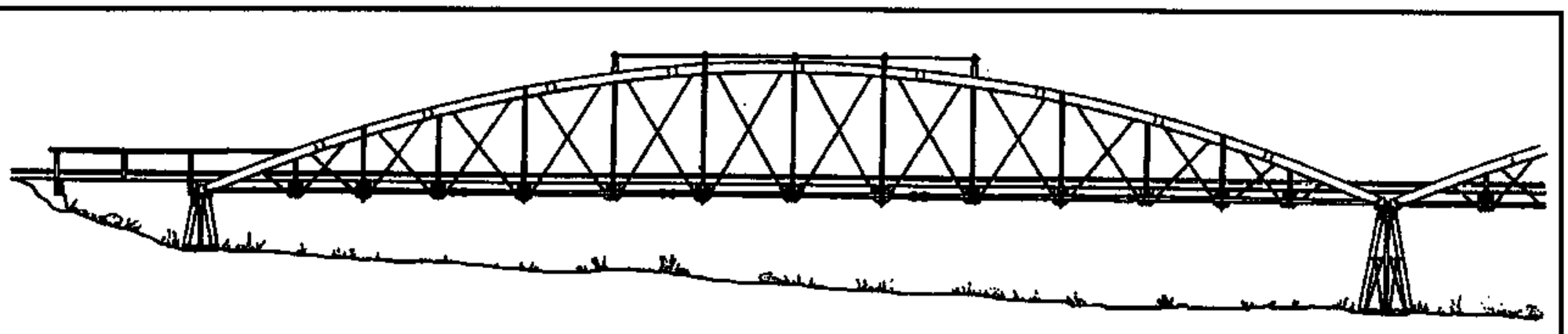

**Figure 2.** Fort Laramie Bridge, near Fort Laramie, Wyoming. Delineated by Chris Payne in U.S. Department of the Interior, Historic American Engineering Record (HAER), No. WY-1, "North Platte River Bowstring Truss Bridge," 1995. Prints and Photographs Division, Library of Congress, Washington, D.C.

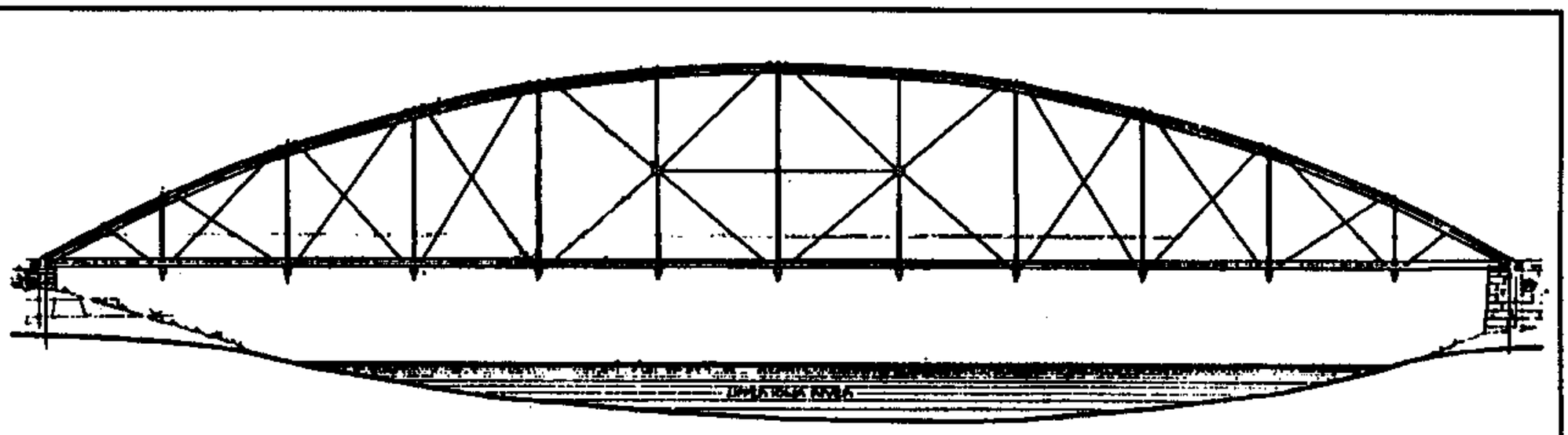

**Figure 3.** Freeport Bridge, Decorah, Iowa. Delineated by Clayton Fraser in U.S. Department of the Interior, Historic American Engineering Record (HAER), No. IA-19, "Freeport Bridge," 1995. Prints and Photographs Division, Library of Congress, Washington, D.C.

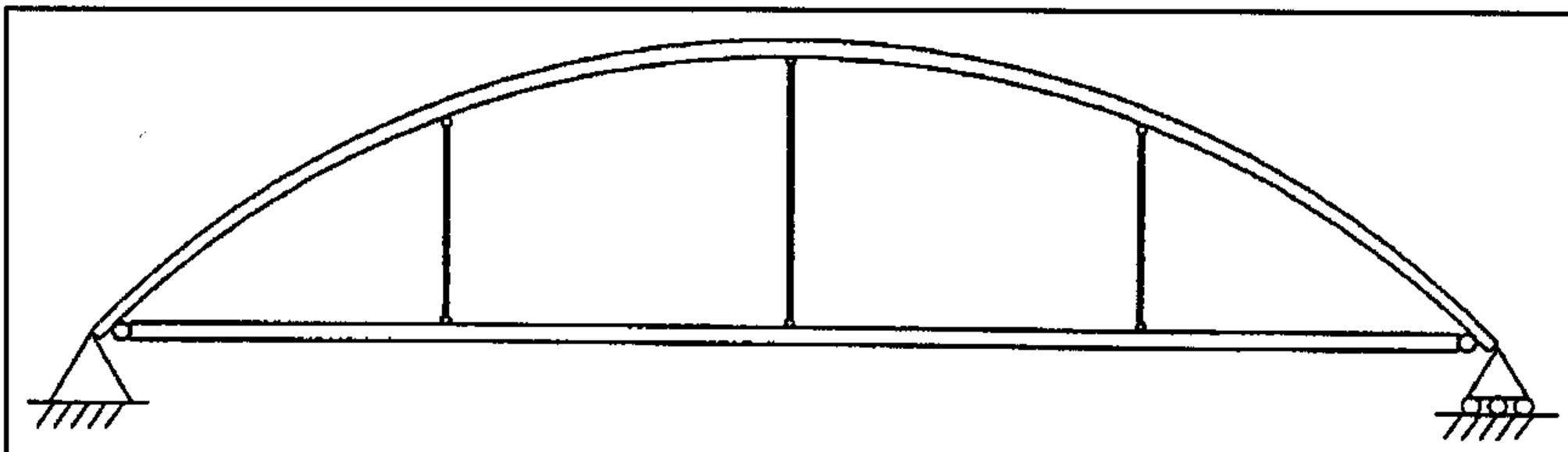

**Figure 4.** A PURE TIED ARCH. The arch is continuous and able to resist bending moments. Equilibrium can only be satisfied if the arch is able to resist bending moments.

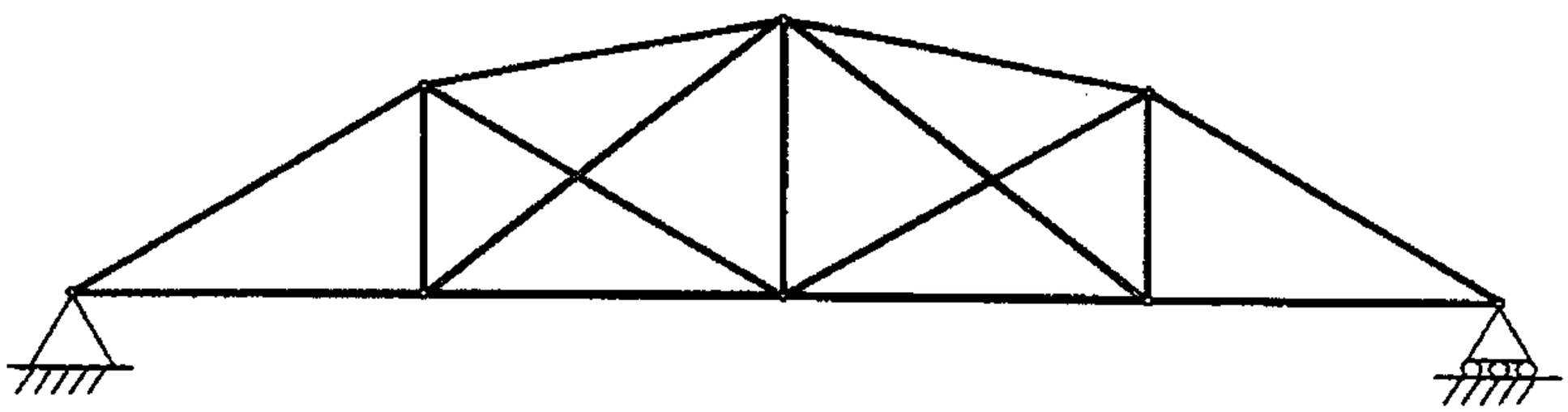

**Figure 5.** AN IDEAL TRUSS. All joints are pinned. All members are able to resist tension and compression. Equilibrium is satisfied by axial forces only.

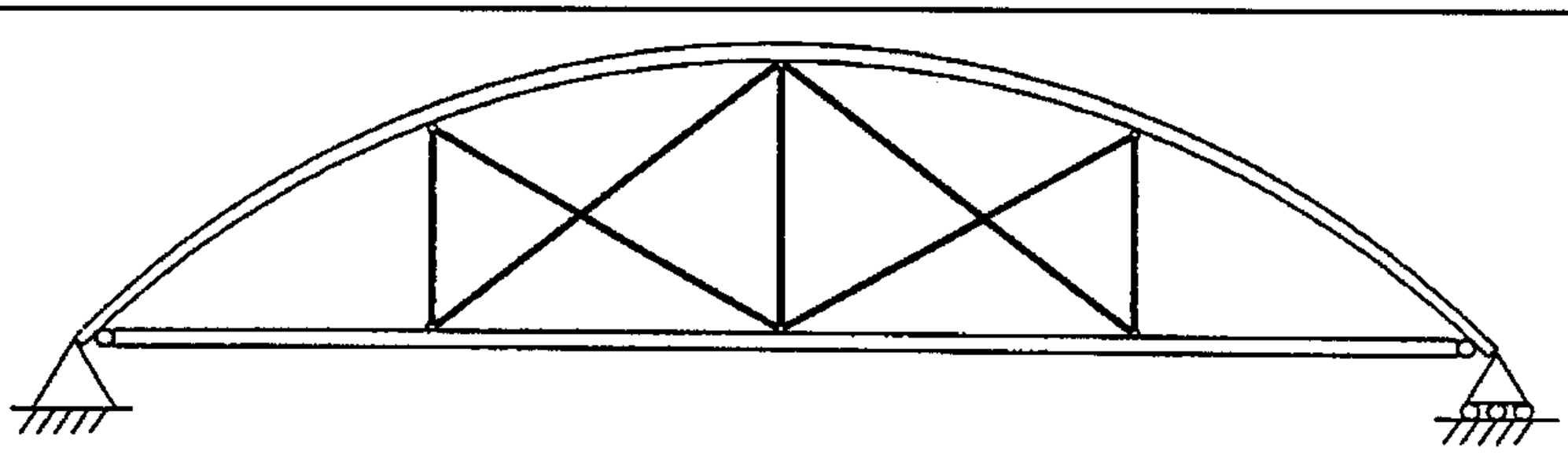

**Figure 6.** A TYPICAL BOWSTRING BRIDGE. The top chord is continuous and able to resist bending moments. All other members can carry only tension. The dead load causes some pretension in the lower chord, the verticals, and the diagonals.

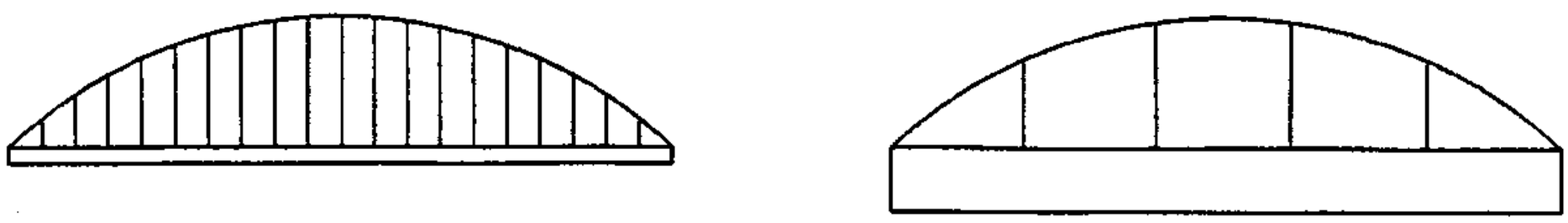

**Figure 7.** An illustration of competing design issues in floor systems. A light floor system can be constructed with many costly connections (left). Fewer connections can be used, but the floor system will be much more heavy and expensive (right).

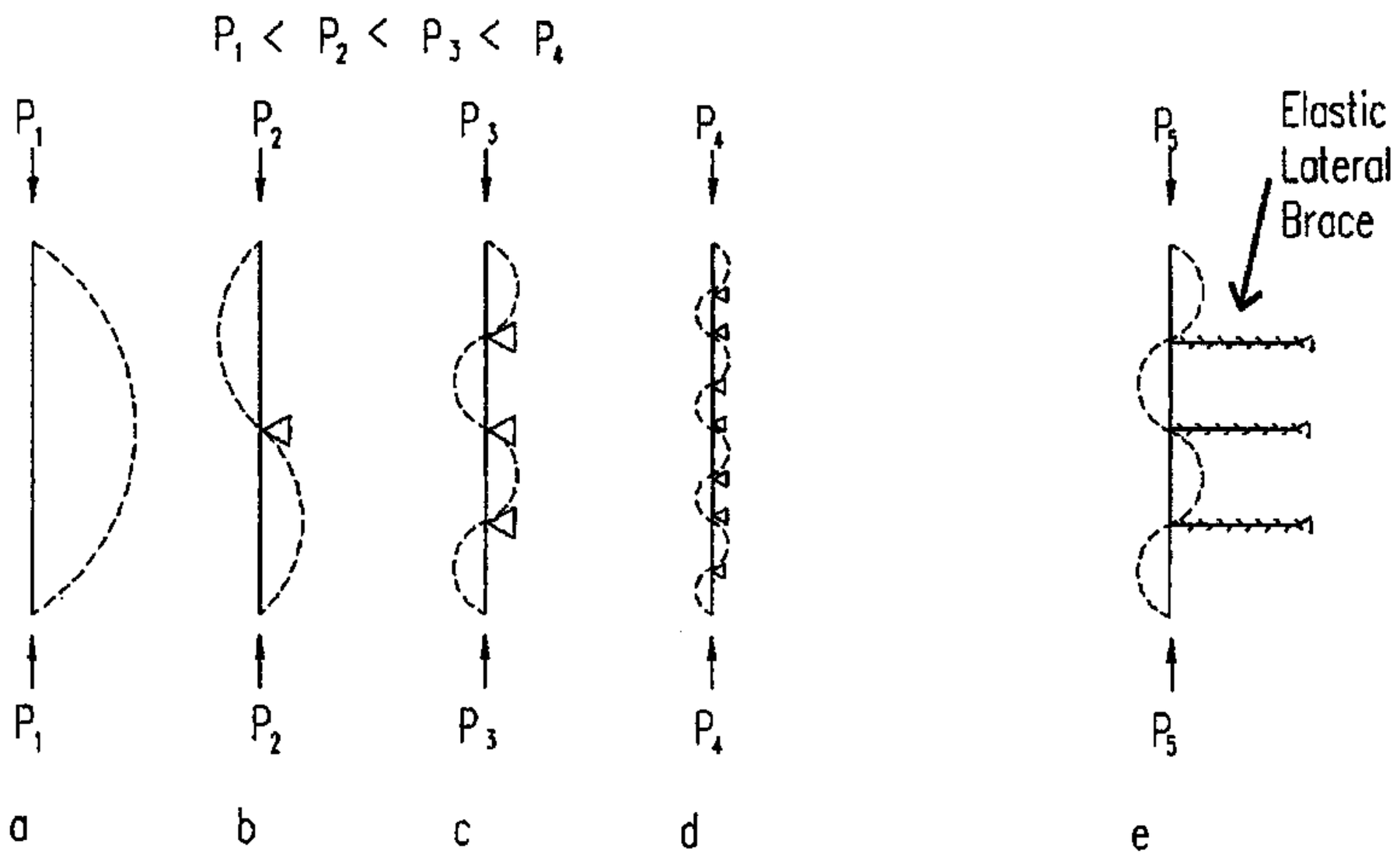


**Figure 8.** Members in compression will become unstable and deform in the shape of half-waves (a). With added bracing, the critical buckling load is increased and the deformed shape is a series of waves with nodes at bracing locations (b, c, d). Actual braces are not rigid but elastic (e).

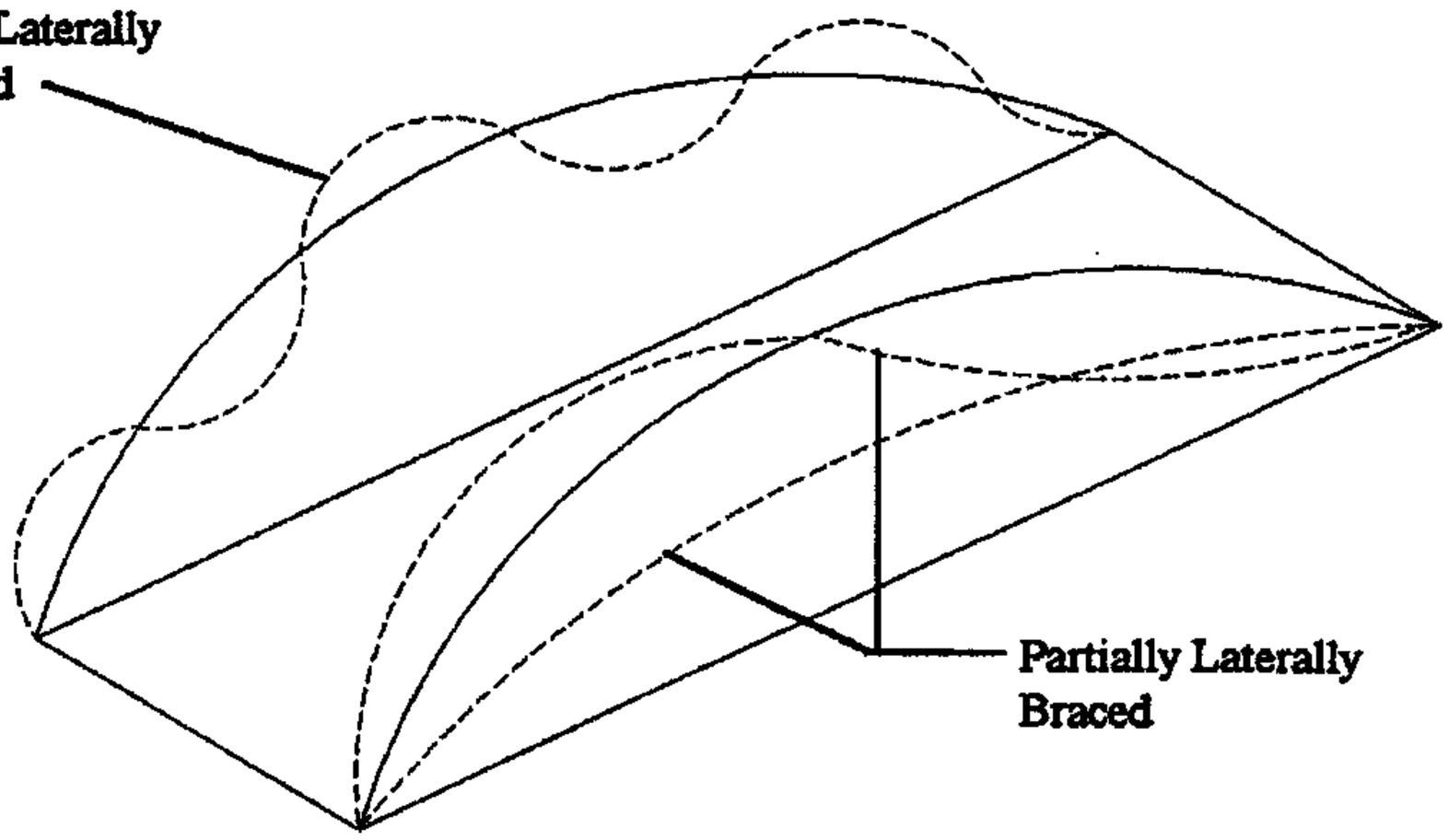


**Figure 9.** The fundamental buckled mode shape of a bowstring truss' top chord depends on the amount of bracing provided.

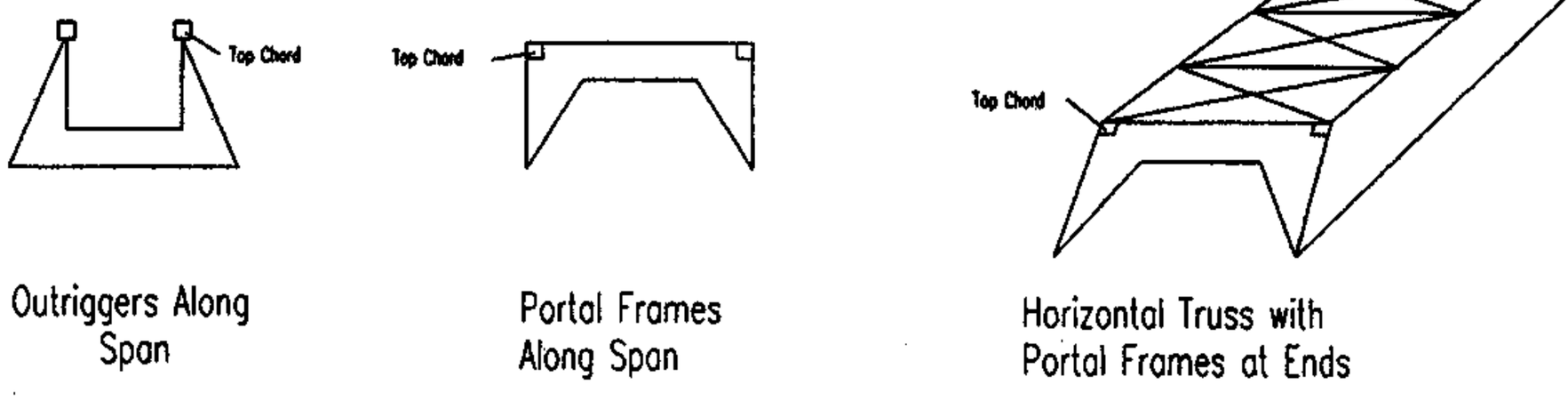


**Figure 10.** Three methods for laterally stabilizing top chords in compression: outriggers, portal frames, and a horizontal truss with end portal frames.

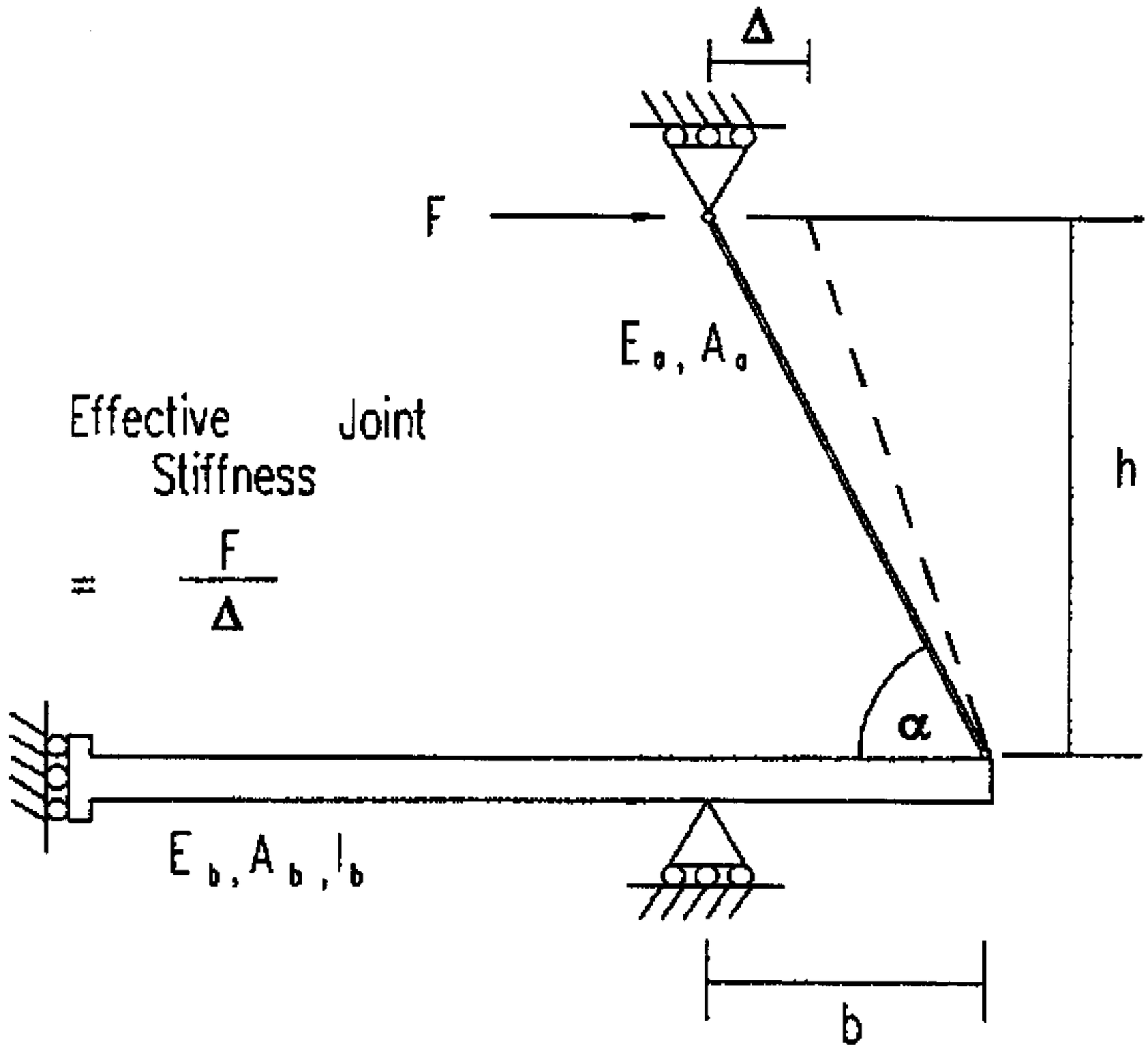


**Figure 11.** Outrigger bracing model for the Fremont Mill and Fort Laramie bridges. Parameters affecting the outrigger's efficiency are the floor beam properties $E_b$, $I_b$, and $A_b$; the outrigger member properties $E_a$ and $A_a$; and the outrigger height $h$ and length $b$.

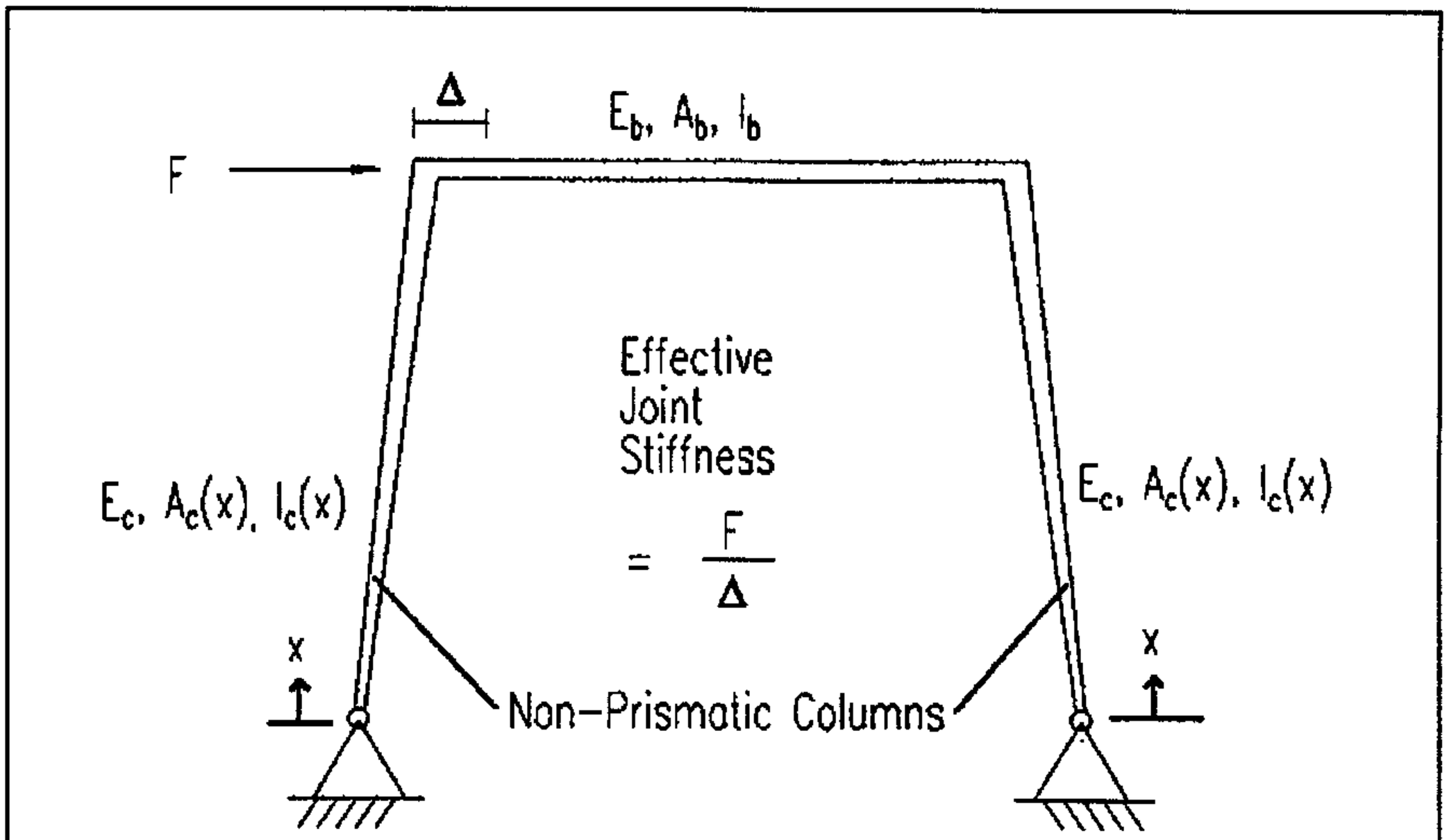


**Figure 12.** Portal-frame bracing model for the Freeport Bridge. Parameters affecting the portal frame's efficiency are the floor beam properties $E_b$, $I_b$, and $A_b$; and the column properties $E_c$, $A_c$, and $I_c$.

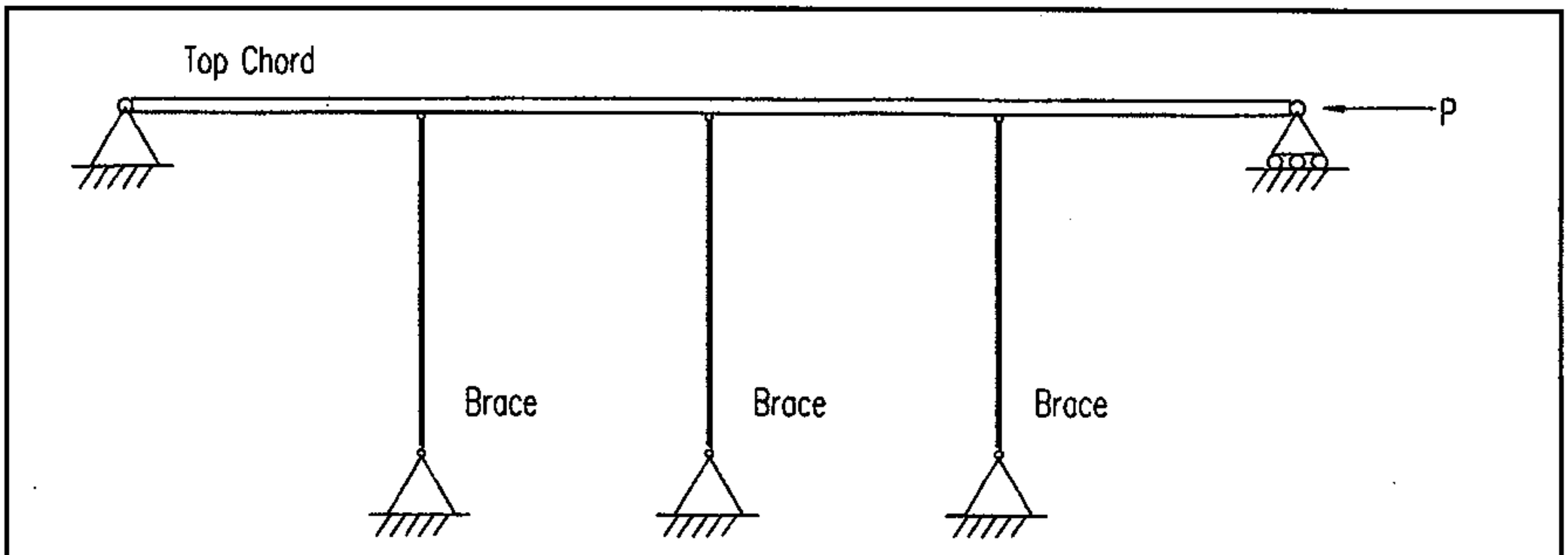


**Figure 13.** Each bridge's top chord is modeled as a member with a series of elastic braces in the horizontal plane.

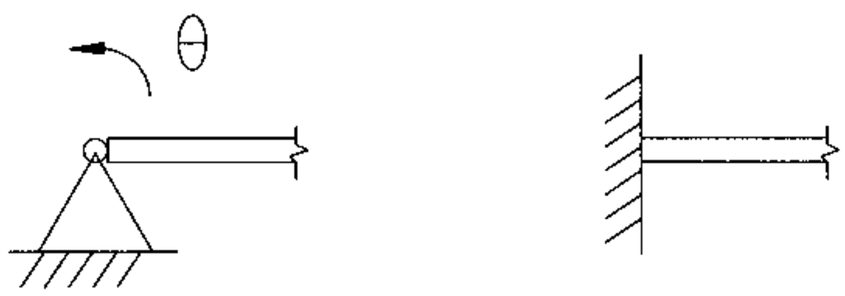


**Figure 14.** Pinned-end boundary condition (left) allows rotational movement θ. Fixed-end boundary condition (right) does not.

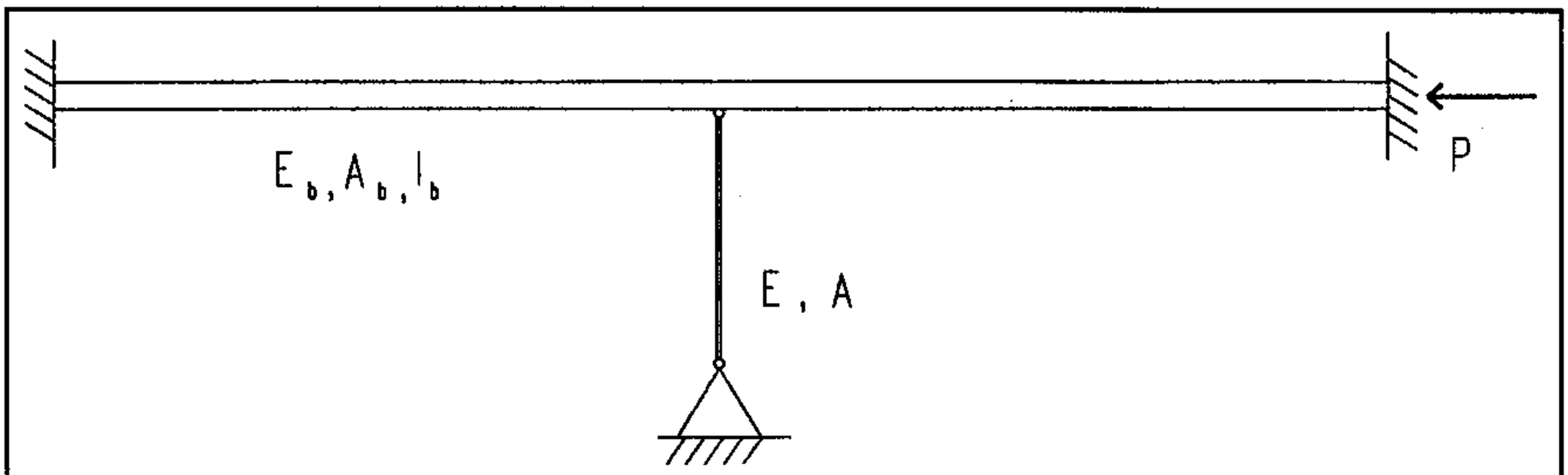


**Figure 15.** Fixed-end beam with a single brace.

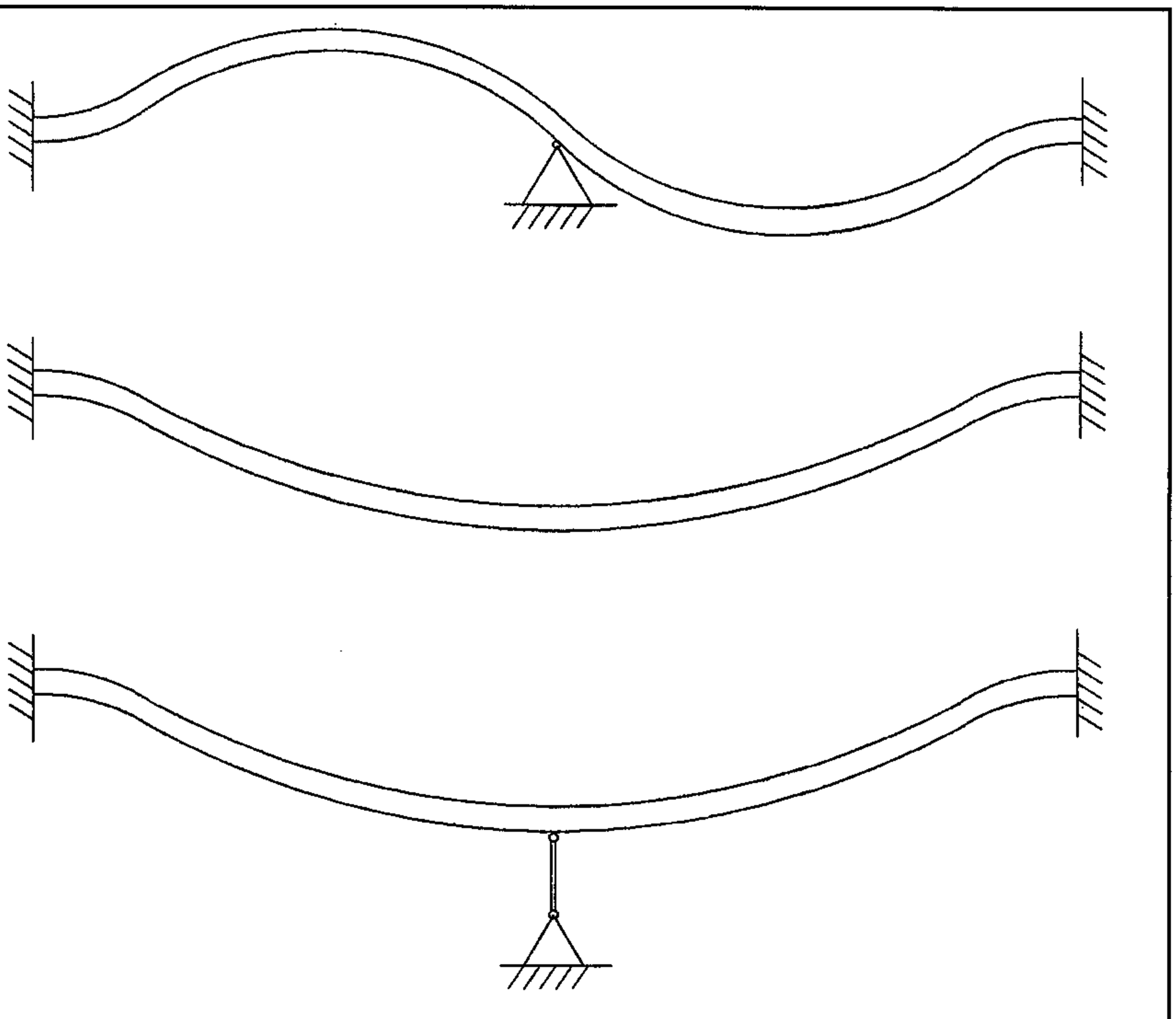

**Figure 16.** Buckled mode shapes of a fixed-end beam with a single brace (top), an unbraced fixed-end beam (center), and a partially-braced fixed-end beam (bottom).

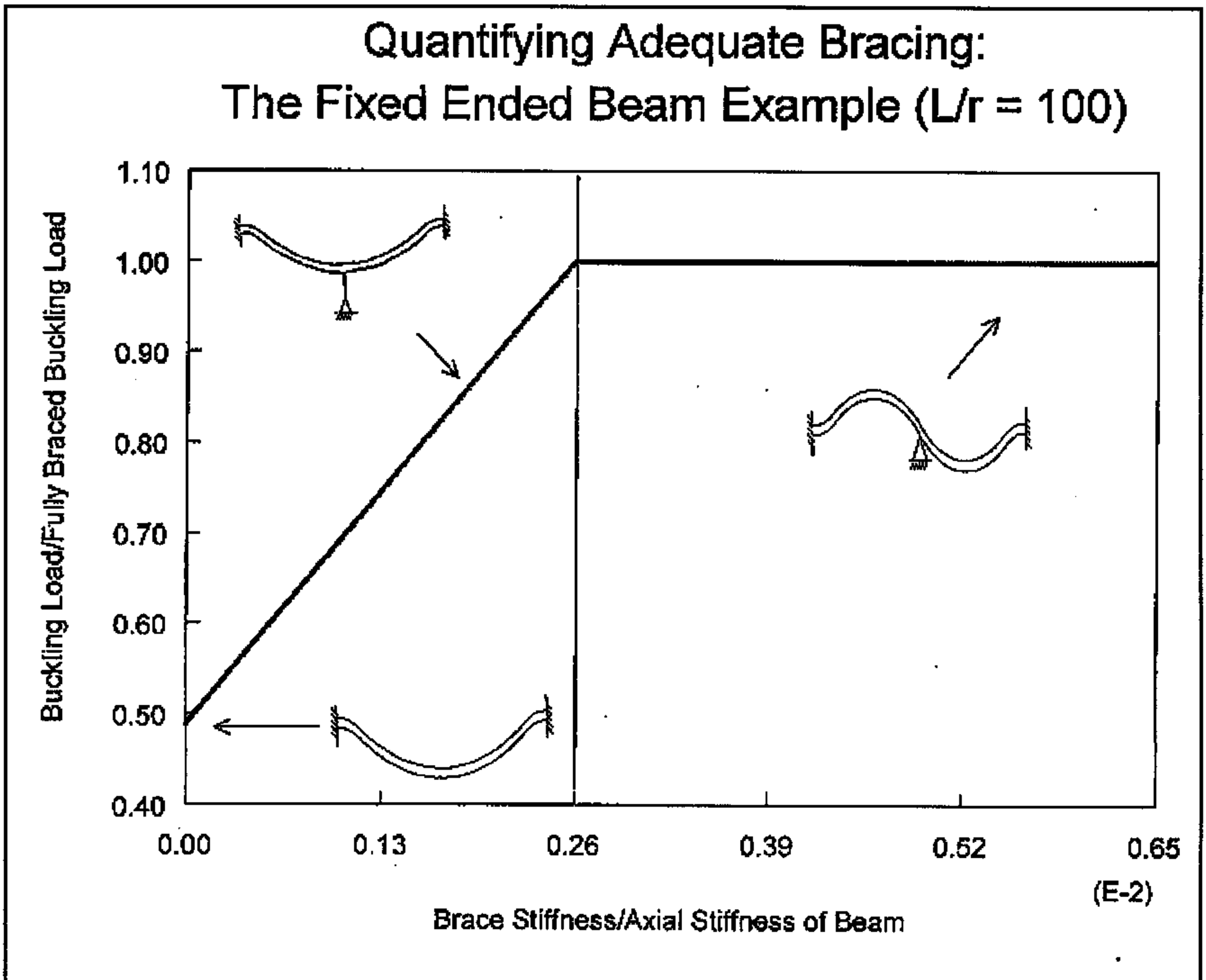


**Figure 17.** Buckling load in a beam of slenderness ratio 100, as a function of brace stiffness. Buckling load is normalized by the buckling load of a fully braced beam, and brace stiffness is normalized by the beam's axial stiffness.

**Figure 18.** Squire Whipple's original bowstring bridge is a tied arch with a divergent top chord. Photograph courtesy Ohio Historical Society.

Comparison of Element Forces Predicted by
STAN2D and Whipple in a 7 Panel Arch Truss
Full Span Live Load of 4.79 kN/m² (100 psf)
(Compressive Forces are Negative)

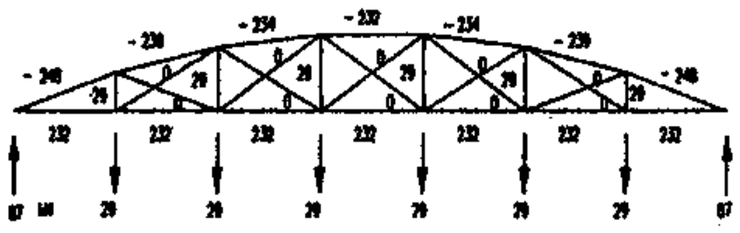

Whipple

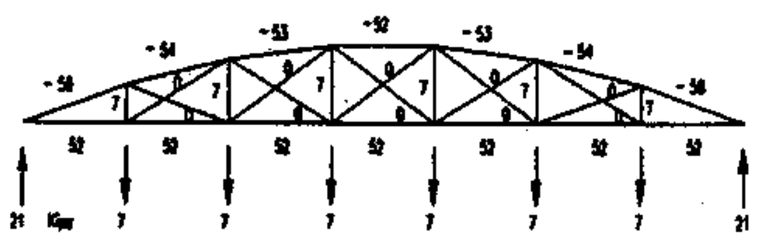

(SI Units)

(English Units)

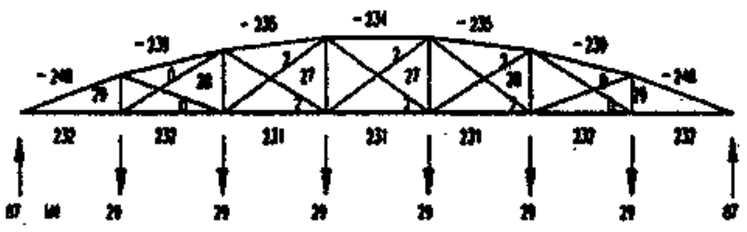

STAN2D

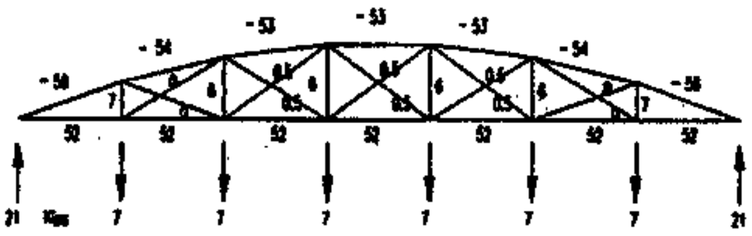

**Figure 19.** A comparison of member forces predicted by Whipple (1872) and modern structural analysis for the uniform load case.

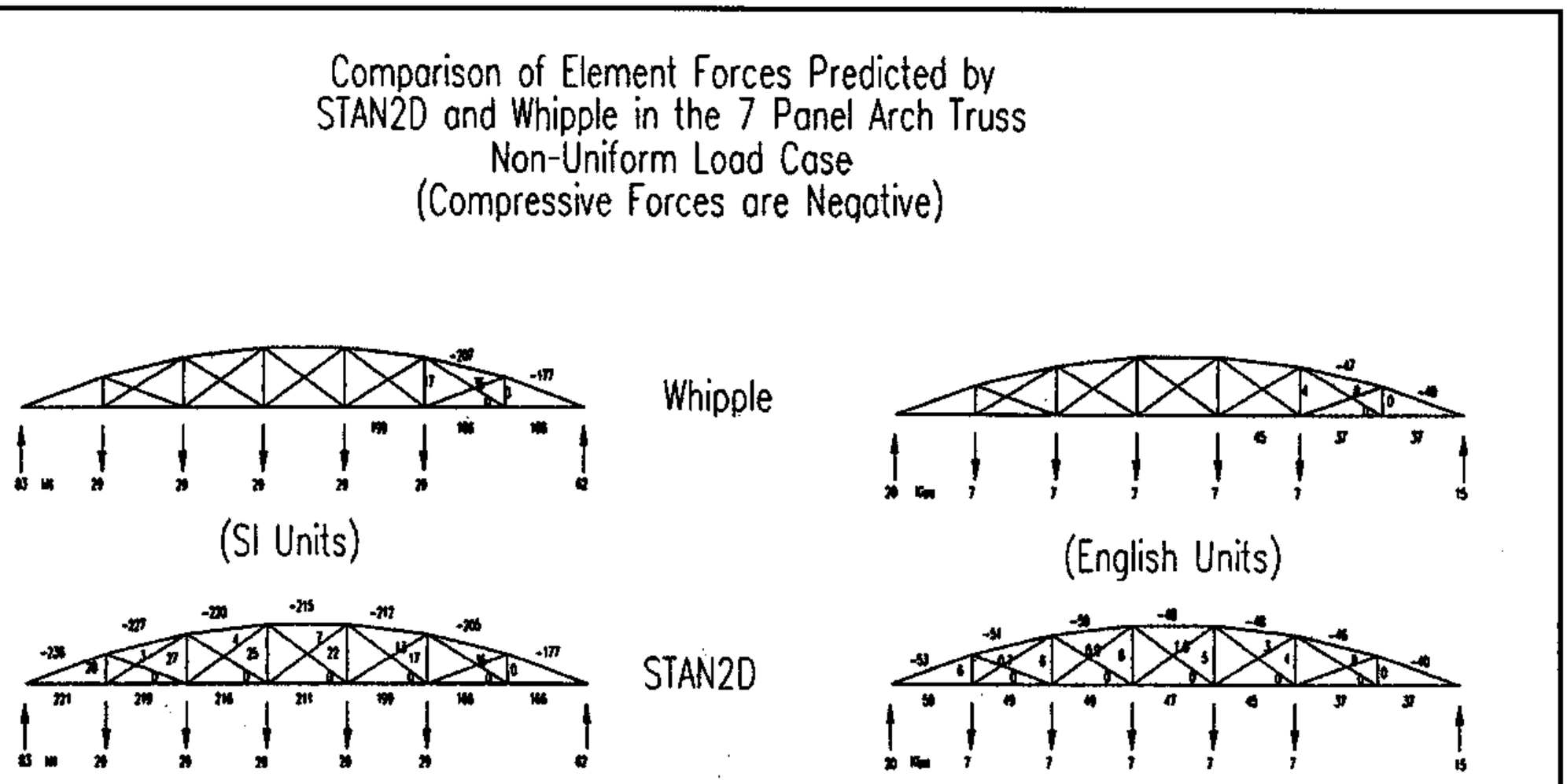


**Figure 20.** Comparison of member forces predicted by Whipple (1872) and modern structural analysis for a non-uniform load case. Whipple's analysis is incomplete because he uses it only to size one of the first diagonals.

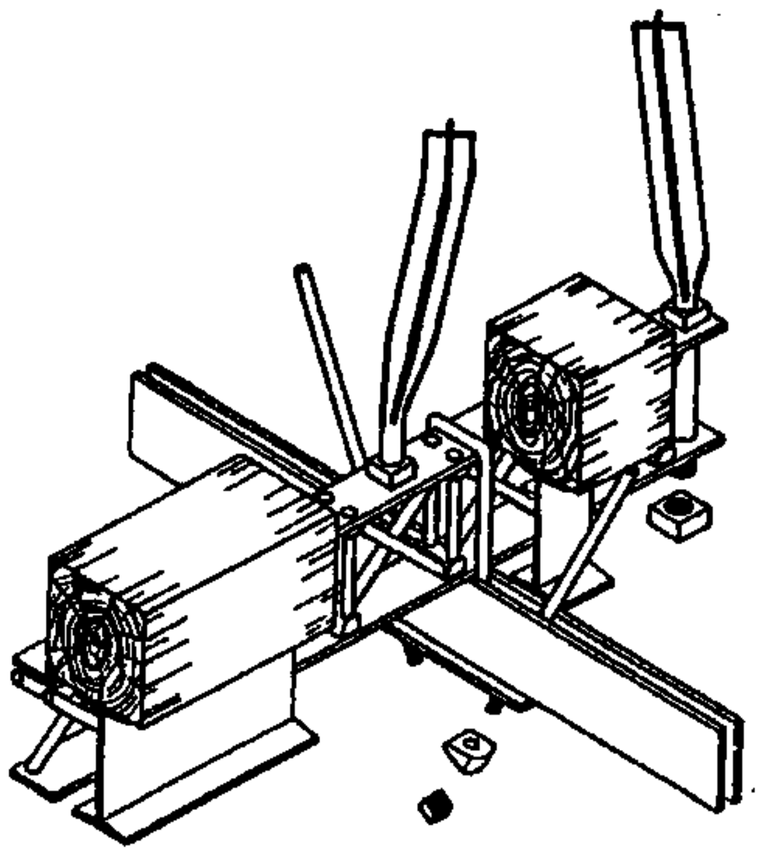

**Figure 21.** Diagonal connection detail from Fremont Mill Bridge. Delineated by Roger Chien in HAER No. IA-58, "Fremont Mill Bridge," 1995.

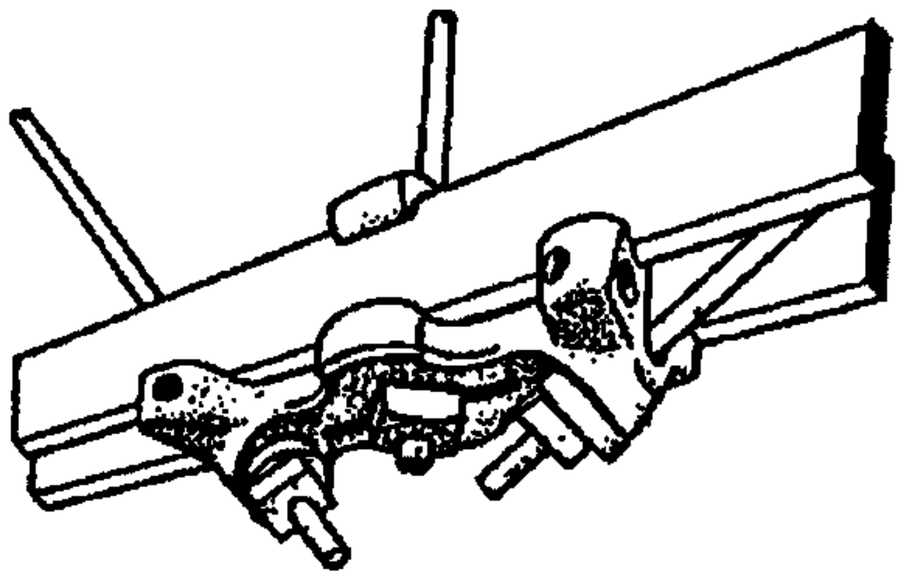

**Figure 22.** Diagonal connection detail from Fort Laramie Bridge. Delineated by Chris Payne in HAER No. WY-1, "North Platte River Bowstring Truss Bridge," 1993.

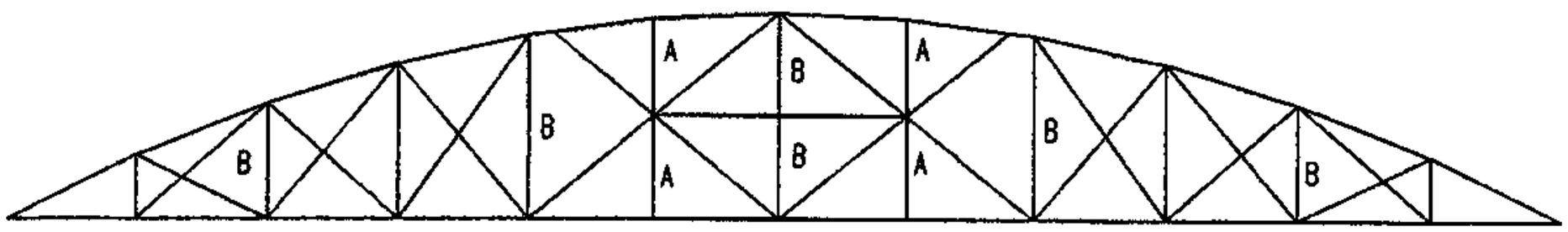


**Figure 23.** The Freeport Bridge's center diagonals span two panels, thereby decreasing the structure's dead load. Further weight reduction is accomplished by the substitution of this suspension rods (A) for more substantial vertical posts (B).

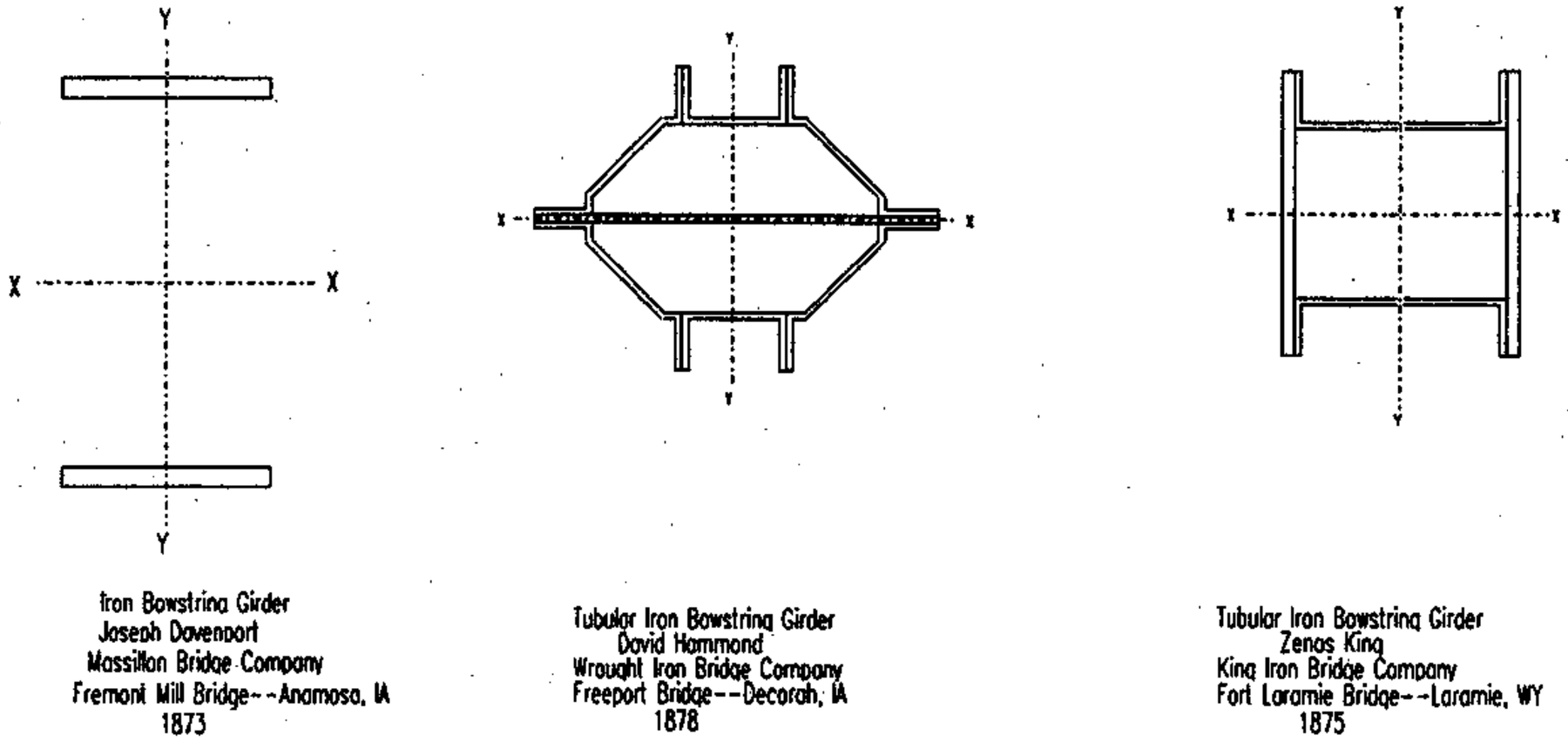


**Figure 24.** Cross sections of the Fremont Mill, Freeport, and Fort Laramie bridges' top chords.

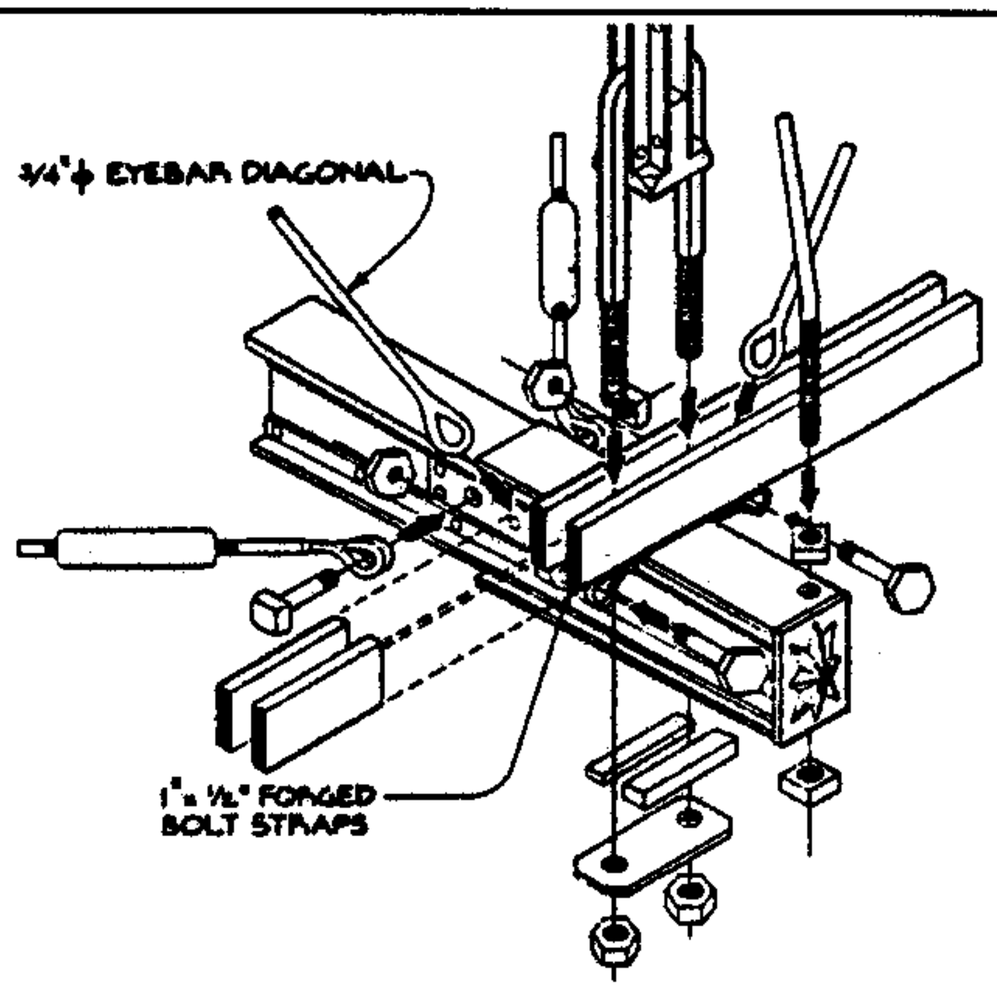


**Figure 25.** Diagonal connection detail from Freeport Bridge. Delineated by Clayton B. Fraser in HAER No. IA-19, "Freeport Bridge," 1995.

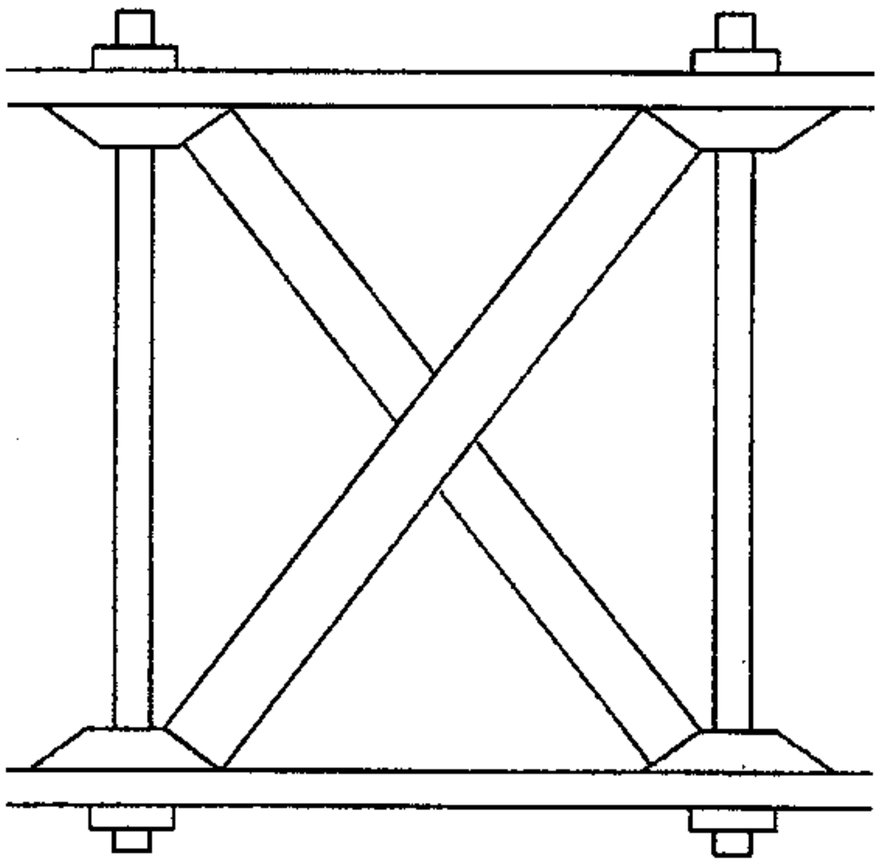

**Figure 26.** The Fremont Mill Bridge's top chord is a Howe truss formed from gas pipe and boiler plate.

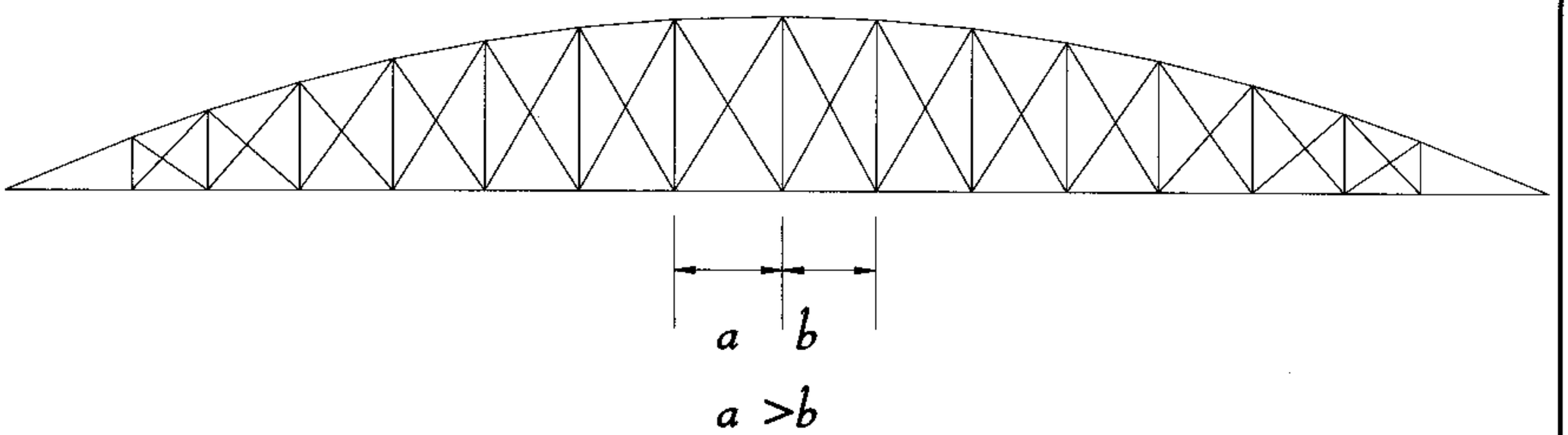


**Figure 27.** The Fremont Mill Bridge is not symmetric. The center vertical does not lie along the structure's geometric center.

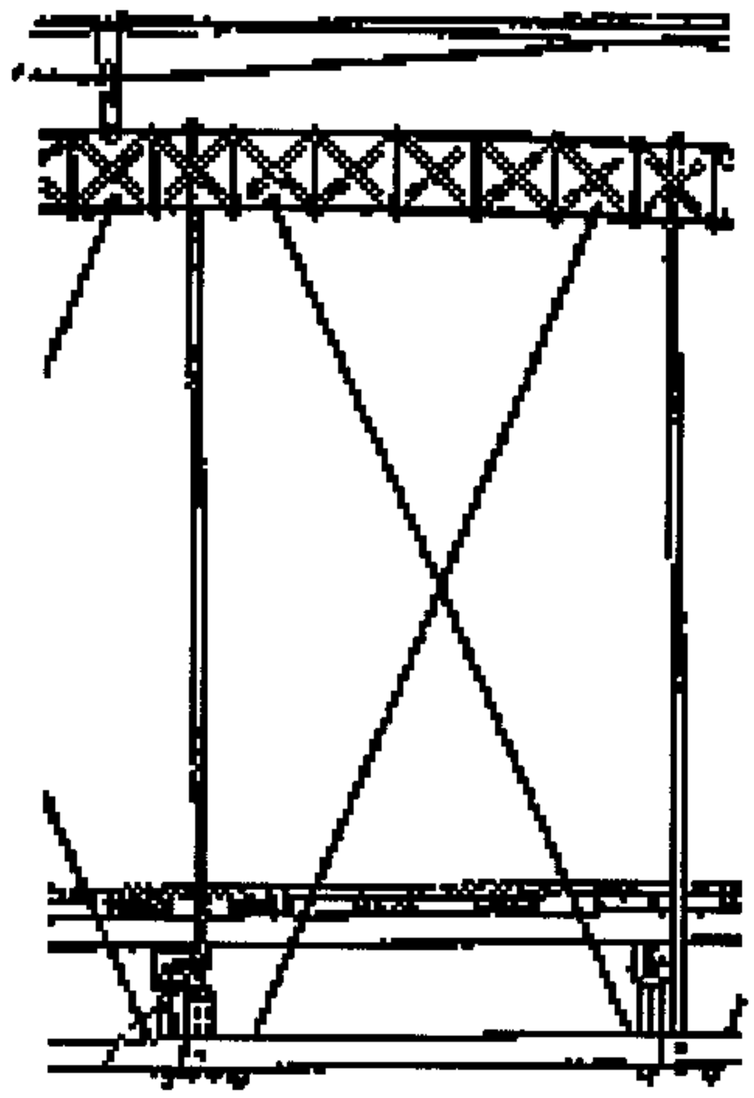

**Figure 28.** Detail of the Fremont Mill Bridge. Eccentrically connected diagonals cause local bending in the chords' boiler plates. Delineated by Erick McEvoy in HAER No. IA-58, "Fremont Mill Bridge," 1995.

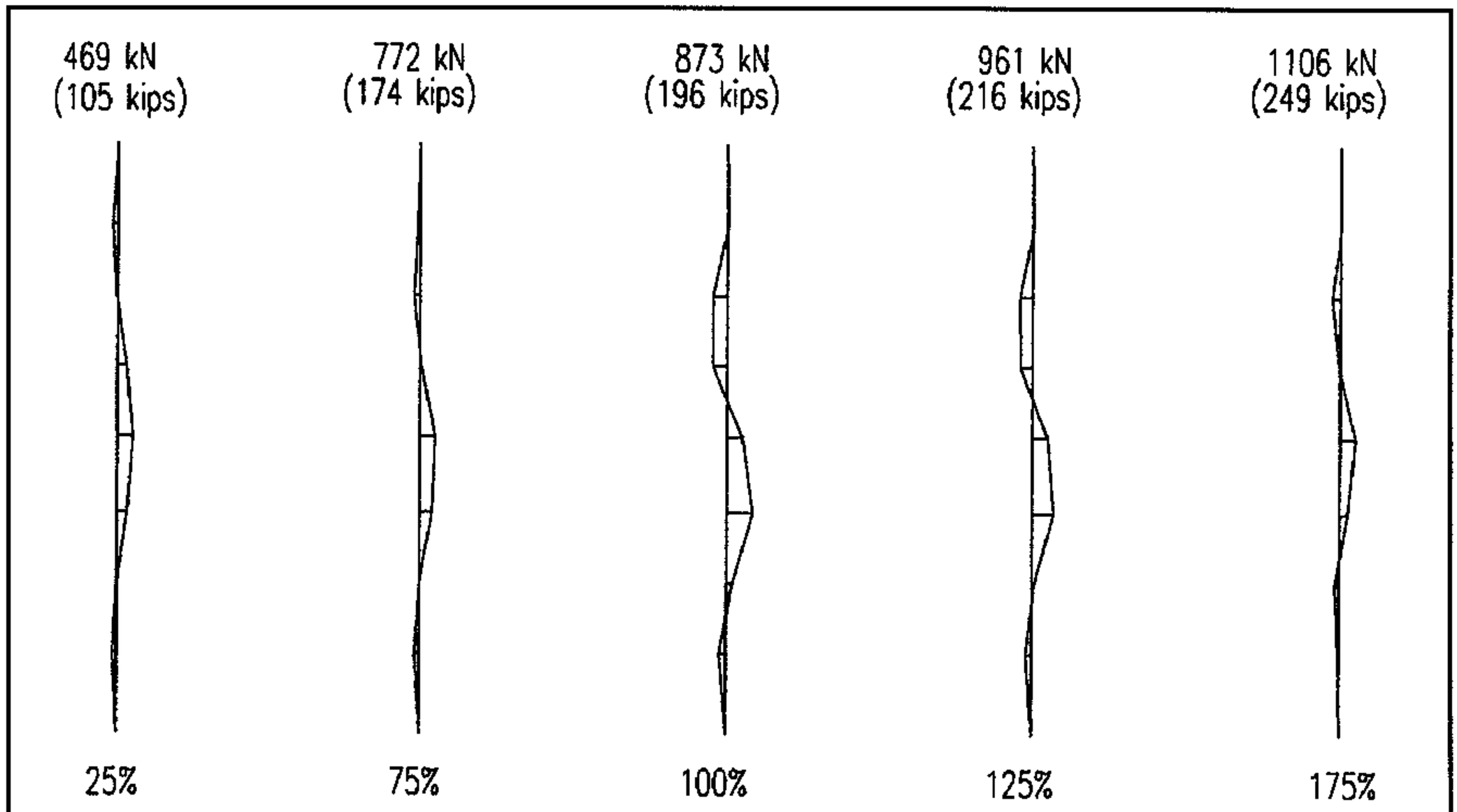


**Figure 29.** Buckled mode shape for the Fremont Mill Bridge's top chord (center), and buckled mode shapes resulting from variations in outrigger brace stiffness.

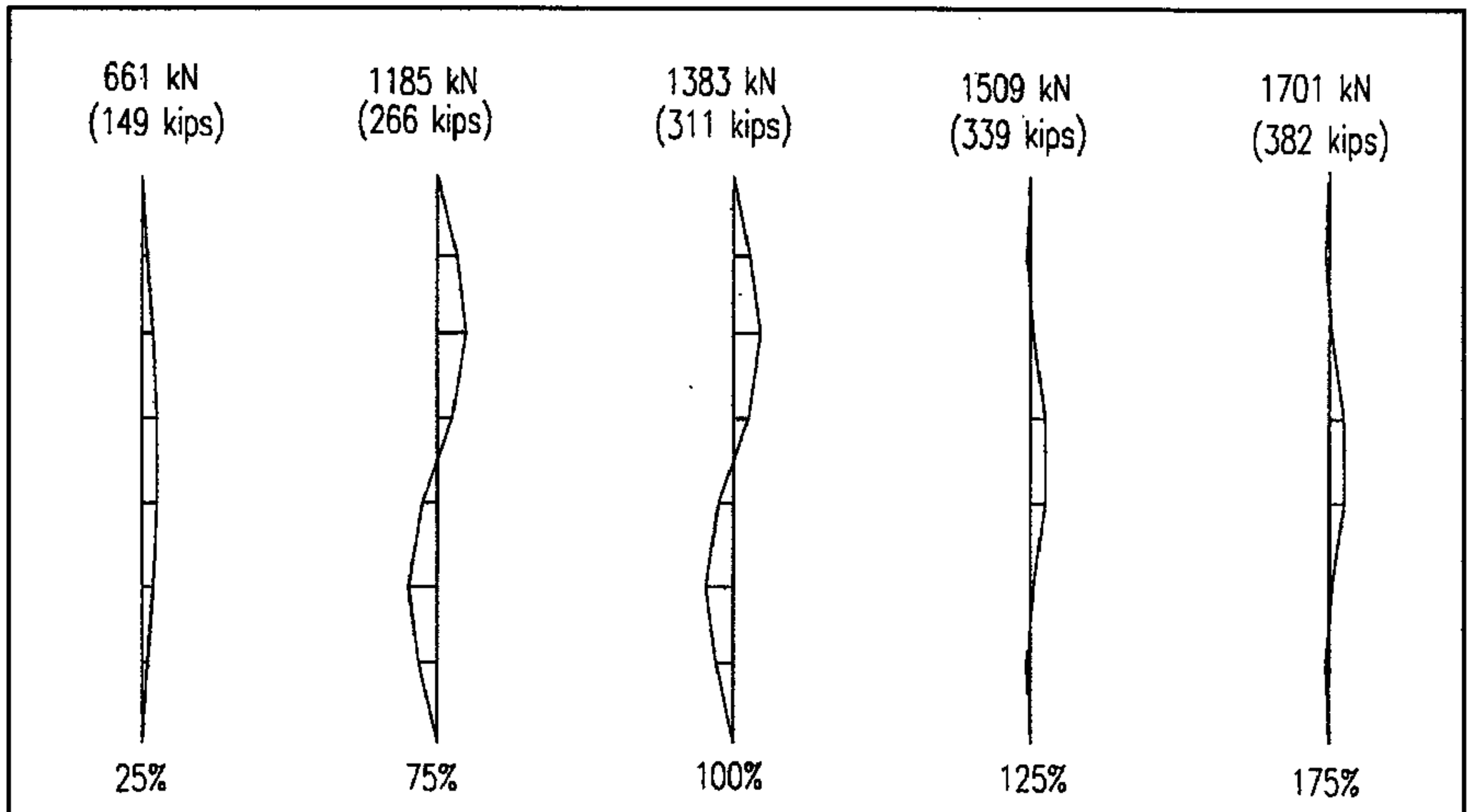


**Figure 30.** Buckled mode shape for the Fort Laramie Bridge's top chord (center), and buckled mode shapes resulting from variations in outrigger brace stiffness.

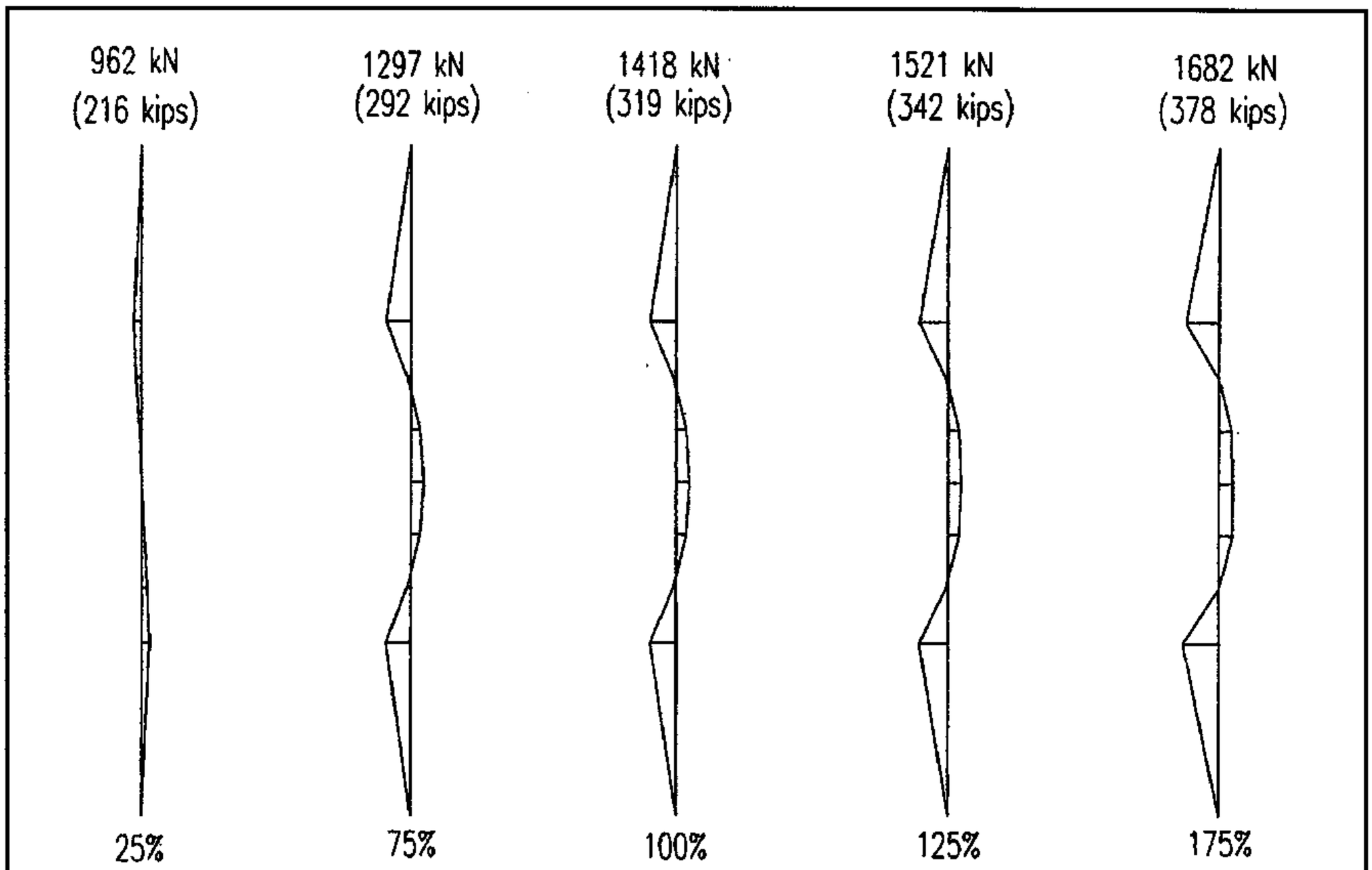


**Figure 31.** Buckled mode shape for the Freeport Bridge's top chord (center), and buckled mode shapes resulting from variations in outrigger brace stiffness.

**APPENDICES**

Appendix A
- Mathematica code used in the lateral stability analyses.
- Example of using the code to determine the buckling load and buckled-mode shape of the Freeport Bridge's top chord.

Appendix B
- Member forces in the Fremont Mill Bridge under a full-span live load of 3.83 kN/m$^2$ (80 psf).
- Joint and member numbering scheme used for static analyses of the Fremont Mill Bridge.
- Table of member stresses in the Fremont Mill Bridge under various loading conditions.

Appendix C
- Member forces in the Fort Laramie Bridge under a full-span live load of 3.83 kN/m$^2$ (80 psf).
- Joint and member numbering scheme used for static analyses of the Fort Laramie Bridge.
- Table of member stresses in the Fort Laramie Bridge under various loading conditions.

Appendix D
- Member forces in the Freeport Bridge under a full-span live load of 3.83 kN/m$^2$ (80 psf).
- Joint and member numbering scheme used for static analyses of the Freeport Bridge.
- Table of member stresses in the Freeport Bridge under various loading conditions.

## APPENDIX A: MATHEMATICA CODE

```
(*The following is the package used in performing the lateral
stability study of the iron bowstring bridges.  It consists of a
series of subroutines programmed using Mathematica 2.2 for
Windows.  It uses the geometric stiffness matrix approximation to
the non-linear element stiffness matrix for plane frames.*)

(*The opening passages describe what is done by each
subroutine.*)

(*Instructions for use of the package:
1.   Clear x,y,B,and the arbitrary displacement to which all
     others will be referenced.
2.   Set the directory to the one which contains this
     package.
3.   Load the package.
4.   Enter the properties of the network--lengths of each
     element, followed by their c factors, then the
     stiffnesses of the joints.
5.   Enter the displacement vector.
6.   Enter another displacement vector without the
     displacement to which all others will be referenced.
7.   Solve for buckling loads using the Results subroutine.
8.   Set B = to the critical buckling load.
9.   Set x = to the Shapes subroutine.
10.  Set y = to the Mult subroutine.
11.  Set the arbitrary displacement (to which all other
     displacements will be referenced) equal to one.
12.  Solve for the buckled mode shape using the Disp
     subroutine.*)

(*An example of the proper use of this package is included
following the code.*)

IBC::usage="
IBC[m_,n_,e_,i_,L_,C_] creates the first submatrix in the
geometric stiffness matrix of a network.  It assumes pinned
boundary conditions exist at the beginning of the network and
formulates the submatrix according to those boundary conditions.
Inputs are m for the dimensions of the network matrix (ie twice
```

```
the number of nodes in the network), n is the submatrix number
(in this case, it should be one since it is the first element in
the network), e is the elastic modulus, i is the moment of
inertia, L is the length of the member, C is the coefficient of
the load taken by the member."

JBC::usage="
JBC[m_,n_,e_,i ,L_,C_] creates the last submatrix in the
geometric stiffness matrix of a network.  It assumes pinned
boundary conditions exist at the end of the network and
formulates the submatrix according to those boundary conditions.
Inputs are m for the dimensions of the network matrix (ie twice
the number of nodes in the network), n is the submatrix number
(in this case, it should be m/2 since it is the last element in
the network), e is the elastic modulus, i is the moment of
inertia, L is the length of the member, C is the coefficient of
the load taken by the member."

Inter::usage="
Inter[m_,n_,e_,i_,L_,C_] creates the intermediate submatrices in
the geometric stiffness matrix of a network.  It assumes two
degrees of freedom at each end of the element--vertical
displacement and rotation.  Inputs are m for the dimensions of
the network matrix (ie twice the number of nodes in the network),
n is the submatrix number, e is the elastic modulus, i is the
moment of inertia, L is the length of the member, C is the
coefficient of the load taken by the member."

Submatrix::usage="
Submatrix[m_,n_,e_,i_,L_,C_] is a function used by the FullMatrix
function when assembling the system stiffness matrix.  The
Submatrix function chooses the right submatrix routine (IBC,JBC,
or Inter) while the FullMatrix routine goes through its loops in
assembling the system stiffness matrix.  Inputs are m for the
dimensions of the network matrix (ie twice the number of nodes in
the network), n is the submatrix number, e is the elastic
modulus, i is the moment of inertia, L is the length of the
member, C is the coefficient of the load taken by the member."

FullMatrix::usage="
```

```
FullMatrix[m_,e_,i_,list_List] creates the network geometric
stiffness matrix by summing all of the appended submatrices of
the network and any braces in the network.  Inputs are m for the
dimensions of the network matrix (ie twice the number of nodes in
the network), e is the elastic modulus, i is the moment of
inertia, and list contains all of the properties of the network,
element lengths and c factors followed by effective stiffnesses
of any braces, i.e. {L1,Cl,L2,C2,....,Kl,K2,K3,....}."

Brace::usage="
Brace[m_,list_List] creates the effective stiffness matrix of any
braces on the network.  Inputs are m for the dimensions of the
network matrix (twice the number of nodes in the network) and
list is the list containing all of the properties of the network,
i.e. {Ll,Cl,L2,C2,....,Kl,K2,K3,....}."

Loads::usage="
Loads[m_,L_] takes the determinant of the system stiffness matrix
m, sets it equal to zero, and solves for the critical buckling
loads L.  Use the capital letter B for the variable L. That is,
the command would read Loads [m,B], where m is the system
stiffness matrix."

Results::usage="
Results[m_,e_,i_,list_List,L_] combines the FullMatrix subroutine
and the Loads subroutine to solve for the buckling loads of a
network."

ZeroMatrix::usage="
ZeroMatrix[m_] creates a zero matrix of dimension m."

Shapes::usage="
Once the critical buckling load of the system is determined and
the variable B is set equal to that buckling load, the subroutine
Shapes[m_,e_,i_,list_List] will substitute that critical buckling
load back into the system stiffness matrix and returns the new
system stiffness matrix.  Inputs are m for the dimension of the
network matrix (twice the number of nodes), e for the elastic
modulus, i for the moment of inertia, and list for the network
properties, {Ll,Cl...,Kl,...}."
```

```
Mult::usage="
Mult[disp_List,list_List,v_] multiplies the system stiffness
matrix evaluated at the critical buckling load (the matrix formed
by the Shapes subroutine) by the displacement vector to obtain
the equations which will describe the buckled mode shape of the
network. Inputs are disp for the displacement vector, list for
backsubstituted network matrix, and v for the number of degrees
of freedom (the number of elements in the displacement vector)."

Disp::usage="
After setting one of the degrees of freedom in the problem equal
to 1, the Disp[equs_List,var_,list_List,n_] function can be used.
The Disp[equs_List,var_,list_List,n_] subroutine then solves for
the remaining displacements in terms of the chosen degree of
freedom."

Submatrix[m_,n_,e_,i_,L_,C_]:=
     If[n==1,IBC[m,n,e,i,L,C],
          If[n==m/2-1,JBC[m,n,e,i,L,C],
               Inter[m,n,e,i,L,C]],0];

Inter[m_,n_,e_,i_,L_,C_]:=
     Block[{f,g,o,p,s,t,u,v,w,x},
     s={};t={};u={};v={};w={};x={};
     a=0;j=0;k=0;
     f=12*e*i/L^3+B*6*C/(5*L);
     g=6*e*i/L^2+B*C/10;
     o=4*e*i/L+B*2*C*L/15;
     p=2*e*i/L-B*C*L/30;
     AppendTo[s,f];
     AppendTo[s,g];
     AppendTo[s,-f];
     AppendTo[s,g];
     AppendTo[t,g];
     AppendTo[t,o];
     AppendTo[t,-g];
     AppendTo[t,p];
     AppendTo[u,-f];
     AppendTo[u,-g];
     AppendTo[u,f];
     AppendTo[u,-g];
```

```
AppendTo[v,g];
AppendTo[v,p];
AppendTo[v,-g];
AppendTo[v,o];
While[j<2*(n-1),
      j=j+1;
      PrependTo[s,0];
      PrependTo[t,0];
      PrependTo[u,0];
      PrependTo[v,0]];
While[k<m-2*n-2,
      k=k+1;
      AppendTo[s,0];
      AppendTo[t,0];
      AppendTo[u,0];
      AppendTo[v,0]];
While[a<m,
      a=a+1;
      AppendTo[x,0]];
AppendTo[w,s];
AppendTo[w,t];
AppendTo[w,u];
AppendTo[w,v];
j=0;k=0;
While[j<2*(n-1),
      j=j+1;
      PrependTo[w,x]];
While[k<m-2*n-2,
      k=k+1;
      AppendTo[w,x]];
Return[w]];

JBC[m_,n_,e_,i_,L_,C_]:=
      Block[{f,g,o,p,s,t,u,v,w,x},
      s={};t={};u={};v={};w={};x={};
      a=0;j=0;k=0;
      f=12*e*i/L^3+B*6*C/(5*L);
      g=6*e*i/L^2+B*C/10;
      o=4*e*i/L+B*2*C*L/15;
      p=2*e*i/L-B*C*L/30;
      AppendTo[s,f];
```

```
AppendTo[s,g];
AppendTo[s,0];
AppendTo[s,g];
AppendTo[t,g];
AppendTo[t,o];
AppendTo[t,0];
AppendTo[t,p];
AppendTo[u,0];
AppendTo[u,0];
AppendTo[u,l];
AppendTo[u,0];
AppendTo[v,g];
AppendTo[v,p];
AppendTo[v,0];
AppendTo[v,o];
While[j<2*(n-1),
      j=j+1;
      PrependTo[s,0];
      PrependTo[t,0];
      PrependTo[u,0];
      PrependTo[v,0]];
While[k<m-2*n-2,
      k=k+1;
      AppendTo[s,0];
      AppendTo[t,0];
      AppendTo[u,0];
      AppendTo[v,0]];
While[a<m,
      a=a+1;
      AppendTo[x,0]];
AppendTo[w,s];
AppendTo[w,t];
AppendTo[w,u];
AppendTo[w,v];
j=0;k=0;
While[j<2*(n-1),
      j=j+1;
      PrependTo[w,x]];
While[k<m-2*n-2,
      k=k+1;
      AppendTo[w,x]];
```

```
      Return[w]];

IBC[m_,n_,e_,i_,L_,C_]:=
      Block[{f,g,o,p,s,t,u,v,w,x},
      s={};t={};u={};v={};w={};x={};
      a=0;j=0;k=0;
      f=12*e*i/L^3+B*6*C/(5*L);
      g=6*e*i/L^2+B*C/10;
      o=4*e*i/L+B*2*C*L/15;
      p=2*e*i/L-B*C*L/30;
      AppendTo[s,1];
      AppendTo[s,0];
      AppendTo[s,0];
      AppendTo[s,0];
      AppendTo[t,0];
      AppendTo[t,o];
      AppendTo[t,-g];
      AppendTo[t,p];
      AppendTo[u,0];
      AppendTo[u,-g];
      AppendTo[u,f];
      AppendTo[u,-g];
      AppendTo[v,0];
      AppendTo[v,p];
      AppendTo[v,-g];
      AppendTo[v,o];
      While[j<2*(n-1),
            j=j+1;
            PrependTo[s,0];
            PrependTo[t,0];
            PrependTo[u,0];
            PrependTo[v,0]];
      While[k<m-2*n-2,
            k=k+1;
            AppendTo[s,0];
            AppendTo[t,0];
            AppendTo[u,0];
            AppendTo[v,0]];
      While[a<m,
            a=a+1;
            AppendTo[x,0]];
```

```
AppendTo[w,s];
AppendTo[w,t];
AppendTo[w,u];
AppendTo[w,v];
j=0;k=0;
While[j<2*(n-1),
      j=j+1;
      PrependTo[w,x]];
While[k<m-2*n-2,
      k=k+1;
      AppendTo[w,x]];
Return[w]];

Brace[m_,list_List]:=
      Block[{j,k,s,w},
      k=0;s={};w={};j=0;
      While[k<m/2-2,
      s={};
      k=k+1;
      AppendTo[s,list[[(m-2)+k]]];
      While[j<2*k,
      j=j+1;
      PrependTo[s,0]];
      j=0;
      While[j<m-2*k-1,
      j=j+1;
      AppendTo[s,0]];
      j=0;
      AppendTo[w,s];
      AppendTo[w,ZeroRow[m]]];
      PrependTo[w,ZeroRow[m]];
      PrependTo[w,ZeroRow[m]];
      AppendTo[w,ZeroRow[m]];
      AppendTo[w,ZeroRow[m]];
      Return[w]];

FullMatrix[m_,e_,i_,list_List]:=
      Block[{f,g,d,w,x,y},
      f=0;g=0;d=0;x=ZeroMatrix[m];
      w=ZeroMatrix[m];y={};
      While[d<(m/2)-1,
```

```
            d=d+1;
            f=2*d-1;
            g=2*d;
            w=Submatrix[m,d,e,i,list[[f]],list[[g]]]+
            ];
      x=w+Brace[m,list];
      Return[x]];

ZeroMatrix[m_]:=
      Block[{k,s,w},
      k=0;s={};w={};
      While[k<m,
            k=k+1;
            AppendTo[s,0]];
      k=0;
      While[k<m,
            k=k+1;
            AppendTo[w,s]];
      Return[w]];

Loads[m_,L_]:=
      Block[{s},
      s=N[Solve[{Det[m]==0},{L}]];
      Return[s]];

Results[m_,e_,i_,list_List,L_]:=
      Block[{x,z},
      x=FullMatrix[m,e,i,list];
      z=Loads[x,B];
      Return[z]];

Shapes[m_,e_,i_,list_List]:=
      Block[{x},
      x=FullMatrix[m,e,i,list];
      Return[x]];

Disp[equs_List,list_List,n_]:=
      Block[{s,j,w},
      j=0;s=0;w={};
      While[j<n-1,
      j=j+1;
```

```
      s=equs[[j]]==0;
      AppendTo[w,s]];
      x=N[Solve[w,list]];
      Return[x]];

Mult[disp_List,list List,v_]:=
      Block[{s,k,a,j,z},
      s=0;k=0;j=0;z={};
      While[j<v,
      j=j+1;
      a=list[[j]];
      While[k<v,
      k=k+1;
      s=s+a[[k]]*disp[[k]]];
      AppendTo[z,s];
      k=0;s=0;];
      Return[z]];
```

## APPENDIX A: MATHEMATICA EXAMPLE

```
(*The following is an example of using the lateral stability package to solve
  for the critical buckling load and buckled mode shape of the Hammond
  Bowstring.*)

(*In this example, the horizontal displacement at node 16, denoted v16, will
  be chosen to be the degree of freedom to which all other displacements will
  be referenced.*)

(*Sysprop will be the list of all the properties of the network--element
  lengths followed by their c factors and then all the effective joint
  stiffnesses provided by the portal frame braces.*)

(*DOF will be the displacement vector, and DOF2 will be the displacement
  vector without the horizontal displacement at node 16.*)

(*C:\ECIV220\Hammond will be the directory which contains the package, and
  GEOMPN is the name of the package to be loaded.*)

(*Out of plane displacements are denoted by "v" followed by the node number,
  and rotational displacements are denoted by "t" followed by the node
  number.*)

(*The Hammond bowstring contains 9 nodes, which means there are 18 degrees of
  freedom in the lateral stability problem.  Hence dimension of the system
  stiffness matrix is 18.  The moment of inertia of the top chord around the
  y axis is 0.0001108 m^4.  The elastic modulus of iron is taken to be 2.0e8
  kPa.  Metric units are used for this example.  Buckling loads will be given
  in kN, and buckled mode shapes are dimensionless.*)

Clear[B]
Clear[x]
Clear[y]
Clear[v16]
SetDirectory["c:\eciv220\hammond"]
C:\ECIV220\HAMMOND
<<`geompn`
sysprop={13.284,1,4.215,.95,3.997,.96,3.996,.95,
3.966,.95,3.997,.96,4.215,.95,13.284,1,226,401,
87,532,87,401,226}
{13.284, 1, 4.215, 0.95, 3.997, 0.96, 3.996, 0.95, 3.966, 0.95, 3.997, 0.96,
  4.215, 0.95, 13.284, 1, 226, 401, 87, 532, 87, 401, 226}
dof={v1,t1,v4,t4,v8,t8,v12,t12,v16,t16,v20,t20,v24,
t24,v28,t28,v32,t32}
{v1, t1, v4, t4, v8, t8, v12, t12, v16, t16, v20, t20, v24, t24, v28, t28,
  v32, t32}
dof2=Delete[dof,9]
```

```
{v1, t1, v4, t4, v8, t8, v12, t12, t16, v20, t20, v24, t24, v28, t28, v32,
  t32}
Results[18,200000000,.0001108,sysprop,B]
{{B -> -80346.6}, {B -> -63926.9}, {B -> -47863.5}, {B -> -35030.4},
 {B -> -25426.7}, {B -> -18111.}, {B -> -16184.8}, {B -> -13835.),
 {B -> -9443.39}, {B -> -6919.24}, {B -> -5358.77}, {B -> -4085.51},
 {B -> -3518.97}, {B -> -3294.16}, {B -> -1517.71}, {B -> -1418.32}}
B=-1418.32
-1418.32
x=Shapes[18,200000000,.0001108,sysprop]
y=Mult[dof,x,Length[x]]
v16=1
1
Disp[y,dof2,Length[x]]
{{v1 -> 0., t1 -> -0.709279, v4 -> -1.96392, t4 -> 0.441381, v8 -> -0.203902,
 t8 -> 0.351358, v12 -> 0.773652, t12 -> 0.137775, t16 -> -0.00138043,
 v20 -> 0.768116, t20 -> -0.138109, v24 -> -0.206613, t24 -> -0.349764,
 v28 -> -1.95796, t28 -> -0.439132, v32 -> 0., t32 -> 0.706264}}
```

# APPENDIX B: FREMONT MILL BRIDGE

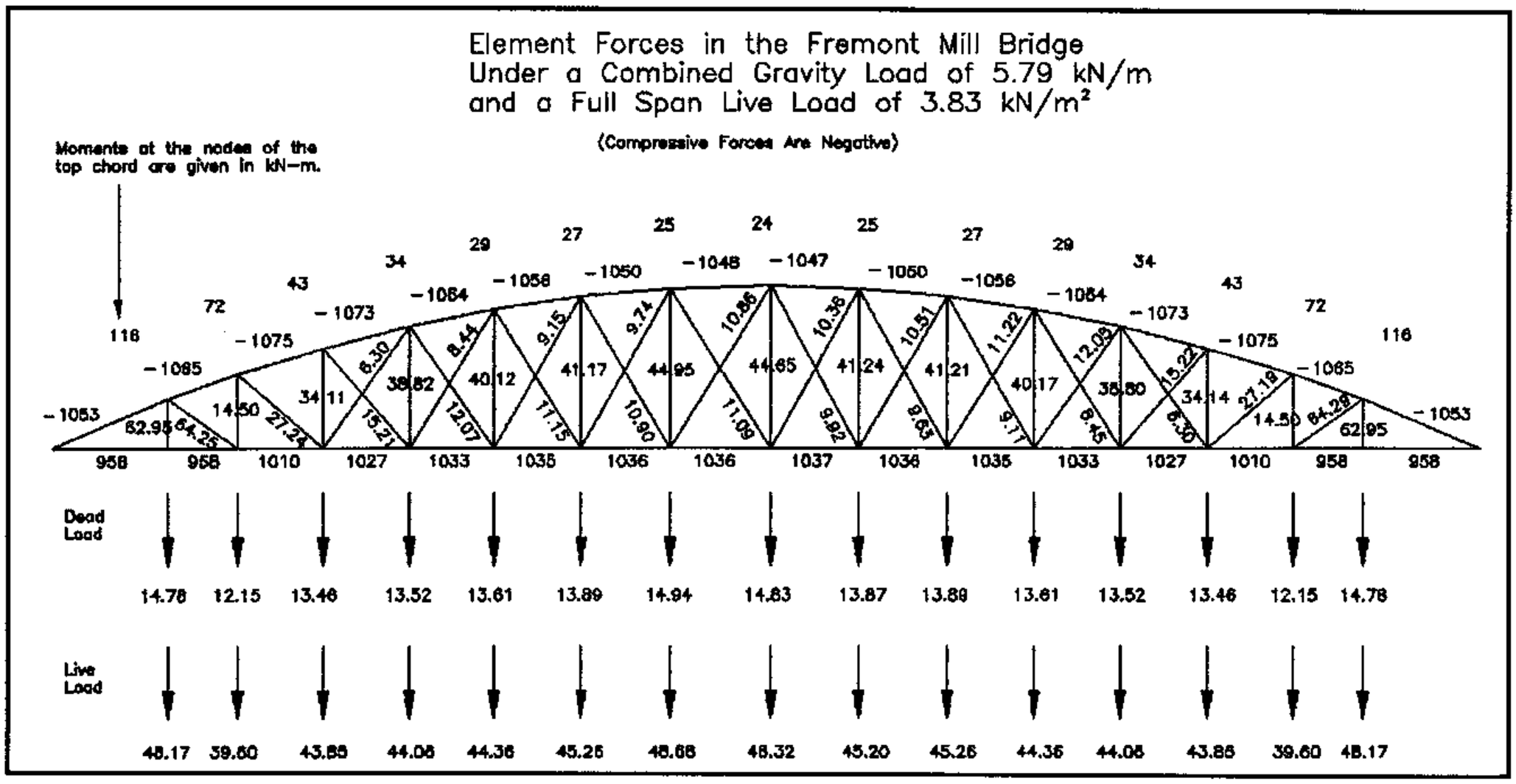


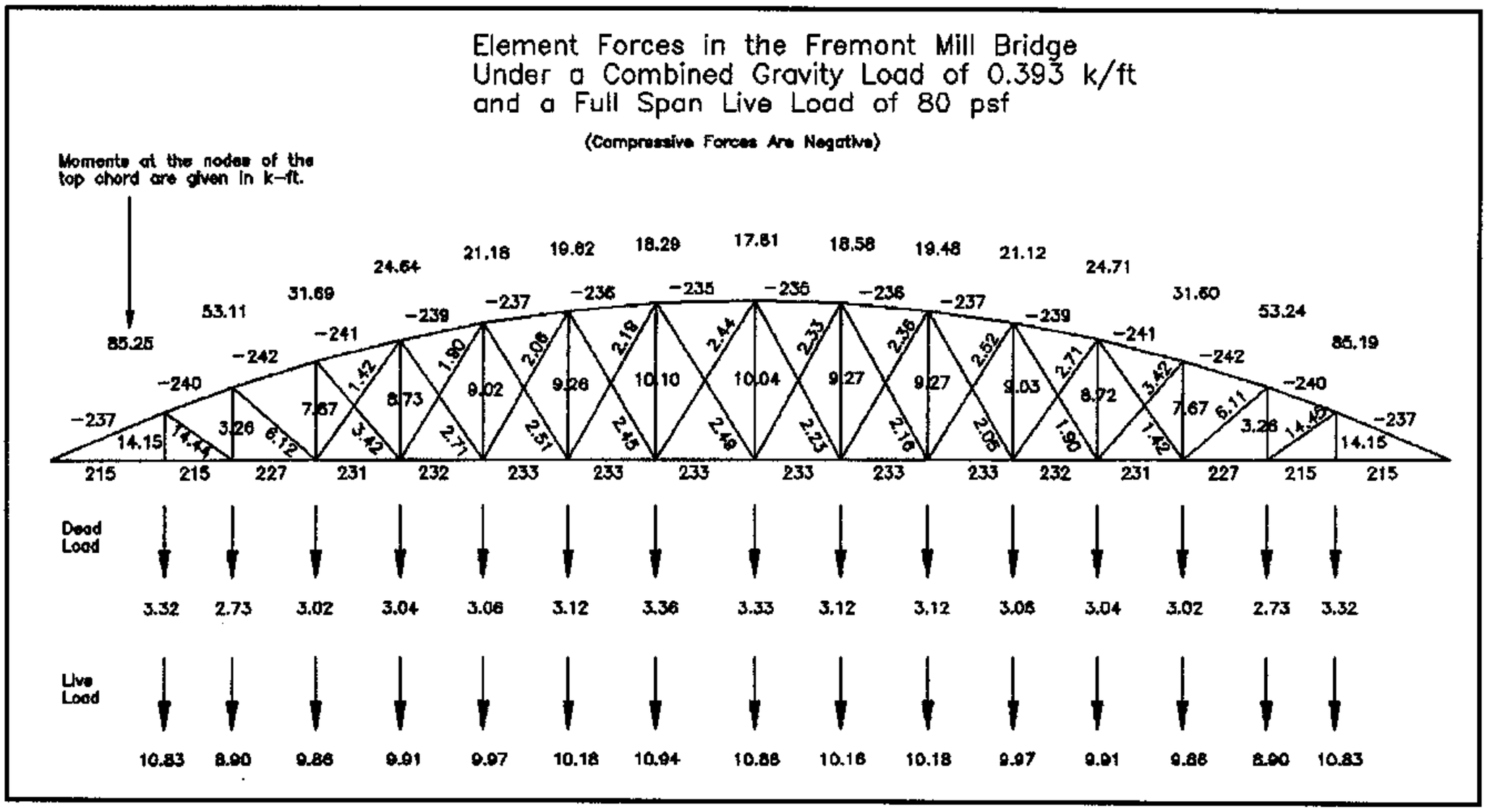

# Joint and Element Numbering Scheme for Static Analysis of the Davenport Bowstring

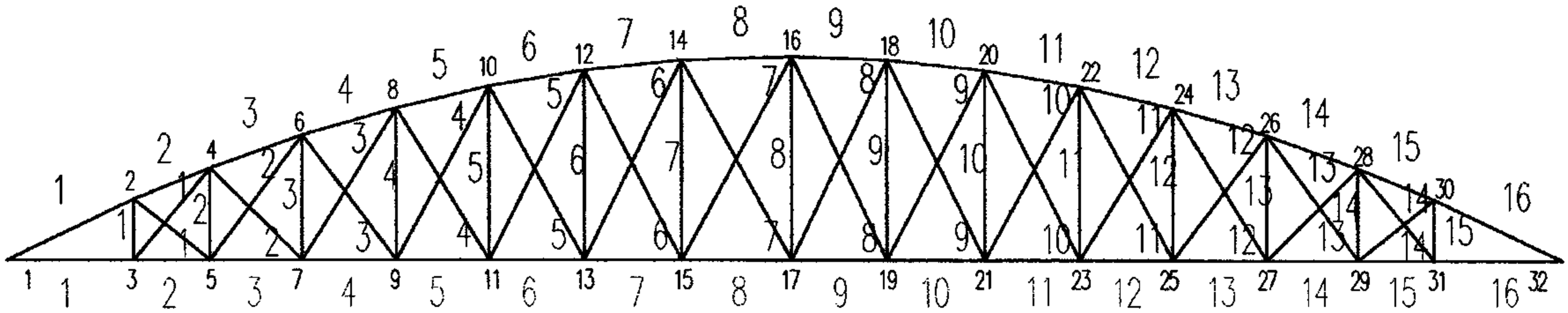

1 = Node Number
1 = Top Chord
1 = Verticals
1 = Bottom Chord
1 = D–Diagonals
1 = U–Diagonals

Elements of a particular type are grouped together, numbered from left to right, and entered into STAN2D in the following order:

1. Top Chord
2. Verticals
3. Bottom Chord
4. D–Diagonals
5. U–Diagonals

## Element Forces and Stresses in Fremont Mill Bridge Under Different Loading Conditions

"% Axial" is the percentage of stress in top chord due to axial force. "—" denotes elements eliminated from analysis.
Negative signs indicate compression.

| Element Type | No. | Gravity Load Force (kN) | Gravity Load Stress (MPa) | Gravity Load % Axial | Gravity + Full-Span Live Load Force (kN) | Gravity + Full-Span Live Load Stress (MPa) | Gravity + Full-Span Live Load % Axial | Gravity + Half-Span Live Load Force (kN) | Gravity + Half-Span Live Load Stress (MPa) | Gravity + Half-Span Live Load % Axial | Concentrated Load, Node 3 Force (kN) | Concentrated Load, Node 3 Stress (MPa) | Concentrated Load, Node 3 % Axial |
|---|---|---|---|---|---|---|---|---|---|---|---|---|---|
| Top | 1 | -247.26 | -50.37 | 0.63 | -1053.28 | -214.36 | 0.63 | -827.20 | -175.26 | 0.61 | -294.10 | -68.55 | 0.55 |
| Top | 2 | -250.04 | -50.73 | 0.64 | -1065.37 | -215.92 | 0.64 | -826.64 | -175.19 | 0.61 | -283.56 | -67.19 | 0.55 |
| Top | 3 | -252.13 | -44.20 | 0.74 | -1075.14 | -187.67 | 0.74 | -823.46 | -148.69 | 0.72 | -281.27 | -49.92 | 0.73 |
| Top | 4 | -250.67 | -39.93 | 0.81 | -1072.67 | -167.66 | 0.83 | -806.84 | -135.40 | 0.77 | -273.73 | -42.28 | 0.84 |
| Top | 5 | -248.51 | -38.04 | 0.84 | -1064.03 | -160.07 | 0.86 | -761.70 | -129.94 | 0.76 | -266.65 | -39.39 | 0.87 |
| Top | 6 | -246.35 | -37.68 | 0.84 | -1055.95 | -155.85 | 0.88 | -753.38 | -124.69 | 0.78 | -261.42 | -37.97 | 0.89 |
| Top | 7 | -244.72 | -37.79 | 0.84 | -1050.13 | -153.67 | 0.88 | -721.40 | -119.46 | 0.78 | -257.87 | -37.48 | 0.89 |
| Top | 8 | -243.84 | -37.75 | 0.83 | -1047.88 | -152.13 | 0.89 | -685.46 | -111.42 | 0.79 | -255.69 | -36.91 | 0.89 |
| Top | 9 | -243.88 | -37.76 | 0.83 | -1046.79 | -152.27 | 0.89 | -639.84 | -92.79 | 0.89 | -254.27 | -36.81 | 0.89 |
| Top | 10 | -244.72 | -37.80 | 0.84 | -1050.01 | -153.52 | 0.88 | -603.25 | -82.74 | 0.94 | -254.19 | -37.00 | 0.89 |
| Top | 11 | -246.35 | -37.89 | 0.84 | -1055.98 | -155.80 | 0.88 | -572.19 | -76.72 | 0.94 | -254.92 | -37.47 | 0.88 |
| Top | 12 | -248.88 | -37.35 | 0.86 | -1064.05 | -160.14 | 0.86 | -547.63 | -73.61 | 0.96 | -256.28 | -38.45 | 0.86 |
| Top | 13 | -251.71 | -37.12 | 0.88 | -1072.89 | -167.58 | 0.83 | -526.48 | -73.76 | 0.93 | -257.85 | -40.23 | 0.83 |
| Top | 14 | -255.40 | -36.47 | 0.90 | -1075.17 | -187.78 | 0.74 | -511.25 | -80.11 | 0.82 | -258.20 | -44.93 | 0.74 |
| Top | 15 | -259.29 | -35.93 | 0.93 | -1065.43 | -215.88 | 0.64 | -491.19 | -90.53 | 0.70 | -255.56 | -51.59 | 0.64 |
| Top | 16 | -264.70 | -35.31 | 0.97 | -1053.31 | -214.31 | 0.63 | -474.57 | -88.36 | 0.69 | -252.41 | -51.18 | 0.64 |
| Vertical | 1 | 14.76 | 9.18 | | 62.95 | 39.10 | | 62.95 | 39.10 | | 36.46 | 23.89 | |
| Vertical | 2 | 3.46 | 2.15 | | 14.50 | 9.01 | | 202.26 | 12.58 | | 3.34 | 2.07 | |
| Vertical | 3 | 9.45 | 5.87 | | 34.11 | 21.19 | | 31.66 | 19.66 | | 7.76 | 4.82 | |
| Vertical | 4 | 11.67 | 7.25 | | 38.82 | 24.11 | | 23.20 | 14.41 | | 8.78 | 5.46 | |
| Vertical | 5 | 12.74 | 7.91 | | 40.12 | 24.92 | | 11.01 | 6.84 | | 9.67 | 6.01 | |
| Vertical | 6 | 13.88 | 8.62 | | 41.17 | 25.57 | | -1.24 | -0.77 | | 10.20 | 6.33 | |
| Vertical | 7 | 14.94 | 9.28 | | 44.95 | 27.92 | | -11.12 | -6.91 | | 10.81 | 6.72 | |
| Vertical | 8 | 14.83 | 9.21 | | 44.65 | 27.73 | | -33.43 | -20.77 | | 10.66 | 6.62 | |
| Vertical | 9 | 13.87 | 8.61 | | 41.24 | 25.81 | | -45.22 | -28.09 | | 9.76 | 6.06 | |
| Vertical | 10 | 13.89 | 8.63 | | 41.21 | 25.60 | | -32.63 | -20.27 | | 9.72 | 6.04 | |
| Vertical | 11 | 13.61 | 8.45 | | 40.17 | 24.95 | | -21.74 | -13.50 | | 9.45 | 5.87 | |
| Vertical | 12 | 13.52 | 8.40 | | 38.80 | 24.10 | | -13.31 | -8.27 | | 9.09 | 5.65 | |
| Vertical | 13 | 13.46 | 8.36 | | 34.14 | 21.20 | | -8.04 | -4.99 | | 7.94 | 4.93 | |
| Vertical | 14 | 12.15 | 7.55 | | 14.50 | 9.00 | | -11.10 | -6.89 | | 3.09 | 1.92 | |
| Vertical | 15 | 14.76 | 9.18 | | 62.95 | 39.10 | | 14.76 | 9.18 | | 14.76 | 9.18 | |
| Bottom | 1 | 224.81 | 58.09 | | 957.72 | 247.47 | | 751.01 | 194.06 | | 265.98 | 68.73 | |
| Bottom | 2 | 224.81 | 58.09 | | 957.72 | 247.47 | | 751.01 | 194.06 | | 264.74 | 68.41 | |
| Bottom | 3 | 237.03 | 61.25 | | 1010.08 | 261.00 | | 778.13 | 201.07 | | 265.54 | 68.61 | |
| Bottom | 4 | 241.56 | 62.42 | | 1026.86 | 265.34 | | 766.63 | 198.10 | | 261.53 | 67.58 | |
| Bottom | 5 | 243.14 | 62.83 | | 1032.37 | 266.76 | | 745.69 | 192.69 | | 258.65 | 66.83 | |
| Bottom | 6 | 243.74 | 62.98 | | 1034.70 | 267.36 | | 718.76 | 185.73 | | 256.39 | 66.25 | |
| Bottom | 7 | 243.75 | 62.98 | | 1035.90 | 267.68 | | 685.38 | 177.10 | | 254.49 | 65.76 | |
| Bottom | 8 | 243.75 | 62.98 | | 1035.67 | 267.62 | | 639.24 | 165.18 | | 252.81 | 65.32 | |
| Bottom | 9 | 243.75 | 62.98 | | 1036.62 | 267.86 | | 600.80 | 155.24 | | 251.81 | 65.07 | |
| Bottom | 10 | 243.75 | 62.98 | | 1036.02 | 267.71 | | 566.46 | 146.37 | | 250.79 | 64.80 | |
| Bottom | 11 | 243.75 | 62.98 | | 1034.72 | 267.37 | | 537.35 | 136.85 | | 249.76 | 64.54 | |
| Bottom | 12 | 243.75 | 62.98 | | 1032.39 | 266.77 | | 512.84 | 132.52 | | 248.62 | 64.24 | |
| Bottom | 13 | 243.75 | 62.98 | | 1026.88 | 265.35 | | 489.85 | 126.58 | | 246.79 | 63.77 | |
| Bottom | 14 | 243.75 | 62.98 | | 1010.15 | 261.02 | | 465.57 | 120.30 | | 242.29 | 62.61 | |
| Bottom | 15 | 243.75 | 62.98 | | 957.75 | 247.48 | | 432.86 | 111.85 | | 229.54 | 59.31 | |
| Bottom | 16 | 243.75 | 62.98 | | 957.75 | 247.48 | | 432.87 | 111.85 | | 229.54 | 59.31 | |
| Diag D | 1 | 14.99 | 52.58 | | 64.25 | 255.45 | | 41.14 | 144.33 | | 6.28 | 22.05 | |
| Diag D | 2 | 6.05 | 21.22 | | 27.24 | 95.57 | | 5.37 | 18.85 | | — | — | |
| Diag D | 3 | 2.43 | 8.53 | | 15.21 | 53.38 | | — | — | | — | — | |
| Diag D | 4 | 1.06 | 3.72 | | 12.07 | 42.36 | | — | — | | — | — | |
| Diag D | 5 | 0.01 | 0.02 | | 11.15 | 39.14 | | — | — | | 0.14 | 0.49 | |
| Diag D | 6 | — | — | | 10.90 | 38.24 | | — | — | | 0.83 | 2.29 | |
| Diag D | 7 | — | — | | 11.09 | 38.91 | | — | — | | 1.28 | 4.48 | |
| Diag D | 8 | — | — | | 9.92 | 34.82 | | — | — | | 1.39 | 4.87 | |
| Diag D | 9 | — | — | | 9.63 | 33.78 | | — | — | | 1.53 | 5.37 | |
| Diag D | 10 | — | — | | 9.11 | 31.95 | | — | — | | 1.59 | 5.57 | |
| Diag D | 11 | — | — | | 8.45 | 29.66 | | — | — | | 1.57 | 5.53 | |
| Diag D | 12 | — | — | | 6.30 | 22.11 | | — | — | | 1.15 | 4.03 | |
| Diag D | 13 | — | — | | — | — | | — | — | | — | — | |
| Diag D | 14 | — | — | | — | — | | — | — | | — | — | |
| Diag U | 1 | — | — | | — | — | | — | — | | 1.81 | 6.35 | |
| Diag U | 2 | — | — | | — | — | | 9.97 | 34.96 | | 6.74 | 23.65 | |
| Diag U | 3 | 0.00 | 0.00 | | 6.30 | 22.10 | | 27.00 | 94.74 | | 6.96 | 24.43 | |
| Diag U | 4 | 0.00 | 0.00 | | 8.44 | 29.60 | | 40.26 | 141.26 | | 5.54 | 19.46 | |
| Diag U | 5 | 0.00 | 0.00 | | 9.15 | 32.09 | | 54.14 | 189.96 | | 4.54 | 15.95 | |
| Diag U | 6 | 0.00 | 0.00 | | 9.74 | 34.17 | | 69.00 | 242.10 | | 4.08 | 14.33 | |
| Diag U | 7 | 0.00 | 0.00 | | 10.86 | 38.12 | | 87.83 | 308.17 | | 4.00 | 14.03 | |
| Diag U | 8 | 0.00 | 0.00 | | 10.36 | 36.36 | | 80.46 | 282.32 | | 3.51 | 12.31 | |
| Diag U | 9 | 0.00 | 0.00 | | 10.51 | 36.87 | | 68.34 | 239.80 | | 3.34 | 11.72 | |
| Diag U | 10 | 0.00 | 0.00 | | 11.22 | 39.35 | | 54.87 | 192.53 | | 3.33 | 11.70 | |
| Diag U | 11 | 0.00 | 0.00 | | 12.05 | 42.29 | | 43.01 | 150.93 | | 3.39 | 11.90 | |
| Diag U | 12 | 0.00 | 0.00 | | 15.22 | 53.40 | | 35.33 | 123.98 | | 4.06 | 14.25 | |
| Diag U | 13 | 0.00 | 0.00 | | 27.19 | 95.39 | | 32.43 | 113.79 | | 6.90 | 24.21 | |
| Diag U | 14 | 0.00 | 0.00 | | 64.29 | 225.58 | | 40.12 | 140.79 | | 15.64 | 54.87 | |

## Element Forces and Stresses in Fremont Mill Bridge Under Different Loading Conditions

"% Axial" is the percentage of stress in top chord due to axial force. "—" denotes elements eliminated from analysis.
Negative signs indicate compression.

| Element Type | No. | Concentrated Load, Node 5 Force (kN) | Stress (MPa) | % Axial | Concentrated Load, Node 7 Force (kN) | Stress (MPa) | % Axial | Concentrated Load, Node 9 Force (kN) | Stress (MPa) | % Axial | Concentrated Load, Node 11 Force (kN) | Stress (MPa) | % Axial |
|---|---|---|---|---|---|---|---|---|---|---|---|---|---|
| Top | 1 | -298.22 | -61.87 | 0.62 | -296.90 | -59.23 | 0.65 | -293.63 | -58.19 | 0.65 | -289.98 | -57.53 | 0.65 |
| Top | 2 | -301.52 | -62.30 | 0.63 | -301.99 | -59.89 | 0.65 | -299.15 | -58.90 | 0.66 | -295.34 | -58.22 | 0.66 |
| Top | 3 | -295.13 | -59.90 | 0.64 | -305.41 | -56.19 | 0.70 | -304.36 | -51.69 | 0.76 | -300.73 | -50.97 | 0.76 |
| Top | 4 | -286.67 | -46.12 | 0.80 | -299.05 | -55.36 | 0.70 | -305.18 | -54.23 | 0.73 | -302.25 | -46.50 | 0.84 |
| Top | 5 | -277.35 | -40.96 | 0.87 | -289.24 | -44.68 | 0.84 | -298.65 | -53.99 | 0.72 | -302.73 | -52.54 | 0.74 |
| Top | 6 | -270.14 | -38.75 | 0.90 | -280.51 | -40.33 | 0.90 | -290.11 | -43.99 | 0.85 | -297.60 | -51.87 | 0.74 |
| Top | 7 | -264.90 | -37.75 | 0.91 | -273.69 | -38.65 | 0.91 | -282.47 | -40.09 | 0.91 | -290.33 | -43.43 | 0.86 |
| Top | 8 | -261.49 | -37.57 | 0.90 | -268.89 | -38.10 | 0.91 | -276.57 | -38.85 | 0.92 | -283.98 | -39.81 | 0.92 |
| Top | 9 | -259.31 | -37.44 | 0.89 | -265.45 | -38.14 | 0.90 | -272.09 | -38.56 | 0.91 | -276.60 | -39.18 | 0.92 |
| Top | 10 | -258.72 | -37.57 | 0.89 | -264.22 | -38.26 | 0.89 | -269.94 | -38.86 | 0.90 | -275.80 | -39.30 | 0.91 |
| Top | 11 | -259.05 | -37.99 | 0.88 | -264.06 | -38.63 | 0.88 | -269.19 | -39.28 | 0.89 | -274.32 | -39.85 | 0.89 |
| Top | 12 | -260.10 | -38.95 | 0.86 | -264.72 | -39.56 | 0.86 | -269.45 | -40.18 | 0.87 | -274.13 | -40.79 | 0.87 |
| Top | 13 | -261.40 | -40.76 | 0.83 | -265.69 | -41.39 | 0.83 | -270.08 | -42.04 | 0.83 | -274.42 | -42.68 | 0.83 |
| Top | 14 | -261.62 | -45.42 | 0.74 | -265.75 | -46.02 | 0.75 | -269.97 | -46.64 | 0.75 | -274.14 | -47.24 | 0.75 |
| Top | 15 | -258.76 | -52.12 | 0.64 | -262.63 | -52.77 | 0.64 | -266.59 | -53.43 | 0.64 | -270.50 | -54.08 | 0.65 |
| Top | 16 | -255.43 | -51.89 | 0.64 | -259.09 | -52.31 | 0.64 | -262.83 | -52.94 | 0.64 | -266.53 | -53.57 | 0.64 |
| Vertical | 1 | 14.76 | 9.18 | | 14.78 | 9.18 | | 14.78 | 9.18 | | 14.78 | 9.18 | |
| Vertical | 2 | 20.78 | 12.91 | | 0.88 | 0.56 | | 0.57 | 0.36 | | 0.74 | 0.46 | |
| Vertical | 3 | 4.51 | 2.80 | | 23.39 | 14.53 | | 5.13 | 3.19 | | 6.26 | 3.89 | |
| Vertical | 4 | 5.78 | 3.59 | | 3.16 | 1.97 | | 23.82 | 14.79 | | 6.46 | 4.01 | |
| Vertical | 5 | 7.49 | 4.65 | | 4.82 | 2.99 | | 3.21 | 2.00 | | 23.99 | 14.90 | |
| Vertical | 6 | 9.02 | 5.60 | | 6.92 | 4.30 | | 4.93 | 3.06 | | 3.99 | 2.48 | |
| Vertical | 7 | 10.73 | 6.67 | | 9.34 | 5.80 | | 7.64 | 4.74 | | 6.15 | 3.82 | |
| Vertical | 8 | 10.85 | 6.74 | | 10.42 | 6.47 | | 9.24 | 5.74 | | 8.02 | 4.98 | |
| Vertical | 9 | 9.80 | 6.09 | | 9.97 | 6.19 | | 9.28 | 5.76 | | 8.37 | 5.20 | |
| Vertical | 10 | 9.75 | 6.05 | | 9.79 | 6.08 | | 9.81 | 6.10 | | 9.29 | 5.77 | |
| Vertical | 11 | 9.46 | 5.87 | | 9.47 | 5.88 | | 9.51 | 5.90 | | 9.52 | 5.92 | |
| Vertical | 12 | 9.08 | 5.64 | | 9.06 | 5.63 | | 9.05 | 5.82 | | 9.05 | 5.62 | |
| Vertical | 13 | 7.90 | 4.91 | | 7.84 | 4.87 | | 7.79 | 4.84 | | 7.74 | 4.81 | |
| Vertical | 14 | 2.90 | 1.80 | | 2.66 | 1.66 | | 2.45 | 1.52 | | 2.22 | 1.38 | |
| Vertical | 15 | 14.76 | 9.18 | | 14.78 | 9.18 | | 14.78 | 9.18 | | 14.78 | 9.18 | |
| Bottom | 1 | 270.97 | 70.02 | | 270.16 | 69.81 | | 267.25 | 69.06 | | 263.92 | 68.20 | |
| Bottom | 2 | 270.97 | 70.02 | | 270.16 | 69.81 | | 267.25 | 69.06 | | 263.92 | 68.20 | |
| Bottom | 3 | 276.37 | 71.93 | | 265.76 | 73.84 | | 283.53 | 73.26 | | 279.96 | 72.34 | |
| Bottom | 4 | 272.09 | 70.31 | | 263.98 | 73.36 | | 290.34 | 75.02 | | 288.09 | 74.44 | |
| Bottom | 5 | 267.38 | 69.09 | | 277.66 | 71.75 | | 287.37 | 74.26 | | 292.10 | 75.48 | |
| Bottom | 6 | 263.86 | 68.18 | | 272.63 | 70.45 | | 281.41 | 72.71 | | 289.35 | 74.77 | |
| Bottom | 7 | 261.17 | 67.49 | | 268.78 | 69.45 | | 276.46 | 71.44 | | 283.88 | 73.35 | |
| Bottom | 8 | 258.58 | 66.82 | | 265.32 | 68.56 | | 271.95 | 70.27 | | 278.45 | 71.95 | |
| Bottom | 9 | 256.80 | 66.36 | | 262.93 | 67.94 | | 268.91 | 69.49 | | 274.75 | 70.99 | |
| Bottom | 10 | 255.25 | 65.96 | | 260.66 | 67.35 | | 266.24 | 68.80 | | 271.55 | 70.17 | |
| Bottom | 11 | 253.79 | 65.58 | | 258.68 | 66.84 | | 263.69 | 68.14 | | 268.67 | 69.42 | |
| Bottom | 12 | 252.30 | 65.19 | | 256.76 | 66.35 | | 261.32 | 67.53 | | 265.84 | 68.69 | |
| Bottom | 13 | 250.16 | 64.64 | | 254.24 | 65.70 | | 258.41 | 66.77 | | 262.53 | 67.84 | |
| Bottom | 14 | 245.31 | 63.39 | | 248.98 | 64.34 | | 252.73 | 65.30 | | 256.43 | 66.26 | |
| Bottom | 15 | 232.31 | 60.03 | | 235.66 | 60.89 | | 239.08 | 61.76 | | 242.46 | 62.65 | |
| Bottom | 16 | 232.31 | 60.03 | | 235.66 | 60.89 | | 239.08 | 61.76 | | 242.46 | 62.65 | |
| Diag D | 1 | 16.23 | 56.96 | | 19.25 | 67.56 | | 19.97 | 70.08 | | 19.68 | 69.06 | |
| Diag D | 2 | — | — | | 7.25 | 25.44 | | 10.42 | 36.58 | | 10.86 | 38.10 | |
| Diag D | 3 | — | — | | — | — | | 5.37 | 18.85 | | 7.46 | 26.18 | |
| Diag D | 4 | — | — | | — | — | | — | — | | 5.41 | 18.99 | |
| Diag D | 5 | — | — | | — | — | | — | — | | — | — | |
| Diag D | 6 | — | — | | — | — | | — | — | | — | — | |
| Diag D | 7 | 0.36 | 1.35 | | — | — | | — | — | | — | — | |
| Diag D | 8 | 0.83 | 2.91 | | 0.00 | 0.00 | | — | — | | — | — | |
| Diag D | 9 | 1.10 | 3.86 | | 0.57 | 1.98 | | — | — | | — | — | |
| Diag D | 10 | 1.26 | 4.43 | | 0.87 | 3.05 | | 0.43 | 1.52 | | — | — | |
| Diag D | 11 | 1.33 | 4.67 | | 1.04 | 3.64 | | 0.74 | 2.58 | | 0.42 | 1.46 | |
| Diag D | 12 | 0.95 | 3.35 | | 0.72 | 2.52 | | 0.48 | 1.67 | | 0.24 | 0.83 | |
| Diag D | 13 | — | — | | — | — | | — | — | | — | — | |
| Diag D | 14 | — | — | | — | — | | — | — | | — | — | |
| Diag U | 1 | — | — | | — | — | | — | — | | — | — | |
| Diag U | 2 | 9.07 | 31.84 | | 0.14 | 0.49 | | — | — | | — | — | |
| Diag U | 3 | 10.93 | 38.35 | | 12.54 | 44.01 | | 1.73 | 6.07 | | — | — | |
| Diag U | 4 | 9.06 | 31.76 | | 12.12 | 42.54 | | 12.43 | 43.62 | | 1.63 | 5.71 | |
| Diag U | 5 | 7.06 | 24.76 | | 10.14 | 35.57 | | 11.99 | 42.05 | | 11.73 | 41.16 | |
| Diag U | 6 | 5.56 | 19.52 | | 7.96 | 27.94 | | 10.23 | 35.91 | | 11.31 | 39.68 | |
| Diag U | 7 | 4.94 | 17.33 | | 6.58 | 23.09 | | 8.58 | 30.09 | | 10.32 | 36.22 | |
| Diag U | 8 | 4.16 | 14.58 | | 5.02 | 17.62 | | 6.36 | 22.32 | | 7.75 | 27.20 | |
| Diag U | 9 | 3.86 | 13.53 | | 4.51 | 15.82 | | 5.31 | 18.64 | | 6.36 | 22.33 | |
| Diag U | 10 | 3.75 | 13.15 | | 4.25 | 14.92 | | 4.81 | 16.86 | | 5.43 | 19.04 | |
| Diag U | 11 | 3.72 | 13.06 | | 4.12 | 14.47 | | 4.54 | 15.93 | | 4.98 | 17.46 | |
| Diag U | 12 | 4.35 | 15.26 | | 4.70 | 16.49 | | 5.06 | 17.74 | | 5.41 | 18.99 | |
| Diag U | 13 | 7.21 | 25.29 | | 7.58 | 26.59 | | 7.96 | 27.92 | | 8.33 | 29.24 | |
| Diag U | 14 | 15.96 | 56.00 | | 16.35 | 57.37 | | 16.75 | 58.76 | | 17.14 | 60.14 | |

## Element Forces and Stresses in Fremont Mill Bridge Under Different Loading Conditions

"% Axial" is the percentage of stress in top chord due to axial force. "—" denotes elements eliminated from analysis.
Negative signs indicate compression.

| Element Type | No. | Concentrated Load, Node 13 Force (kN) | Stress (MPa) | % Axial | Concentrated Load, Node 15 Force (kN) | Stress (MPa) | % Axial | Concentrated Load, Node 17 Force (kN) | Stress (MPa) | % Axial |
|---|---|---|---|---|---|---|---|---|---|---|
| Top | 1 | -286.19 | -56.88 | 0.65 | -282.34 | -56.24 | 0.65 | -277.96 | -55.50 | 0.65 |
| Top | 2 | -291.33 | -57.55 | 0.65 | -287.25 | -56.87 | 0.65 | -282.61 | -56.10 | 0.65 |
| Top | 3 | -296.49 | -50.35 | 0.76 | -292.12 | -49.73 | 0.76 | -287.13 | -49.04 | 0.76 |
| Top | 4 | -298.14 | -45.78 | 0.84 | -293.53 | -45.17 | 0.84 | -288.21 | -44.50 | 0.84 |
| Top | 5 | -299.12 | -44.66 | 0.87 | -294.59 | -43.23 | 0.88 | -288.96 | -42.52 | 0.88 |
| Top | 6 | -300.15 | -51.22 | 0.76 | -296.19 | -44.02 | 0.87 | -290.58 | -41.54 | 0.90 |
| Top | 7 | -296.80 | -50.79 | 0.75 | -298.06 | -50.01 | 0.77 | -293.17 | -42.89 | 0.88 |
| Top | 8 | -290.92 | -42.94 | 0.88 | -296.59 | -49.82 | 0.77 | -296.90 | -49.69 | 0.77 |
| Top | 9 | -285.18 | -40.02 | 0.92 | -291.36 | -42.57 | 0.88 | -296.96 | -49.70 | 0.77 |
| Top | 10 | -281.79 | -39.89 | 0.91 | -287.76 | -40.57 | 0.92 | -293.95 | -43.49 | 0.87 |
| Top | 11 | -279.76 | -40.30 | 0.90 | -285.28 | -40.88 | 0.90 | -291.41 | -41.62 | 0.90 |
| Top | 12 | -278.95 | -41.39 | 0.87 | -284.00 | -41.97 | 0.87 | -289.73 | -42.62 | 0.88 |
| Top | 13 | -278.88 | -43.34 | 0.83 | -283.59 | -43.92 | 0.83 | -288.93 | -44.57 | 0.84 |
| Top | 14 | -278.43 | -47.87 | 0.75 | -282.82 | -48.47 | 0.75 | -287.81 | -49.17 | 0.76 |
| Top | 15 | -274.52 | -54.75 | 0.65 | -278.60 | -55.43 | 0.65 | -283.25 | -56.20 | 0.65 |
| Top | 16 | -270.32 | -54.21 | 0.64 | -274.18 | -54.86 | 0.65 | -278.55 | -55.59 | 0.65 |
| Vertical | 1 | 14.78 | 9.18 | | 14.78 | 9.18 | | 14.78 | 9.18 | |
| Vertical | 2 | 0.97 | 0.60 | | 1.22 | 0.76 | | 1.50 | 0.93 | |
| Vertical | 3 | 6.47 | 4.02 | | 6.75 | 4.19 | | 7.08 | 4.40 | |
| Vertical | 4 | 7.54 | 4.69 | | 7.84 | 4.87 | | 8.29 | 5.15 | |
| Vertical | 5 | 7.02 | 4.36 | | 7.55 | 4.69 | | 8.02 | 4.98 | |
| Vertical | 6 | 24.25 | 15.06 | | 7.38 | 4.58 | | 7.27 | 4.52 | |
| Vertical | 7 | 5.52 | 3.43 | | 25.01 | 15.54 | | 7.45 | 4.63 | |
| Vertical | 8 | 6.89 | 4.28 | | 6.49 | 4.03 | | 24.97 | 15.51 | |
| Vertical | 9 | 7.39 | 4.59 | | 6.56 | 4.07 | | 6.51 | 4.04 | |
| Vertical | 10 | 8.58 | 5.33 | | 7.84 | 4.87 | | 7.17 | 4.45 | |
| Vertical | 11 | 9.13 | 5.67 | | 8.56 | 5.32 | | 7.94 | 4.93 | |
| Vertical | 12 | 9.10 | 5.65 | | 8.70 | 5.40 | | 8.22 | 5.11 | |
| Vertical | 13 | 7.66 | 4.77 | | 7.38 | 4.58 | | 7.04 | 4.38 | |
| Vertical | 14 | 1.98 | 1.23 | | 1.74 | 1.08 | | 1.46 | 0.90 | |
| Vertical | 15 | 14.78 | 9.18 | | 14.78 | 9.18 | | 14.78 | 9.18 | |
| Bottom | 1 | 260.45 | 67.30 | | 256.93 | 66.39 | | 252.92 | 65.35 | |
| Bottom | 2 | 260.45 | 67.30 | | 256.93 | 66.39 | | 252.92 | 65.35 | |
| Bottom | 3 | 276.16 | 71.36 | | 272.30 | 70.36 | | 267.90 | 69.22 | |
| Bottom | 4 | 284.06 | 73.40 | | 279.88 | 72.32 | | 275.10 | 71.09 | |
| Bottom | 5 | 289.17 | 74.72 | | 284.74 | 73.58 | | 279.58 | 72.24 | |
| Bottom | 6 | 292.74 | 75.64 | | 288.95 | 74.66 | | 283.46 | 73.25 | |
| Bottom | 7 | 290.84 | 75.15 | | 292.99 | 75.71 | | 287.80 | 74.32 | |
| Bottom | 8 | 285.02 | 73.65 | | 291.17 | 75.24 | | 291.95 | 75.44 | |
| Bottom | 9 | 280.71 | 72.53 | | 286.64 | 74.07 | | 292.70 | 75.63 | |
| Bottom | 10 | 276.95 | 71.56 | | 282.39 | 72.97 | | 288.42 | 74.53 | |
| Bottom | 11 | 273.63 | 70.71 | | 276.60 | 71.99 | | 284.22 | 73.44 | |
| Bottom | 12 | 270.52 | 69.90 | | 275.10 | 71.09 | | 280.29 | 72.43 | |
| Bottom | 13 | 266.76 | 68.93 | | 270.97 | 70.02 | | 275.75 | 71.25 | |
| Bottom | 14 | 260.23 | 67.24 | | 264.10 | 68.24 | | 268.51 | 69.38 | |
| Bottom | 15 | 245.93 | 63.55 | | 249.46 | 64.46 | | 253.47 | 65.49 | |
| Bottom | 16 | 245.93 | 63.55 | | 249.46 | 64.46 | | 253.46 | 65.49 | |
| Diag D | 1 | 19.28 | 67.66 | | 18.86 | 66.19 | | 18.38 | 64.49 | |
| Diag D | 2 | 10.54 | 36.97 | | 10.12 | 35.51 | | 9.62 | 33.75 | |
| Diag D | 3 | 7.87 | 27.60 | | 7.48 | 26.24 | | 6.89 | 24.18 | |
| Diag D | 4 | 7.06 | 24.78 | | 7.36 | 25.89 | | 6.81 | 23.89 | |
| Diag D | 5 | 6.19 | 21.72 | | 7.65 | 26.85 | | 7.80 | 27.39 | |
| Diag D | 6 | — | — | | 7.13 | 25.03 | | 8.65 | 30.37 | |
| Diag D | 7 | — | — | | — | — | | 8.90 | 31.22 | |
| Diag D | 8 | — | — | | — | — | | — | — | |
| Diag D | 9 | — | — | | — | — | | — | — | |
| Diag D | 10 | — | — | | — | — | | — | — | |
| Diag D | 11 | 0.02 | 0.08 | | — | — | | — | — | |
| Diag D | 12 | — | — | | — | — | | — | — | |
| Diag D | 13 | — | — | | — | — | | — | — | |
| Diag D | 14 | — | — | | — | — | | — | — | |
| Diag U | 1 | — | — | | — | — | | — | — | |
| Diag U | 2 | — | — | | — | — | | — | — | |
| Diag U | 3 | — | — | | — | — | | — | — | |
| Diag U | 4 | — | — | | — | — | | — | — | |
| Diag U | 5 | 0.91 | 3.20 | | — | — | | — | — | |
| Diag U | 6 | 10.73 | 37.65 | | 0.03 | 0.10 | | — | — | |
| Diag U | 7 | 11.06 | 38.81 | | 10.29 | 36.10 | | — | — | |
| Diag U | 8 | 9.03 | 31.68 | | 9.49 | 33.29 | | 8.34 | 29.26 | |
| Diag U | 9 | 7.49 | 26.28 | | 8.46 | 29.68 | | 8.51 | 29.86 | |
| Diag U | 10 | 6.26 | 21.95 | | 7.13 | 25.03 | | 7.92 | 27.80 | |
| Diag U | 11 | 5.45 | 19.14 | | 6.14 | 21.56 | | 6.90 | 24.21 | |
| Diag U | 12 | 5.80 | 20.35 | | 6.35 | 22.29 | | 6.98 | 24.46 | |
| Diag U | 13 | 8.72 | 30.59 | | 9.17 | 32.16 | | 9.67 | 33.94 | |
| Diag U | 14 | 17.55 | 61.56 | | 17.97 | 63.06 | | 18.45 | 64.75 | |

# APPENDIX C: FORT LARAMIE BRIDGE

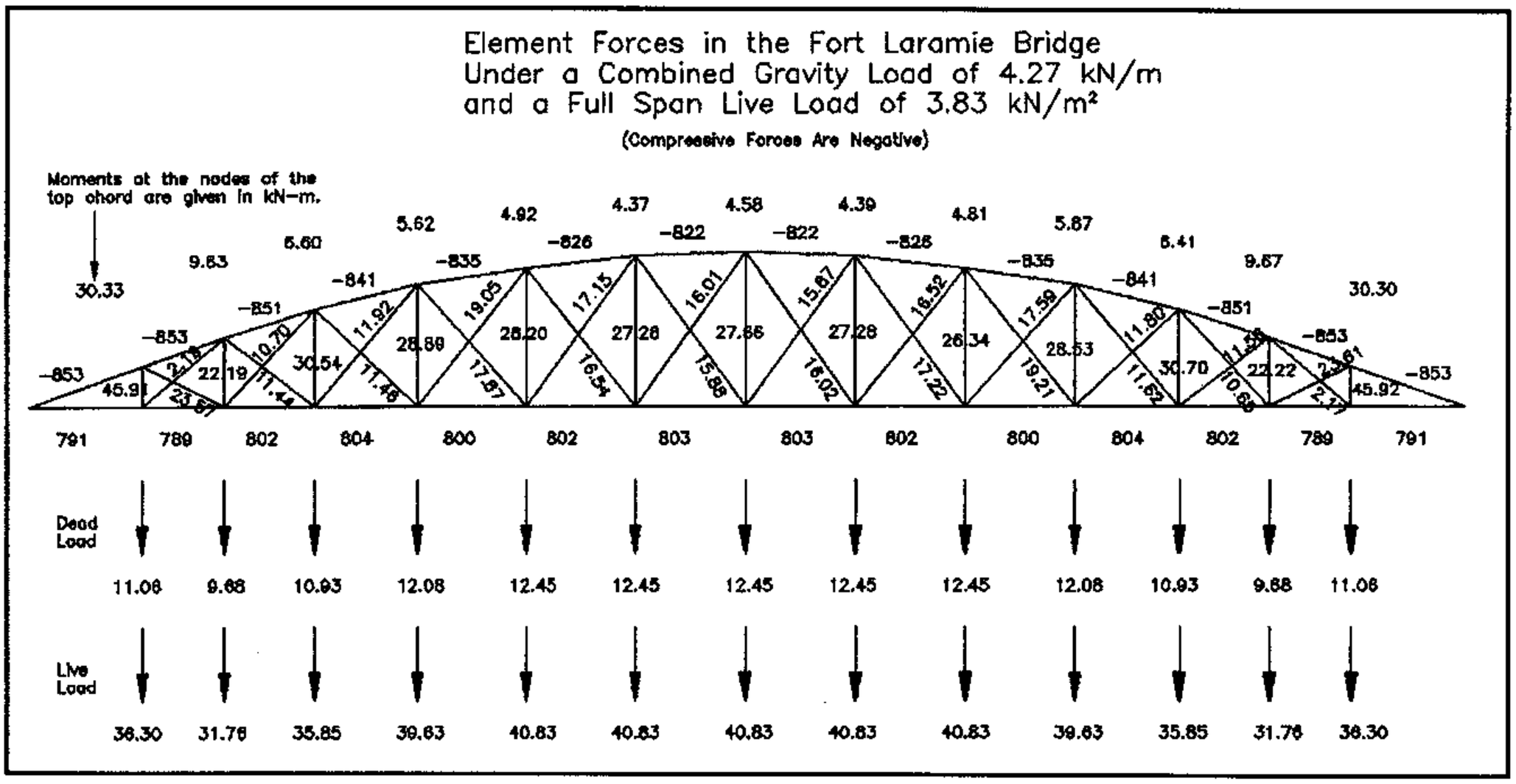


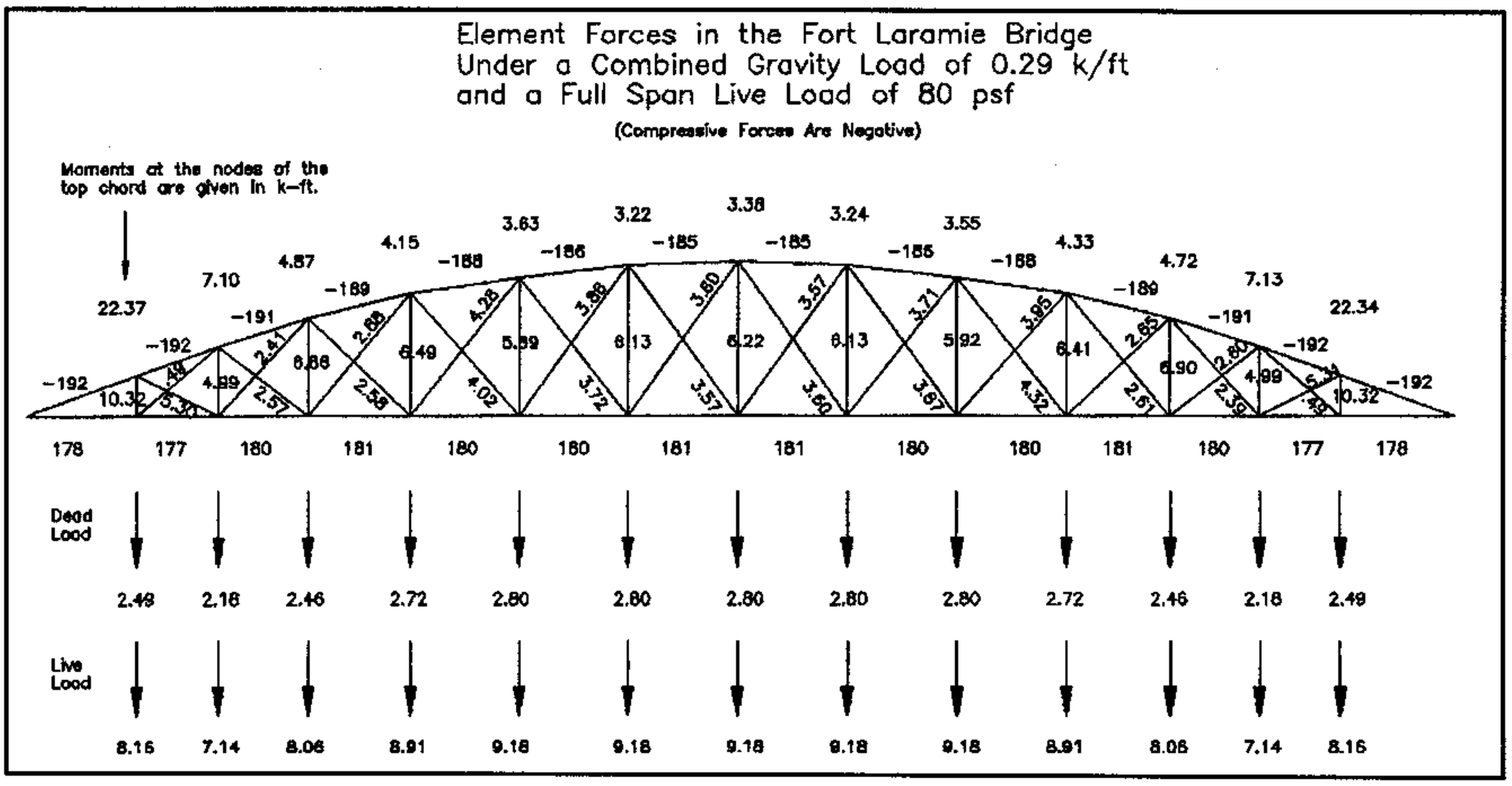

# Joint and Element Numbering Scheme for Static Analysis of King Bowstring

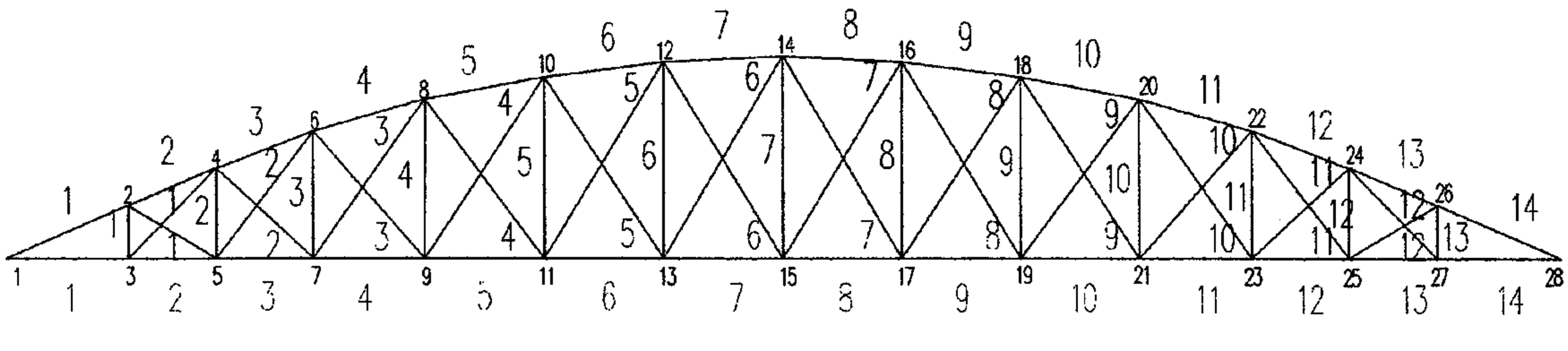

1 = Node Number
1 = Top Chord
1 = Verticals
1 = Bottom Chord
1 = D-Diagonals
1 = U-Diagonals

Elements of a particular type are grouped together, numbered from left to right, and entered into STAN2D in the following order:

1. Top Chord
2. Verticals
3. Bottom Chord
4. D-Diagonals
5. U-Diagonals

## Element Forces and Stresses in Ft. Laramie Bridge Under Different Loading Conditions

"% Axial" is the percentage of stress in top chord due to axial force. "—" denotes elements eliminated from analysis.
Negative signs indicate compression.

| | | Gravity Load | | | Gravity + Full-Span Live Load | | | Gravity + Half-Span Live Load | | | Concentrated Load, Node 3 | | |
|---|---|---|---|---|---|---|---|---|---|---|---|---|---|
| Element Type | No. | Force (kN) | Stress (MPa) | % Axial | Force (kN) | Stress (MPa) | % Axial | Force (kN) | Stress (MPa) | % Axial | Force (kN) | Stress (MPa) | % Axial |
| Top | 1 | -199.28 | -30.42 | 0.60 | -853.12 | -130.23 | 0.60 | -673.87 | -106.65 | 0.58 | -255.01 | -51.33 | 0.46 |
| Top | 2 | -199.24 | -30.42 | 0.60 | -852.93 | -130.21 | 0.60 | -667.89 | -106.05 | 0.58 | -246.43 | -50.54 | 0.45 |
| Top | 3 | -198.78 | -22.11 | 0.83 | -850.96 | -94.63 | 0.83 | -654.25 | -75.85 | 0.79 | -231.94 | -25.34 | 0.84 |
| Top | 4 | -196.35 | -20.67 | 0.87 | -840.57 | -88.49 | 0.87 | -631.50 | -72.16 | 0.80 | -218.64 | -21.28 | 0.94 |
| Top | 5 | -195.04 | -20.16 | 0.89 | -834.95 | -86.31 | 0.89 | -607.17 | -66.49 | 0.84 | -210.59 | -21.66 | 0.89 |
| Top | 6 | -193.04 | -19.70 | 0.90 | -828.38 | -84.32 | 0.90 | -575.89 | -63.62 | 0.83 | -205.30 | -21.17 | 0.89 |
| Top | 7 | -192.04 | -19.47 | 0.91 | -822.11 | -83.35 | 0.91 | -541.73 | -60.44 | 0.82 | -202.21 | -20.42 | 0.91 |
| Top | 8 | -192.04 | -19.47 | 0.91 | -822.12 | -83.35 | 0.91 | -501.27 | -51.39 | 0.90 | -200.78 | -20.29 | 0.91 |
| Top | 9 | -193.05 | -19.65 | 0.90 | -826.44 | -84.13 | 0.90 | -462.63 | -43.51 | 0.98 | -200.74 | -20.36 | 0.91 |
| Top | 10 | -195.08 | -20.26 | 0.88 | -835.14 | -86.74 | 0.88 | -434.41 | -45.64 | 0.87 | -201.99 | -21.01 | 0.88 |
| Top | 11 | -198.37 | -20.60 | 0.88 | -840.63 | -88.17 | 0.88 | -413.51 | -43.72 | 0.87 | -202.67 | -21.16 | 0.88 |
| Top | 12 | -198.74 | -22.12 | 0.83 | -850.80 | -94.68 | 0.83 | -399.69 | -41.00 | 0.90 | -204.61 | -22.70 | 0.80 |
| Top | 13 | -199.18 | -30.40 | 0.60 | -852.67 | -130.12 | 0.60 | -388.87 | -52.48 | 0.68 | -204.69 | -31.11 | 0.60 |
| Top | 14 | -199.22 | -30.40 | 0.60 | -852.86 | -130.14 | 0.60 | -379.54 | -51.60 | 0.68 | -204.55 | -31.10 | 0.60 |
| Vertical | 1 | 10.72 | 17.72 | | 45.91 | 75.88 | | 42.28 | 69.88 | | 25.15 | 41.56 | |
| Vertical | 2 | 5.18 | 8.57 | | 22.19 | 36.68 | | 21.34 | 35.28 | | -1.20 | -1.99 | |
| Vertical | 3 | 7.13 | 11.79 | | 30.54 | 50.47 | | 26.66 | 44.06 | | 3.84 | 6.34 | |
| Vertical | 4 | 6.75 | 9.31 | | 28.89 | 39.84 | | 18.92 | 26.09 | | 6.11 | 8.42 | |
| Vertical | 5 | 6.12 | 7.23 | | 26.20 | 30.94 | | 10.08 | 11.90 | | 6.88 | 8.12 | |
| Vertical | 6 | 6.37 | 6.58 | | 27.28 | 28.18 | | -3.36 | -3.47 | | 6.51 | 6.72 | |
| Vertical | 7 | 6.46 | 5.93 | | 27.66 | 25.37 | | -22.55 | -20.69 | | 6.59 | 6.04 | |
| Vertical | 8 | 6.37 | 6.58 | | 27.28 | 28.19 | | -27.49 | -28.40 | | 6.43 | 6.64 | |
| Vertical | 9 | 6.15 | 7.26 | | 26.34 | 31.10 | | -16.16 | -19.08 | | 6.16 | 7.27 | |
| Vertical | 10 | 6.66 | 9.19 | | 28.53 | 39.35 | | -5.23 | -7.22 | | 6.70 | 9.24 | |
| Vertical | 11 | 7.17 | 11.85 | | 30.70 | 50.75 | | -1.17 | -1.93 | | 7.18 | 11.86 | |
| Vertical | 12 | 5.19 | 8.58 | | 22.22 | 36.72 | | 0.09 | 0.15 | | 5.19 | 8.57 | |
| Vertical | 13 | 10.73 | 17.73 | | 45.92 | 75.91 | | 11.06 | 18.29 | | 10.83 | 17.91 | |
| Bottom | 1 | 184.70 | 35.79 | | 790.69 | 153.23 | | 624.30 | 120.99 | | 235.53 | 45.65 | |
| Bottom | 2 | 184.32 | 35.72 | | 789.04 | 152.92 | | 618.56 | 119.88 | | 223.21 | 43.26 | |
| Bottom | 3 | 187.45 | 38.33 | | 802.47 | 155.52 | | 616.17 | 119.41 | | 213.24 | 41.33 | |
| Bottom | 4 | 187.73 | 36.38 | | 803.64 | 155.74 | | 599.00 | 116.09 | | 207.19 | 40.15 | |
| Bottom | 5 | 186.92 | 36.22 | | 800.17 | 155.07 | | 573.12 | 111.07 | | 202.48 | 39.24 | |
| Bottom | 6 | 187.35 | 36.31 | | 802.04 | 155.44 | | 541.48 | 104.94 | | 199.40 | 38.64 | |
| Bottom | 7 | 187.57 | 36.35 | | 802.97 | 155.62 | | 500.97 | 97.09 | | 197.62 | 38.30 | |
| Bottom | 8 | 187.57 | 36.35 | | 802.98 | 155.62 | | 460.39 | 89.22 | | 196.15 | 38.01 | |
| Bottom | 9 | 187.36 | 36.31 | | 802.07 | 155.44 | | 428.87 | 83.11 | | 194.85 | 37.76 | |
| Bottom | 10 | 186.98 | 36.24 | | 800.45 | 155.13 | | 403.02 | 78.10 | | 193.61 | 37.52 | |
| Bottom | 11 | 187.75 | 36.38 | | 803.73 | 155.76 | | 384.62 | 74.54 | | 193.74 | 37.55 | |
| Bottom | 12 | 187.41 | 36.32 | | 802.28 | 155.48 | | 369.61 | 71.63 | | 192.91 | 37.39 | |
| Bottom | 13 | 184.25 | 35.71 | | 788.78 | 152.87 | | 352.17 | 68.25 | | 189.32 | 36.69 | |
| Bottom | 14 | 184.63 | 35.78 | | 790.40 | 153.18 | | 352.17 | 68.25 | | 189.58 | 36.74 | |
| Diag D | 1 | 5.51 | 19.32 | | 23.57 | 82.71 | | 12.16 | 42.66 | | — | — | |
| Diag D | 2 | 2.67 | 9.38 | | 11.44 | 40.14 | | — | — | | — | — | |
| Diag D | 3 | 2.68 | 9.39 | | 11.46 | 40.21 | | — | — | | — | — | |
| Diag D | 4 | 4.18 | 8.24 | | 17.87 | 35.25 | | — | — | | 0.82 | 1.62 | |
| Diag D | 5 | 3.86 | 7.62 | | 16.54 | 32.62 | | — | — | | 2.09 | 4.13 | |
| Diag D | 6 | 3.71 | 7.32 | | 15.88 | 31.33 | | — | — | | 2.39 | 4.71 | |
| Diag D | 7 | 3.74 | 7.38 | | 16.02 | 31.59 | | — | — | | 2.81 | 5.55 | |
| Diag D | 8 | 4.02 | 7.93 | | 17.22 | 33.98 | | — | — | | 3.36 | 6.64 | |
| Diag D | 9 | 4.49 | 8.85 | | 19.21 | 37.88 | | — | — | | 4.03 | 7.94 | |
| Diag D | 10 | 2.71 | 9.52 | | 11.62 | 40.76 | | — | — | | 2.40 | 8.43 | |
| Diag D | 11 | 2.49 | 8.73 | | 10.65 | 37.35 | | — | — | | 2.27 | 7.98 | |
| Diag D | 12 | 0.51 | 1.78 | | 2.17 | 7.60 | | — | — | | 0.35 | 1.21 | |
| Diag U | 1 | 0.51 | 1.80 | | 2.19 | 7.69 | | 7.67 | 26.90 | | 16.46 | 57.76 | |
| Diag U | 2 | 2.50 | 8.77 | | 10.70 | 37.55 | | 19.32 | 67.77 | | 14.76 | 51.79 | |
| Diag U | 3 | 2.78 | 9.77 | | 11.92 | 41.82 | | 26.45 | 92.82 | | 9.32 | 32.70 | |
| Diag U | 4 | 4.45 | 8.78 | | 19.05 | 37.58 | | 41.78 | 82.40 | | 7.61 | 15.01 | |
| Diag U | 5 | 4.01 | 7.90 | | 17.15 | 33.82 | | 53.55 | 105.61 | | 6.14 | 12.12 | |
| Diag U | 6 | 3.74 | 7.38 | | 16.01 | 31.58 | | 69.64 | 137.35 | | 5.28 | 10.42 | |
| Diag U | 7 | 3.71 | 7.31 | | 15.87 | 31.31 | | 68.68 | 135.47 | | 4.88 | 9.62 | |
| Diag U | 8 | 3.86 | 7.61 | | 16.52 | 32.58 | | 50.88 | 100.36 | | 4.75 | 9.37 | |
| Diag U | 9 | 4.11 | 8.10 | | 17.59 | 34.69 | | 38.55 | 76.05 | | 4.81 | 9.49 | |
| Diag U | 10 | 2.76 | 9.68 | | 11.80 | 41.42 | | 25.26 | 88.64 | | 3.24 | 11.36 | |
| Diag U | 11 | 2.70 | 9.48 | | 11.58 | 40.57 | | 19.28 | 67.64 | | 3.07 | 10.76 | |
| Diag U | 12 | 5.51 | 19.35 | | 23.61 | 82.84 | | 19.91 | 69.84 | | 5.85 | 20.51 | |

## Element Forces and Stresses in Ft. Laramie Bridge Under Different Loading Conditions

"% Axial" is the percentage of stress in top chord due to axial force. "—" denotes elements eliminated from analysis.
Negative signs indicate compression.

| Element Type | No. | Concentrated Load, Node 5 Force (kN) | Stress (MPa) | % Axial | Concentrated Load, Node 7 Force (kN) | Stress (MPa) | % Axial | Concentrated Load, Node 9 Force (kN) | Stress (MPa) | % Axial | Concentrated Load, Node 11 Force (kN) | Stress (MPa) | % Axial |
|---|---|---|---|---|---|---|---|---|---|---|---|---|---|
| Top | 1 | -257.38 | -37.93 | 0.62 | -253.43 | -36.89 | 0.63 | -248.49 | -36.46 | 0.63 | -243.32 | -35.85 | 0.62 |
| Top | 2 | -258.38 | -41.28 | 0.57 | -255.85 | -37.11 | 0.63 | -250.68 | -36.67 | 0.63 | -245.22 | -36.03 | 0.63 |
| Top | 3 | -252.16 | -40.71 | 0.57 | -257.90 | -37.48 | 0.63 | -252.59 | -27.67 | 0.84 | -247.01 | -27.17 | 0.84 |
| Top | 4 | -235.34 | -24.02 | 0.90 | -251.00 | -36.85 | 0.63 | -254.61 | -30.91 | 0.76 | -248.12 | -25.87 | 0.88 |
| Top | 5 | -222.83 | -22.43 | 0.91 | -236.48 | -23.39 | 0.93 | -250.27 | -30.51 | 0.75 | -252.49 | -29.14 | 0.80 |
| Top | 6 | -214.01 | -21.62 | 0.91 | -224.27 | -22.15 | 0.93 | -236.37 | -23.72 | 0.92 | -248.63 | -28.78 | 0.79 |
| Top | 7 | -209.49 | -21.11 | 0.91 | -217.46 | -21.89 | 0.91 | -227.27 | -22.45 | 0.93 | -237.70 | -23.74 | 0.92 |
| Top | 8 | -207.01 | -20.88 | 0.91 | -213.88 | -21.56 | 0.91 | -221.78 | -22.20 | 0.92 | -230.51 | -22.87 | 0.93 |
| Top | 9 | -206.23 | -20.87 | 0.91 | -212.27 | -21.43 | 0.91 | -219.25 | -22.07 | 0.91 | -226.64 | -22.76 | 0.91 |
| Top | 10 | -206.91 | -21.55 | 0.88 | -212.34 | -22.13 | 0.88 | -218.60 | -22.81 | 0.88 | -225.26 | -23.54 | 0.88 |
| Top | 11 | -207.17 | -21.57 | 0.88 | -212.12 | -22.11 | 0.88 | -217.84 | -22.74 | 0.88 | -223.91 | -23.41 | 0.88 |
| Top | 12 | -208.80 | -23.12 | 0.83 | -231.41 | -23.57 | 0.83 | -218.73 | -24.12 | 0.83 | -224.38 | -24.73 | 0.83 |
| Top | 13 | -208.63 | -31.62 | 0.61 | -212.97 | -32.18 | 0.61 | -218.00 | -32.82 | 0.61 | -223.43 | -33.45 | 0.61 |
| Top | 14 | -208.36 | -31.60 | 0.61 | -212.55 | -32.15 | 0.61 | -217.40 | -32.76 | 0.61 | -222.57 | -33.37 | 0.61 |
| Vertical | 1 | 10.02 | 16.57 | | 11.06 | 18.29 | | 11.06 | 18.29 | | 11.06 | 18.29 | |
| Vertical | 2 | 16.33 | 27.00 | | 3.04 | 5.02 | | 5.02 | 8.29 | | 5.01 | 8.28 | |
| Vertical | 3 | -0.67 | -1.10 | | 18.31 | 30.26 | | 6.14 | 10.15 | | 7.22 | 11.93 | |
| Vertical | 4 | 3.03 | 4.17 | | -0.67 | -0.93 | | 17.00 | 23.45 | | 5.65 | 7.80 | |
| Vertical | 5 | 6.33 | 7.48 | | 4.22 | 4.98 | | 1.39 | 1.64 | | 15.89 | 18.76 | |
| Vertical | 6 | 6.78 | 7.01 | | 6.28 | 6.49 | | 4.40 | 4.55 | | 2.40 | 2.48 | |
| Vertical | 7 | 6.65 | 6.10 | | 6.85 | 6.29 | | 6.27 | 5.75 | | 4.96 | 4.55 | |
| Vertical | 8 | 6.47 | 6.69 | | 6.50 | 6.72 | | 6.66 | 6.88 | | 6.38 | 6.59 | |
| Vertical | 9 | 6.17 | 7.28 | | 6.17 | 7.29 | | 6.17 | 7.28 | | 6.22 | 7.34 | |
| Vertical | 10 | 6.72 | 9.27 | | 6.75 | 9.30 | | 6.78 | 9.35 | | 6.80 | 9.38 | |
| Vertical | 11 | 7.18 | 11.87 | | 7.18 | 11.88 | | 7.19 | 11.88 | | 7.19 | 11.88 | |
| Vertical | 12 | 5.18 | 8.57 | | 5.18 | 8.56 | | 5.17 | 8.55 | | 5.14 | 8.49 | |
| Vertical | 13 | 10.91 | 18.03 | | 10.99 | 18.17 | | 11.06 | 18.29 | | 11.06 | 18.29 | |
| Bottom | 1 | 238.64 | 46.25 | | 235.00 | 45.54 | | 230.40 | 44.65 | | 225.60 | 43.72 | |
| Bottom | 2 | 237.46 | 46.02 | | 235.00 | 45.54 | | 230.40 | 44.65 | | 225.60 | 43.72 | |
| Bottom | 3 | 229.66 | 44.51 | | 241.35 | 46.77 | | 238.10 | 46.14 | | 232.71 | 45.10 | |
| Bottom | 4 | 219.77 | 42.59 | | 233.26 | 45.20 | | 241.85 | 46.87 | | 237.12 | 45.95 | |
| Bottom | 5 | 212.63 | 41.21 | | 223.20 | 43.25 | | 235.25 | 45.59 | | 240.27 | 46.56 | |
| Bottom | 6 | 208.15 | 40.34 | | 217.17 | 42.09 | | 227.15 | 44.02 | | 237.58 | 46.04 | |
| Bottom | 7 | 204.78 | 39.69 | | 212.78 | 41.23 | | 221.39 | 42.91 | | 230.39 | 44.65 | |
| Bottom | 8 | 202.28 | 39.20 | | 209.01 | 40.51 | | 216.87 | 42.03 | | 224.91 | 43.59 | |
| Bottom | 9 | 200.19 | 38.80 | | 206.08 | 39.94 | | 212.86 | 41.25 | | 220.12 | 42.66 | |
| Bottom | 10 | 198.34 | 38.44 | | 203.55 | 39.45 | | 209.56 | 40.61 | | 215.94 | 41.85 | |
| Bottom | 11 | 198.02 | 38.38 | | 202.72 | 39.29 | | 208.16 | 40.34 | | 213.94 | 41.46 | |
| Bottom | 12 | 196.84 | 38.15 | | 201.17 | 38.99 | | 206.16 | 39.95 | | 211.46 | 40.98 | |
| Bottom | 13 | 192.95 | 37.39 | | 196.93 | 38.16 | | 201.50 | 39.05 | | 206.31 | 39.98 | |
| Bottom | 14 | 193.12 | 37.43 | | 197.01 | 38.18 | | 201.50 | 39.05 | | 206.31 | 39.98 | |
| Diag D | 1 | 6.84 | 24.01 | | 9.44 | 33.11 | | 9.08 | 31.87 | | 8.65 | 30.34 | |
| Diag D | 2 | — | — | | 5.29 | 18.55 | | 5.97 | 20.94 | | 5.76 | 20.21 | |
| Diag D | 3 | — | — | | — | — | | 7.28 | 25.54 | | 6.48 | 22.74 | |
| Diag D | 4 | — | — | | — | — | | — | — | | 10.79 | 21.27 | |
| Diag D | 5 | 0.58 | 1.14 | | — | — | | — | — | | — | — | |
| Diag D | 6 | 1.47 | 2.91 | | 0.30 | 0.58 | | — | — | | — | — | |
| Diag D | 7 | 2.15 | 4.24 | | 1.44 | 2.83 | | 0.46 | 0.90 | | — | — | |
| Diag D | 8 | 2.90 | 5.71 | | 2.38 | 4.69 | | 1.80 | 3.55 | | 1.10 | 2.17 | |
| Diag D | 9 | 3.70 | 7.29 | | 3.33 | 6.58 | | 2.91 | 5.75 | | 2.48 | 4.89 | |
| Diag D | 10 | 2.18 | 7.66 | | 1.94 | 6.80 | | 1.66 | 5.82 | | 1.36 | 4.77 | |
| Diag D | 11 | 2.12 | 7.45 | | 1.96 | 6.86 | | 1.76 | 6.18 | | 1.54 | 5.41 | |
| Diag D | 12 | 0.23 | 0.81 | | 0.10 | 0.36 | | — | — | | — | — | |
| Diag U | 1 | 1.57 | 5.51 | | — | — | | — | — | | — | — | |
| Diag U | 2 | 20.41 | 71.63 | | 2.84 | 9.97 | | 0.39 | 1.36 | | 0.68 | 2.40 | |
| Diag U | 3 | 15.24 | 53.48 | | 18.80 | 65.98 | | 1.37 | 4.81 | | 0.13 | 0.44 | |
| Diag U | 4 | 11.53 | 22.75 | | 16.24 | 32.04 | | 19.21 | 37.88 | | 2.52 | 4.97 | |
| Diag U | 5 | 7.58 | 14.94 | | 10.20 | 20.12 | | 13.71 | 27.04 | | 16.81 | 33.16 | |
| Diag U | 6 | 6.41 | 12.63 | | 7.58 | 14.95 | | 9.89 | 19.50 | | 12.35 | 24.35 | |
| Diag U | 7 | 5.71 | 11.26 | | 6.64 | 13.09 | | 7.66 | 15.11 | | 9.28 | 18.31 | |
| Diag U | 8 | 5.39 | 10.62 | | 6.08 | 12.00 | | 6.90 | 13.61 | | 7.73 | 15.25 | |
| Diag U | 9 | 5.32 | 10.49 | | 5.87 | 11.58 | | 6.51 | 12.84 | | 7.19 | 14.19 | |
| Diag U | 10 | 3.58 | 12.57 | | 3.96 | 13.90 | | 4.40 | 15.43 | | 4.86 | 17.05 | |
| Diag U | 11 | 3.33 | 11.68 | | 3.62 | 12.69 | | 3.95 | 13.87 | | 4.32 | 15.15 | |
| Diag U | 12 | 6.08 | 21.35 | | 6.34 | 22.26 | | 6.67 | 23.40 | | 7.07 | 24.80 | |

## Element Forces and Stresses in Ft. Laramie Bridge Under Different Loading Conditions

"% Axial" is the percentage of stress in top chord due to axial force. "—" denotes elements eliminated from analysis.
Negative signs indicate compression.

| Element Type | No. | Concentrated Load, Node 13 Force (kN) | Stress (MPa) | % Axial | Concentrated Load, Node 15 Force (kN) | Stress (MPa) | % Axial |
|---|---|---|---|---|---|---|---|
| Top | 1 | -238.15 | -35.24 | 0.62 | -232.97 | -34.62 | 0.62 |
| Top | 2 | -239.79 | -35.39 | 0.62 | -234.36 | -34.75 | 0.62 |
| Top | 3 | -241.36 | -26.54 | 0.84 | -235.71 | -25.93 | 0.83 |
| Top | 4 | -242.13 | -25.22 | 0.88 | -236.04 | -24.66 | 0.88 |
| Top | 5 | -245.04 | -25.48 | 0.88 | -238.50 | -24.88 | 0.88 |
| Top | 6 | -249.52 | -28.33 | 0.81 | -241.56 | -24.00 | 0.92 |
| Top | 7 | -247.73 | -28.16 | 0.81 | -247.83 | -28.07 | 0.81 |
| Top | 8 | -239.35 | -23.97 | 0.92 | -247.83 | -28.07 | 0.81 |
| Top | 9 | -234.02 | -23.49 | 0.92 | -241.56 | -24.00 | 0.92 |
| Top | 10 | -231.92 | -24.26 | 0.88 | -238.56 | -25.01 | 0.88 |
| Top | 11 | -229.99 | -24.08 | 0.88 | -236.07 | -24.78 | 0.88 |
| Top | 12 | -230.02 | -25.34 | 0.83 | -235.67 | -25.95 | 0.83 |
| Top | 13 | -228.86 | -34.09 | 0.62 | -234.30 | -34.73 | 0.62 |
| Top | 14 | -227.74 | -33.99 | 0.62 | -232.91 | -34.60 | 0.62 |
| Vertical | 1 | 11.06 | 18.29 | | 11.06 | 18.29 | |
| Vertical | 2 | 5.03 | 8.32 | | 5.07 | 8.38 | |
| Vertical | 3 | 7.14 | 11.80 | | 7.13 | 11.79 | |
| Vertical | 4 | 7.15 | 9.86 | | 7.00 | 9.66 | |
| Vertical | 5 | 4.82 | 5.69 | | 6.04 | 7.13 | |
| Vertical | 6 | 16.89 | 17.44 | | 4.94 | 5.10 | |
| Vertical | 7 | 3.59 | 3.29 | | 17.55 | 16.10 | |
| Vertical | 8 | 5.72 | 5.91 | | 4.96 | 5.12 | |
| Vertical | 9 | 6.34 | 7.49 | | 6.09 | 7.19 | |
| Vertical | 10 | 6.82 | 9.40 | | 6.90 | 9.52 | |
| Vertical | 11 | 7.19 | 11.88 | | 7.18 | 11.87 | |
| Vertical | 12 | 5.11 | 8.44 | | 5.06 | 8.39 | |
| Vertical | 13 | 11.06 | 18.29 | | 11.06 | 18.29 | |
| Bottom | 1 | 220.79 | 42.79 | | 215.99 | 41.86 | |
| Bottom | 2 | 220.79 | 42.79 | | 215.99 | 41.86 | |
| Bottom | 3 | 227.41 | 44.07 | | 222.11 | 43.04 | |
| Bottom | 4 | 231.23 | 44.81 | | 225.45 | 43.69 | |
| Bottom | 5 | 235.17 | 45.57 | | 228.66 | 44.31 | |
| Bottom | 6 | 240.66 | 46.64 | | 234.47 | 45.44 | |
| Bottom | 7 | 239.21 | 46.36 | | 240.39 | 46.59 | |
| Bottom | 8 | 232.73 | 45.10 | | 240.40 | 46.59 | |
| Bottom | 9 | 227.42 | 44.07 | | 234.49 | 45.44 | |
| Bottom | 10 | 222.32 | 43.08 | | 228.74 | 44.33 | |
| Bottom | 11 | 219.71 | 42.58 | | 225.49 | 43.70 | |
| Bottom | 12 | 216.76 | 42.01 | | 222.06 | 43.04 | |
| Bottom | 13 | 211.11 | 40.91 | | 215.91 | 41.84 | |
| Bottom | 14 | 211.11 | 40.91 | | 215.91 | 41.84 | |
| Diag D | 1 | 8.25 | 28.96 | | 7.85 | 27.55 | |
| Diag D | 2 | 5.37 | 18.83 | | 5.01 | 17.57 | |
| Diag D | 3 | 6.17 | 21.66 | | 5.68 | 19.94 | |
| Diag D | 4 | 9.12 | 17.99 | | 8.65 | 17.06 | |
| Diag D | 5 | 11.23 | 22.15 | | 9.56 | 18.86 | |
| Diag D | 6 | — | — | | 12.33 | 24.32 | |
| Diag D | 7 | — | — | | — | — | |
| Diag D | 8 | 0.31 | 0.61 | | — | — | |
| Diag D | 9 | 2.06 | 4.05 | | 1.55 | 3.05 | |
| Diag D | 10 | 1.06 | 3.72 | | 0.77 | 2.70 | |
| Diag D | 11 | 1.32 | 4.64 | | 1.10 | 3.88 | |
| Diag D | 12 | — | — | | — | — | |
| Diag U | 1 | — | — | | — | — | |
| Diag U | 2 | 0.91 | 3.19 | | 1.12 | 3.94 | |
| Diag U | 3 | 0.56 | 1.96 | | 0.86 | 3.01 | |
| Diag U | 4 | 0.89 | 1.75 | | 1.49 | 2.95 | |
| Diag U | 5 | 1.07 | 2.11 | | — | — | |
| Diag U | 6 | 14.44 | 28.48 | | — | — | |
| Diag U | 7 | 10.98 | 21.66 | | 12.32 | 24.31 | |
| Diag U | 8 | 8.57 | 16.90 | | 9.54 | 18.82 | |
| Diag U | 9 | 7.88 | 15.55 | | 8.57 | 16.90 | |
| Diag U | 10 | 5.32 | 18.67 | | 5.78 | 20.29 | |
| Diag U | 11 | 4.68 | 16.42 | | 5.04 | 17.69 | |
| Diag U | 12 | 7.47 | 26.20 | | 7.87 | 27.60 | |

# APPENDIX D: FREEPORT BRIDGE

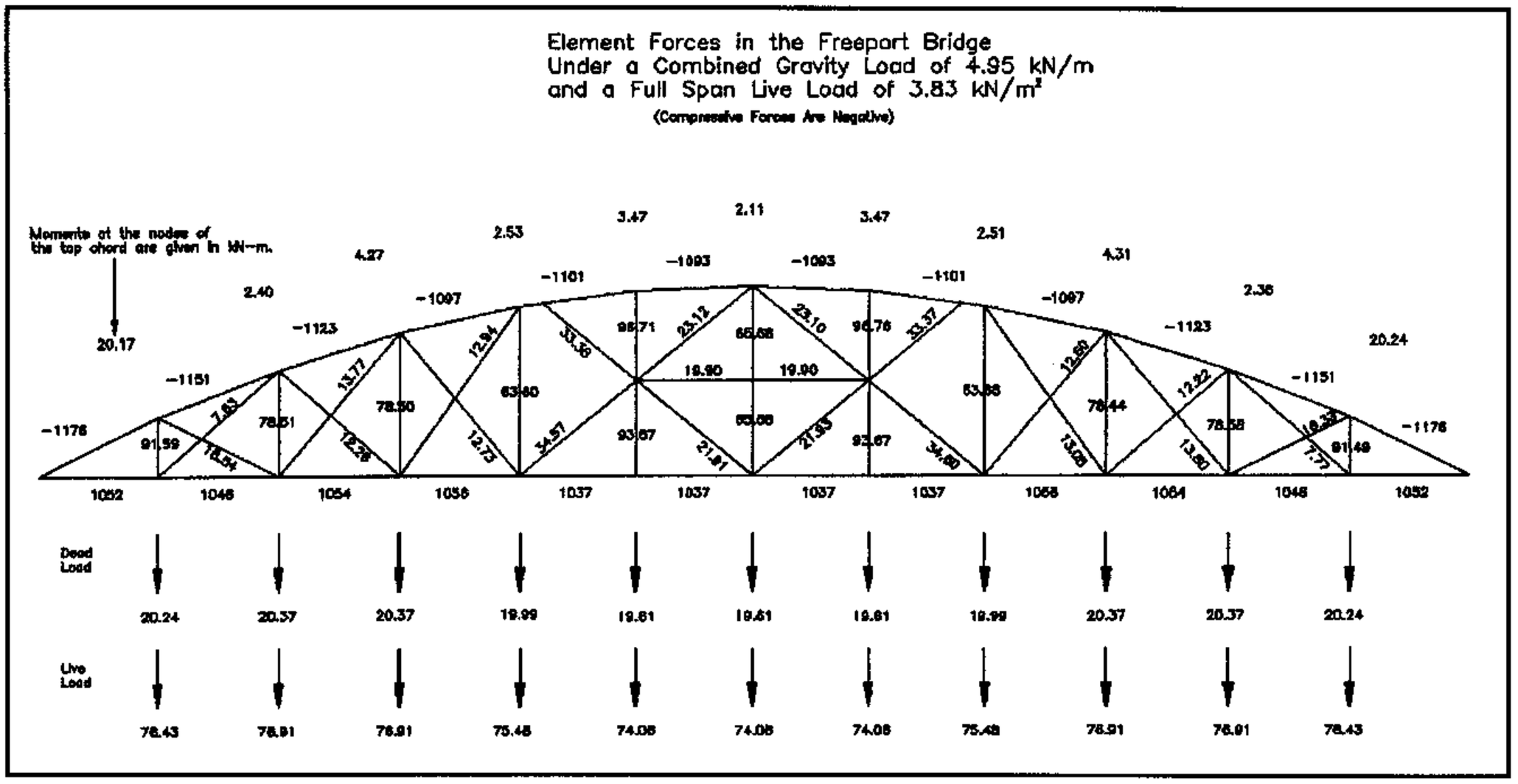


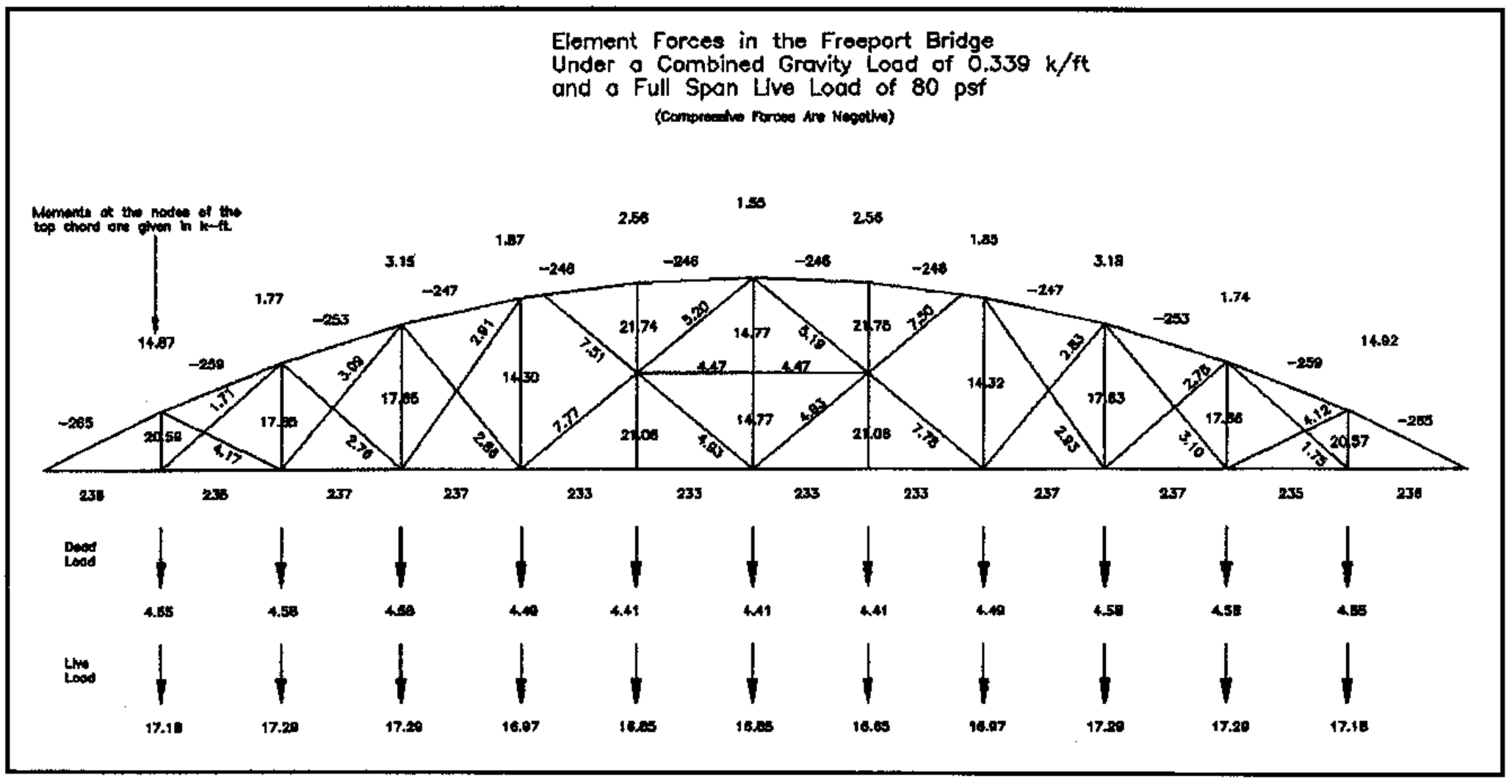

# Joint and Element Numbering Scheme for Static Analysis of Hammond Bowstring

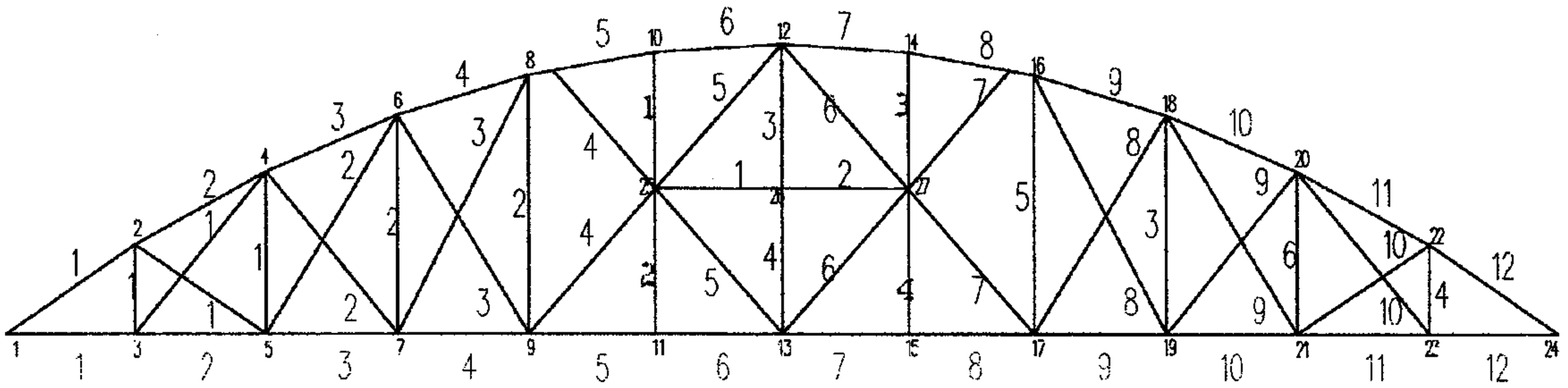

1 = Node Number
1 = Top Chord
1 = Angle Verticals
1 = Web Verticals
1 = Square Verticals
1 = Bottom Chord
1 = D-Diagonals
1 = U-Diagonals
1 = Horizontal Braces

Elements of a particular type are grouped numbered from left to right, and entered into STAN2D in the following order:

1. Top Chord
2. Angle Verticals
3. Web Verticals
4. Square Verticals
5. Bottom Chord
6. D-Diagonals
7. U-Diagonals
8. Horizontal Braces

## Element Forces and Stresses in Freeport Bridge Under Different Loading Conditions

"% Axial" is the percentage of stress in top chord due to axial force. "—" denotes elements eliminated from analysis.
Negative signs indicate compression.

| Element Type | No. | Gravity Load Force (kN) | Gravity Load Stress (MPa) | Gravity Load % Axial | Gravity + Full-Span Live Load Force (kN) | Gravity + Full-Span Live Load Stress (MPa) | Gravity + Full-Span Live Load % Axial | Gravity + Half-Span Live Load Force (kN) | Gravity + Half-Span Live Load Stress (MPa) | Gravity + Half-Span Live Load % Axial | Concentrated Load, Node 3 Force (kN) | Concentrated Load, Node 3 Stress (MPa) | Concentrated Load, Node 3 % Axial |
|---|---|---|---|---|---|---|---|---|---|---|---|---|---|
| Top | 1 | -246.34 | -31.36 | 0.69 | -1176.46 | -149.77 | 0.69 | -921.78 | -123.60 | 0.66 | -294.70 | -51.89 | 0.50 |
| Top | 2 | -240.94 | -30.89 | 0.69 | -1150.71 | -147.51 | 0.69 | -887.25 | -120.56 | 0.65 | -282.28 | -50.79 | 0.49 |
| Top | 3 | -235.18 | -22.76 | 0.91 | -1123.17 | -108.69 | 0.91 | -848.85 | -100.54 | 0.74 | -258.13 | -27.39 | 0.83 |
| Top | 4 | -229.70 | -22.28 | 0.91 | -1097.03 | -106.39 | 0.91 | -797.67 | -122.27 | 0.57 | -243.64 | -23.16 | 0.93 |
| Top | 5 | -230.58 | -21.97 | 0.92 | -1101.19 | -104.91 | 0.92 | -759.63 | -160.51 | 0.42 | -239.93 | -22.94 | 0.92 |
| Top | 6 | -228.80 | -21.81 | 0.92 | -1092.73 | -104.17 | 0.92 | -751.24 | -159.77 | 0.41 | -238.08 | -22.77 | 0.92 |
| Top | 7 | -228.80 | -21.81 | 0.92 | -1092.72 | -104.17 | 0.92 | -644.75 | -120.11 | 0.47 | -235.64 | -22.37 | 0.93 |
| Top | 8 | -230.57 | -21.97 | 0.92 | -1101.18 | -104.91 | 0.92 | -647.84 | -120.39 | 0.47 | -237.47 | -22.53 | 0.93 |
| Top | 9 | -229.73 | -22.30 | 0.91 | -1097.14 | -106.48 | 0.91 | -550.69 | -97.33 | 0.50 | -235.43 | -22.74 | 0.91 |
| Top | 10 | -235.22 | -22.78 | 0.91 | -1123.36 | -108.79 | 0.91 | -528.82 | -60.44 | 0.77 | -240.44 | -23.18 | 0.91 |
| Top | 11 | -241.02 | -30.93 | 0.69 | -1151.08 | -141.71 | 0.69 | -511.98 | -55.22 | 0.82 | -245.88 | -31.42 | 0.69 |
| Top | 12 | -246.43 | -31.40 | 0.69 | -1176.92 | -149.98 | 0.69 | -501.87 | -54.33 | 0.81 | -251.12 | -31.88 | 0.69 |
| Angle Vert | 1 | 19.18 | 10.84 | | 91.59 | 51.75 | | 84.07 | 47.50 | | 30.33 | 17.13 | |
| Angle Vert | 2 | 16.44 | 9.29 | | 78.50 | 44.35 | | 55.08 | 31.12 | | 15.15 | 8.56 | |
| Angle Vert | 3 | 16.42 | 9.28 | | 78.44 | 44.32 | | -6.61 | -3.73 | | 16.47 | 9.31 | |
| Angle Vert | 4 | 19.16 | 10.82 | | 91.49 | 51.69 | | 20.24 | 11.44 | | 19.28 | 10.89 | |
| Web Vert | 1 | 16.44 | 10.21 | | 78.51 | 48.76 | | 62.09 | 38.57 | | 10.39 | 6.46 | |
| Web Vert | 2 | 13.32 | 8.27 | | 63.60 | 39.50 | | 7.22 | 4.49 | | 13.42 | 8.34 | |
| Web Vert | 3 | 13.75 | 8.54 | | 65.68 | 40.80 | | -32.66 | -28.69 | | 13.98 | 8.68 | |
| Web Vert | 4 | 13.75 | 8.54 | | 65.68 | 40.79 | | -32.66 | -28.69 | | 13.98 | 8.68 | |
| Web Vert | 5 | 13.33 | 8.28 | | 63.68 | 39.55 | | -17.52 | -10.88 | | 13.40 | 8.32 | |
| Web Vert | 6 | 16.45 | 10.22 | | 78.58 | 48.81 | | 7.68 | 4.77 | | 16.52 | 10.26 | |
| Square Vert | 1 | 20.25 | 31.39 | | 96.71 | 149.93 | | 93.65 | 145.20 | | 21.19 | 32.85 | |
| Square Vert | 2 | 19.61 | 30.41 | | 93.67 | 145.23 | | 93.67 | 145.23 | | 19.61 | 30.41 | |
| Square Vert | 3 | 20.26 | 31.41 | | 96.76 | 150.02 | | 38.53 | 59.73 | | 20.84 | 32.32 | |
| Square Vert | 4 | 19.61 | 30.41 | | 93.67 | 145.23 | | 19.61 | 30.41 | | 19.61 | 30.41 | |
| Bottom | 1 | 220.22 | 42.68 | | 1051.73 | 203.82 | | 823.78 | 159.65 | | 262.84 | 50.94 | |
| Bottom | 2 | 219.03 | 42.45 | | 1046.05 | 202.72 | | 809.69 | 156.92 | | 246.17 | 47.71 | |
| Bottom | 3 | 220.68 | 42.77 | | 1053.92 | 204.25 | | 780.55 | 151.27 | | 237.91 | 46.11 | |
| Bottom | 4 | 221.04 | 42.84 | | 1055.64 | 204.58 | | 751.02 | 145.55 | | 234.25 | 45.40 | |
| Bottom | 5 | 217.17 | 42.09 | | 1037.15 | 201.00 | | 644.65 | 124.93 | | 226.34 | 43.86 | |
| Bottom | 6 | 217.17 | 42.09 | | 1037.15 | 201.00 | | 644.65 | 124.93 | | 226.34 | 43.86 | |
| Bottom | 7 | 217.16 | 42.09 | | 1037.13 | 201.00 | | 536.24 | 103.92 | | 223.63 | 43.34 | |
| Bottom | 8 | 217.16 | 42.09 | | 1037.13 | 201.00 | | 536.24 | 103.92 | | 223.63 | 43.34 | |
| Bottom | 9 | 221.05 | 42.84 | | 1055.72 | 204.60 | | 505.17 | 97.90 | | 226.48 | 43.89 | |
| Bottom | 10 | 220.71 | 42.77 | | 1054.10 | 204.28 | | 475.00 | 92.05 | | 225.54 | 43.71 | |
| Bottom | 11 | 219.11 | 42.46 | | 1046.45 | 202.80 | | 449.12 | 87.04 | | 223.44 | 43.30 | |
| Bottom | 12 | 220.33 | 42.70 | | 1052.24 | 203.92 | | 449.12 | 87.04 | | 224.52 | 43.51 | |
| Diag D | 1 | 3.88 | 13.62 | | 18.54 | 65.06 | | — | — | | — | — | |
| Diag D | 2 | 2.57 | 9.01 | | 12.26 | 43.03 | | — | — | | — | — | |
| Diag D | 3 | 2.66 | 9.35 | | 12.73 | 44.65 | | — | — | | — | — | |
| Diag D | 4 | 6.99 | 10.84 | | 33.38 | 51.76 | | — | — | | 4.30 | 6.67 | |
| Diag D | 5 | 4.59 | 7.11 | | 21.91 | 33.97 | | — | — | | 2.65 | 4.11 | |
| Diag D | 6 | 4.84 | 7.50 | | 23.10 | 35.81 | | — | — | | 3.62 | 5.61 | |
| Diag D | 7 | 7.24 | 11.23 | | 34.60 | 53.64 | | — | — | | 6.40 | 9.93 | |
| Diag D | 8 | 2.73 | 9.59 | | 13.05 | 45.78 | | — | — | | 2.29 | 8.04 | |
| Diag D | 9 | 2.89 | 10.14 | | 13.80 | 48.44 | | — | — | | 2.60 | 9.14 | |
| Diag D | 10 | 1.63 | 5.71 | | 7.77 | 27.28 | | — | — | | 1.45 | 5.08 | |
| Diag U | 1 | 1.60 | 5.60 | | 7.63 | 26.76 | | 18.91 | 66.35 | | 22.37 | 78.50 | |
| Diag U | 2 | 2.88 | 10.11 | | 13.77 | 48.30 | | 45.68 | 160.29 | | 12.95 | 45.44 | |
| Diag U | 3 | 2.71 | 9.51 | | 12.94 | 45.40 | | 51.50 | 180.71 | | 6.37 | 22.35 | |
| Diag U | 4 | 7.24 | 11.22 | | 34.57 | 53.60 | | 138.21 | 214.28 | | 10.28 | 15.94 | |
| Diag U | 5 | 4.84 | 7.50 | | 23.12 | 35.84 | | 138.23 | 214.31 | | 6.78 | 10.51 | |
| Diag U | 6 | 4.59 | 7.12 | | 21.93 | 34.00 | | 139.86 | 216.84 | | 6.17 | 9.57 | |
| Diag U | 7 | 6.99 | 10.83 | | 33.37 | 51.73 | | 128.61 | 199.40 | | 8.20 | 12.71 | |
| Diag U | 8 | 2.64 | 9.25 | | 12.60 | 44.20 | | 48.71 | 170.91 | | 3.26 | 11.42 | |
| Diag U | 9 | 2.56 | 8.97 | | 12.22 | 42.86 | | 40.47 | 141.99 | | 3.03 | 10.62 | |
| Diag U | 10 | 3.84 | 13.47 | | 18.33 | 64.32 | | 28.83 | 101.15 | | 4.19 | 14.69 | |
| Horizontal | 1 | 4.17 | 6.46 | | 19.90 | 30.85 | | — | — | | 4.26 | 6.60 | |
| Horizontal | 2 | 4.17 | 6.46 | | 19.90 | 30.85 | | — | — | | 4.26 | 6.60 | |

## Element Forces and Stresses in Freeport Bridge Under Different Loading Conditions

"% Axial" is the percentage of stress in top chord due to axial force. "—" denotes elements eliminated from analysis.
Negative signs indicate compression.

| Element Type | No. | Concentrated Load, Node 5 Force (kN) | Stress (MPa) | % Axial | Concentrated Load, Node 7 Force (kN) | Stress (MPa) | % Axial | Concentrated Load, Node 9 Force (kN) | Stress (MPa) | % Axial | Concentrated Load, Node 11 Force (kN) | Stress (MPa) | % Axial |
|---|---|---|---|---|---|---|---|---|---|---|---|---|---|
| Top | 1 | -293.37 | -34.13 | 0.76 | -288.18 | -35.91 | 0.71 | -283.50 | -35.13 | 0.71 | -278.93 | -34.68 | 0.71 |
| Top | 2 | -289.29 | -37.63 | 0.68 | -284.57 | -35.60 | 0.70 | -279.49 | -34.78 | 0.71 | -274.76 | -34.31 | 0.71 |
| Top | 3 | -279.77 | -36.79 | 0.67 | -282.10 | -36.39 | 0.68 | -276.64 | -25.58 | 0.95 | -271.55 | -25.47 | 0.94 |
| Top | 4 | -259.79 | -24.13 | 0.95 | -274.12 | -35.69 | 0.68 | -275.30 | -29.32 | 0.83 | -269.67 | -25.31 | 0.94 |
| Top | 5 | -249.27 | -24.03 | 0.91 | -260.14 | -27.28 | 0.84 | -270.97 | -28.94 | 0.82 | -280.07 | -30.85 | 0.80 |
| Top | 6 | -247.32 | -23.86 | 0.91 | -258.05 | -25.00 | 0.91 | -268.95 | -25.00 | 0.95 | -277.83 | -30.66 | 0.80 |
| Top | 7 | -242.55 | -22.94 | 0.93 | -249.54 | -23.51 | 0.93 | -256.48 | -23.97 | 0.94 | -263.25 | -24.40 | 0.95 |
| Top | 8 | -244.42 | -23.10 | 0.93 | -251.47 | -23.68 | 0.94 | -258.45 | -24.40 | 0.93 | -265.28 | -25.15 | 0.93 |
| Top | 9 | -241.21 | -23.19 | 0.92 | -246.99 | -23.63 | 0.92 | -252.76 | -24.08 | 0.92 | -258.32 | -24.53 | 0.93 |
| Top | 10 | -245.74 | -23.59 | 0.92 | -251.03 | -23.99 | 0.92 | -256.32 | -24.39 | 0.93 | -261.42 | -24.77 | 0.93 |
| Top | 11 | -250.80 | -31.92 | 0.69 | -255.72 | -32.42 | 0.69 | -260.63 | -32.92 | 0.70 | -265.37 | -33.40 | 0.70 |
| Top | 12 | -255.86 | -32.37 | 0.70 | -260.60 | -32.85 | 0.70 | -265.34 | -33.33 | 0.70 | -269.91 | -33.80 | 0.70 |
| Angle Vert | 1 | 19.66 | 11.11 | | 20.24 | 11.44 | | 20.13 | 11.37 | | 20.01 | 11.31 | |
| Angle Vert | 2 | 9.41 | 5.32 | | 26.69 | 15.08 | | 16.16 | 9.13 | | 16.48 | 9.31 | |
| Angle Vert | 3 | 16.52 | 9.33 | | 16.57 | 9.36 | | 16.62 | 9.39 | | 16.66 | 9.41 | |
| Angle Vert | 4 | 19.40 | 10.96 | | 19.52 | 11.03 | | 19.64 | 11.10 | | 19.76 | 11.16 | |
| Web Vert | 1 | 25.95 | 16.12 | | 16.08 | 9.99 | | 17.00 | 10.56 | | 16.91 | 10.50 | |
| Web Vert | 2 | 11.51 | 7.15 | | 8.34 | 5.18 | | 24.86 | 15.44 | | 11.75 | 7.30 | |
| Web Vert | 3 | 14.26 | 8.85 | | 13.74 | 8.53 | | 12.54 | 7.79 | | 10.69 | 6.64 | |
| Web Vert | 4 | 14.25 | 8.85 | | 13.74 | 8.53 | | 12.54 | 7.79 | | 10.69 | 6.64 | |
| Web Vert | 5 | 13.47 | 8.37 | | 13.48 | 8.38 | | 13.55 | 8.42 | | 13.55 | 8.41 | |
| Web Vert | 6 | 16.59 | 10.30 | | 16.65 | 10.34 | | 16.72 | 10.39 | | 16.79 | 10.43 | |
| Square Vert | 1 | 22.25 | 34.50 | | 23.60 | 36.58 | | 23.32 | 36.16 | | 25.74 | 39.90 | |
| Square Vert | 2 | 19.61 | 30.41 | | 19.61 | 30.41 | | 19.61 | 30.41 | | 44.61 | 69.17 | |
| Square Vert | 3 | 21.44 | 33.24 | | 22.05 | 34.18 | | 22.63 | 35.09 | | 23.31 | 36.14 | |
| Square Vert | 4 | 19.61 | 30.41 | | 19.61 | 30.41 | | 19.61 | 30.41 | | 19.61 | 30.41 | |
| Bottom | 1 | 262.40 | 50.85 | | 257.66 | 49.93 | | 253.48 | 49.12 | | 249.40 | 48.33 | |
| Bottom | 2 | 261.75 | 50.73 | | 257.66 | 49.93 | | 253.35 | 49.10 | | 249.14 | 48.28 | |
| Bottom | 3 | 253.64 | 49.16 | | 263.39 | 51.04 | | 258.97 | 50.19 | | 254.25 | 49.27 | |
| Bottom | 4 | 245.97 | 47.67 | | 257.80 | 49.96 | | 263.67 | 51.10 | | 258.60 | 50.12 | |
| Bottom | 5 | 235.75 | 45.69 | | 243.76 | 47.24 | | 251.76 | 48.79 | | 260.21 | 50.43 | |
| Bottom | 6 | 235.75 | 45.69 | | 243.76 | 47.24 | | 251.76 | 48.79 | | 260.21 | 50.43 | |
| Bottom | 7 | 230.20 | 44.61 | | 236.68 | 45.87 | | 243.23 | 47.14 | | 249.45 | 48.34 | |
| Bottom | 8 | 230.20 | 44.61 | | 236.68 | 45.87 | | 243.23 | 47.14 | | 249.45 | 48.34 | |
| Bottom | 9 | 231.97 | 44.96 | | 237.47 | 46.02 | | 242.96 | 47.08 | | 248.25 | 48.11 | |
| Bottom | 10 | 230.42 | 44.65 | | 235.30 | 45.60 | | 240.18 | 46.55 | | 244.89 | 47.46 | |
| Bottom | 11 | 227.82 | 44.15 | | 232.20 | 45.00 | | 236.58 | 45.85 | | 240.80 | 46.67 | |
| Bottom | 12 | 228.76 | 44.33 | | 233.01 | 45.16 | | 237.25 | 45.98 | | 241.34 | 46.77 | |
| Diag D | 1 | 6.32 | 22.17 | | 7.35 | 25.79 | | 6.66 | 23.36 | | 6.32 | 22.18 | |
| Diag D | 2 | — | — | | 6.18 | 21.68 | | 6.31 | 22.13 | | 5.83 | 20.47 | |
| Diag D | 3 | — | — | | — | — | | 7.89 | 27.67 | | 7.37 | 25.84 | |
| Diag D | 4 | 1.33 | 2.06 | | — | — | | — | — | | 17.07 | 26.47 | |
| Diag D | 5 | 0.59 | 0.91 | | — | — | | — | — | | — | — | |
| Diag D | 6 | 2.41 | 3.74 | | 0.96 | 1.49 | | — | — | | — | — | |
| Diag D | 7 | 5.53 | 8.57 | | 4.76 | 7.37 | | 3.89 | 6.04 | | 3.18 | 4.94 | |
| Diag D | 8 | 1.85 | 6.48 | | 1.40 | 4.91 | | 0.96 | 3.35 | | 0.53 | 1.84 | |
| Diag D | 9 | 2.32 | 8.12 | | 2.03 | 7.11 | | 1.74 | 6.09 | | 1.46 | 5.11 | |
| Diag D | 10 | 1.27 | 4.45 | | 1.09 | 3.81 | | 0.90 | 3.17 | | 0.73 | 2.56 | |
| Diag U | 1 | 0.87 | 3.07 | | — | — | | 0.17 | 0.61 | | 0.35 | 1.21 | |
| Diag U | 2 | 21.61 | 75.81 | | 1.37 | 4.80 | | 0.56 | 1.98 | | 0.88 | 3.07 | |
| Diag U | 3 | 13.37 | 46.92 | | 17.77 | 62.35 | | 0.00 | 0.01 | | — | — | |
| Diag U | 4 | 13.29 | 20.60 | | 18.25 | 28.29 | | 22.01 | 34.13 | | 4.02 | 6.23 | |
| Diag U | 5 | 8.60 | 13.34 | | 12.01 | 18.61 | | 16.20 | 25.12 | | 18.95 | 29.38 | |
| Diag U | 6 | 7.80 | 12.10 | | 9.20 | 14.27 | | 11.08 | 17.17 | | 13.98 | 21.67 | |
| Diag U | 7 | 9.40 | 14.58 | | 10.71 | 16.61 | | 11.95 | 18.53 | | 13.27 | 20.58 | |
| Diag U | 8 | 3.88 | 13.62 | | 4.51 | 15.81 | | 5.13 | 18.00 | | 5.73 | 20.09 | |
| Diag U | 9 | 3.50 | 12.29 | | 3.98 | 13.96 | | 4.45 | 15.63 | | 4.91 | 17.24 | |
| Diag U | 10 | 4.54 | 15.93 | | 4.90 | 17.18 | | 5.25 | 18.42 | | 5.59 | 19.61 | |
| Horizontal | 1 | 4.26 | 6.61 | | 4.80 | 7.45 | | 4.48 | 6.94 | | 2.80 | 4.34 | |
| Horizontal | 2 | 4.26 | 6.61 | | 4.80 | 7.45 | | 4.48 | 6.94 | | 2.80 | 4.34 | |

## Element Forces and Stresses in Freeport Bridge Under Different Loading Conditions

"% Axial" is the percentage of stress in top chord due to axial force. "—" denotes elements eliminated from analysis.
Negative signs indicate compression.

| Element Type | No. | Concentrated Load, Node 13 Force (kN) | Stress (MPa) | % Axial |
|---|---|---|---|---|
| Top | 1 | -274.37 | -34.21 | 0.71 |
| Top | 2 | -270.02 | -33.83 | 0.70 |
| Top | 3 | -266.47 | -25.08 | 0.94 |
| Top | 4 | -263.84 | -25.30 | 0.92 |
| Top | 5 | -272.85 | -26.10 | 0.92 |
| Top | 6 | -270.81 | -28.63 | 0.83 |
| Top | 7 | -270.81 | -28.63 | 0.83 |
| Top | 8 | -272.85 | -26.08 | 0.92 |
| Top | 9 | -263.87 | -25.29 | 0.92 |
| Top | 10 | -266.51 | -25.11 | 0.93 |
| Top | 11 | -270.11 | -33.88 | 0.70 |
| Top | 12 | -274.48 | -34.26 | 0.71 |
| Angle Vert | 1 | 19.90 | 11.24 | |
| Angle Vert | 2 | 16.73 | 9.45 | |
| Angle Vert | 3 | 16.72 | 9.45 | |
| Angle Vert | 4 | 19.87 | 11.23 | |
| Web Vert | 1 | 16.84 | 10.46 | |
| Web Vert | 2 | 13.04 | 8.10 | |
| Web Vert | 3 | 24.71 | 15.35 | |
| Web Vert | 4 | 24.71 | 15.35 | |
| Web Vert | 5 | 13.06 | 8.11 | |
| Web Vert | 6 | 16.85 | 10.47 | |
| Square Vert | 1 | 23.17 | 35.92 | |
| Square Vert | 2 | 19.61 | 30.41 | |
| Square Vert | 3 | 23.18 | 35.94 | |
| Square Vert | 4 | 19.61 | 30.41 | |
| Bottom | 1 | 245.31 | 47.54 | |
| Bottom | 2 | 244.92 | 47.47 | |
| Bottom | 3 | 249.55 | 48.36 | |
| Bottom | 4 | 253.53 | 49.13 | |
| Bottom | 5 | 255.05 | 49.43 | |
| Bottom | 6 | 255.05 | 49.43 | |
| Bottom | 7 | 255.04 | 49.43 | |
| Bottom | 8 | 255.04 | 49.43 | |
| Bottom | 9 | 253.55 | 49.14 | |
| Bottom | 10 | 249.59 | 48.37 | |
| Bottom | 11 | 245.01 | 47.48 | |
| Bottom | 12 | 245.43 | 47.56 | |
| Diag D | 1 | 5.98 | 20.97 | |
| Diag D | 2 | 5.39 | 18.90 | |
| Diag D | 3 | 6.32 | 22.16 | |
| Diag D | 4 | 15.50 | 24.03 | |
| Diag D | 5 | — | — | |
| Diag D | 6 | 15.58 | 24.15 | |
| Diag D | 7 | 3.28 | 5.09 | |
| Diag D | 8 | 0.08 | 0.27 | |
| Diag D | 9 | 1.18 | 4.12 | |
| Diag D | 10 | 0.56 | 1.95 | |
| Diag U | 1 | 0.52 | 1.83 | |
| Diag U | 2 | 1.17 | 4.09 | |
| Diag U | 3 | 0.05 | 0.18 | |
| Diag U | 4 | 3.27 | 5.06 | |
| Diag U | 5 | — | — | |
| Diag U | 6 | 15.59 | 24.17 | |
| Diag U | 7 | 15.50 | 24.03 | |
| Diag U | 8 | 6.29 | 22.05 | |
| Diag U | 9 | 5.38 | 18.87 | |
| Diag U | 10 | 5.93 | 20.80 | |
| Horizontal | 1 | 3.50 | 5.42 | |
| Horizontal | 2 | 3.50 | 5.42 | |